INFLUENCE OF DISFORMAL COUPLING BETWEEN DARK ENERGY AND DARK MATTER ON OBSERVABLE UNIVERSE

STHARPORN SAPA

A Thesis Submitted to the Graduate School of Naresuan University
in Partial Fulfillment of the Requirements
for the Philosophy Degree in Theoretical Physics
November 2018

Thesis entitled "Influence of Disformal Coupling Between Dark Energy and Dark Matter on Observable Universe" by Stharporn Sapa has been approved by the Graduate School as partial fulfillment of the requirements for the Philosophy in Theoretical Physics of Naresuan University.

Oral Defense Committee

………………………………….Chair

(Phongpichit Channuie, Ph.D.)

………………………………….Advisor

(Khamphee Karwan, Dr. rer. Nat.)

………………………………….Committee

(Pitayuth Wongjun, Ph.D.)

………………………………….Committee

(Teeraparb Chantavat, Ph.D.)

………………………………….Committee

(Pichet Vanichchapongjaroen, Ph.D.)

Approved

………………………………………….

(Prof. Dr. Paisarn Muneesawang)

Associate Dean for Administration and Planning
for Dean of the Graduate School

ACKNOWLEDGEMENT

LIST OF CONTENTS

LIST OF FIGURES

LIST OF FIGURES (CONT.)

Figure   **Page**

ABSTRACT

The purpose of this research is to study cosmological consequences of the coupling between dark energy and dark matter through general disformal transformations. Using dynamical analysis, the influence of general disformal coupling on the evolution of background universe is investigated. We have found two new classes of fixed points for the case where disformal coefficient depends on both scalar field and its kinetic term. One of these classes of the fixed points is the generalization of disformal fixed point found in literature, while the other class of the fixed points occurs only when disformal coefficient depends on kinetic term of the scalar field. For the same value of the parameters of model, the stable fixed points in these classes can take two different physically relevant values. In addition to the background evolution, we also explore properties of density perturbations of the Universe for the case of disformal coupling. We analyze how both linear and non-linear density contrast of matter evolve with time on small scales. Based on this analysis, the growth of large scale structure in the Universe, the spherical collapse of the overdense regions and cluster number counts are investigated. We have found that the disformal coupling can affect an enhancement of the cluster number counts at late time.

CHAPTER I

INTRODUCTION

After Einstein has proposed the general theory of relativity in 1915, this theory has been tested many times until now. For example, the precession of Mercury's orbit [1, 2], gravitational lensing [3, 4, 5], the gravitational deflection of light by the Sun [6, 7, 8]. Moreover, this theory has been being used to describe the macroscopic systems, such as galaxies, clusters of galaxies and also our Universe. However, the general relativity theory encounters with important problems: Firstly this theory cannot describe phenomena at the quantum gravity level. Secondly it cannot be used to explain the present accelerating expansion of the Universe unless the mysterious form of energy with negative pressure, called dark energy, is introduced [9, 10]. These are some reasons why at present the Einstein theory of gravity is faced with many questions as well as the Newton theory. Therefore, physicists modify the Einstein theory of gravity in order to associated with the observations. The important models of modified gravity are scalar tensor theories. These theories reveal an interaction between dark energy and dark matter in some frames. In this work we will study this interaction inspired by general scalar tensor theories.

The observational data of Supernova Type Ia (SN Ia) [11, 12, 13], CMB observation [14, 15, 16], Large-scale structure surveys (LSS) [17, 18, 19] indicated that currently the Universe is in the phase of an accelerating expansion. In order to explain this phenomenon, we can assume that dynamics of the present Universe is dominated by some form of energy e.g. dark energy, or physics of gravity should deviate from Einstein theory of gravity on large scales (greater than 100 Megaparsec). For this reason the cosmological constant has been reconsidered as a source of the accelerating behaviour of the Universe [20]. However, it cannot exactly be identified whether the cosmological constant really drive a present ac-

celeration of the Universe. The ΛCDM model in which the accelerating expansion of the Universe is driven by the cosmological constant, is currently a standard model of the Universe because this model is in agreement with the observational data [21, 22]. Nevertheless, the standard ΛCDM model of the Universe appears to be extremely fine-tuned [23], because from the prediction from particle physics the vacuum energy density is much larger than the observed value of dark energy [20, 24]. This is the reason why physicists have been constructing new theories in order to satisfy with the data from the observations.

In the standard ΛCDM model of cosmology, at the present epoch the Universe appears to be extremely fine-tuned. In attempt to alleviate the fine-tuned problem, the various models of time dependent Λ are proposed, for example dark energy models or the models in which the Λ depends on scale factor a. Here we focus on the model of a scalar field as a dark energy. An important problem of the model of dark energy is the coincidence problem [25, 26] namely why the energy density of dark energy and dark matter are of the same order of magnitude at the present epoch albeit they are evolving differently during the expansion of the Universe. In order to alleviate the coincidence problem, we assume that there is an interaction between dark energy and dark matter [27, 28, 29, 30, 31].

At present, it seems that we have already known very little about properties of the dark energy. For instance, 1) the accelerating expansion of the Universe shows a redshift $z < 1$ [31, 32, 33] so that the dark energy (if exist) should dominate the dynamics of the Universe at late time, 2) the equation of state of dark energy should be $< \omega_d = -1.006 \pm 0.045$ [14]. For the case where gravity obeys Einstein theory, age of the Universe which contain dark energy is older than the Universe which do not contain dark energy. There are many the models of the Universe that have been constructed to explain the accelerating expansion of the Universe, for example the simplest model of the Universe that is ΛCDM, for which $\omega_\Lambda = -1$, quintessence and k-essence model of the Universe in which scalar field plays the role of dark energy with $\omega_\Lambda \neq -1$ [34, 35]. Therefore, investigating the properties of dark energy is an essential topic of cosmology to insight into our universe. We have already known that dark energy does not only influence the expansion rate of the Universe, but also the growth of structure formation and the collapse of

the overdense regions due to gravitational instability which is slowed down by the Hubble drag. There are several methods to follow the evolution of the overdense regions or structure formation, for example N-body simulations [36, 37], the spherical collapse model [38, 39] and other alternative methods [40, 41]. The simplest method to study non-linear structure formation is the spherical collapse which can be derived in both dark energy and modified gravity [42] models. Originally the spherical collapse model was proposed to explain perturbations in pressureless matter. From the work [43], they show that the correction of the relativistic equation for the cosmological background and density contrast can be obtained by using Newtonian cosmology for the case of non-vanishing pressure. In this work we study the effect of dark energy, which has negative pressure, in linear and non-linear regimes, on the structure formation. We also use spherical collapse model together with Press-Schechter or Sheth-Torman formalism to estimate cluster number counts of halos. The cluster number counts can be used to study the influence of the dark energy to overdense regions, test and discriminate among the dark energy models [39]. In the work [44], the authors use spherical collapse model to study the linear and non-linear growth of overdense regions of $f(T)$ model. They compute the number counts of virialization of haloes in order to distinguish the current $f(T)$ and ΛCDM models as well. The study of the influence of dark energy on the structure formation can be performed under the assumption in which dark energy can be both homogeneous and inhomogeneous distributes [39, 45]. In addition, the interaction between dark energy and dark matter remains an open issue in cosmology. There are many works have been proposed to explain the interaction between dark matter and dark energy [46, 47, 48]. Generally, there are many motivation in order to study the interaction between dark energy and dark matter [27, 28, 29, 30, 31, 49, 50, 51].

In this work, we study an interaction between dark energy and dark matter induced by the general disformal transformation (DFT) which is studied in chapter II. We investigate the background Universe, the evolution of the background Universe using Cosmological dynamical analysis and also analyze the stability of fixed points using linear stability theory in chapter III. In chapter IV, we use the perturbation theory and a spherical collapse model to determine linear and non-

linear perturbations and we also study the evolution of spherical collapse regions, structure formation as well. In addition, we investigate how a disformal interaction between dark energy and dark matter influences the growth of large scale structure of the Universe by computing cluster number counts of virialization of haloes in chapter IV. We also compare the result of the disformal coupling with conformal coupling, non-coupling and ΛCDM models in chapter IV. In the last chapter V, we conclude the thesis by summarizing our results and providing encouragement for future research.

1.1 Frequently used symbols and fundamental constants

- Symbol & Definition

- a & Scale factor of the Universe

- t & Cosmic time

- τ & Conformal time

- N & Number of e-foldings

- z & Redshift

- H & Hubble parameter

- $\mathcal{H}$ & Conformal Hubble parameter

- ρ & Energy density

- P & Pressure

- ω & Equation of state

- Ω & Dimensionless density parameters

- S & Action

- $\mathcal{L}$ & Lagrangian density

- R & Ricci scalar

- $g_{\mu\nu}$ & Metric tensor

- $G_{\mu\nu}$ & Einstein tensor

- $T_{\mu\nu}$ & Energy-momentum tensor

- ϕ & Scalar field

- X & Kinetic energy of the scalar field

- $V(\phi)$ & Potential energy of the scalar field

- $C(\phi, X)$ & Conformal coefficient

- $D(\phi, X)$ & Disformal coefficient

- Q & Coupling term between scalar field and non-relativistic matter

- δ_i & Density contrast of component i

1.2 Fundamental constants

- Symbol & Fundamental constants & Numerical value

- c & Speed of light in vacuum & 3×10^8 m/s

- G_N & Newton's gravitational constant & 6.673×10^{-11} Nm^2 kg^{-1}

- k_b & Boltzmann constant & 8.6×10^{-5} eV K^{-1}

- $L_\odot$ & The Sun's luminosity & 3.8×10^{26} watts

- $M_\odot$ & The Sun's mass & 2×10^{30} kg

- $\hbar = h/2\pi$ & Reduced Planck constant & 1.1×10^{-34}Js $= 6.6 \times 10^{-16}$ eVs

- $m_p = \sqrt{\frac{\hbar c}{G}}$ & Planck mass & 1.2211×10^{19} GeV/c^2

- $M_p = \sqrt{\frac{\hbar c}{8\pi G}}$ & Reduced Planck mass & 2.4357×10^{18} GeV

- $l_p = \sqrt{\frac{\hbar G}{c^3}}$ & Planck length & 1.6×10^{-35} m

- $E_p = m_p c^2$ & Planck energy & $2.0 \times 10^9 J = 1.2 \times 10^{19}$ GeV

- $T_p = E_p/k_b$ & Panck Temperature & 1.4×10^{32} K

- H_0 & Present Hubble parameter & 73.45 ± 1.66 km s^{-1} Mpc^{-1}

- Λ & Cosmological constant & 1.11×10^{-52} m^{-2} or $\simeq 10^{-35}$ s^{-2}

- ρ_{vacuum} & Vacuum energy density & 5.96×10^{-27} kg/m$^3 \simeq 10^{-47}$ GeV^4

1.3 The list of conversion factors

- 1 AU = 1.5×10^{11} m

- 1 parsec = 1 pc = 3.261 light years = 3.086×10^{16} m

- 1 year = 1 yr = 3.156×10^7 sec

- Sun mass M$_\odot$ = 1.989×10^{30} kg

- 1 Joule = 1 kgm^2 sec^{-2}

- 1 eV = 1.602×10^{-19} J

CHAPTER II

DISFORMAL TRANSFORMATIONS AND THE COUPLING BETWEEN DARK ENERGY AND DARK MATTER

It is generally accepted that at one time the Universe was dominated by matter (baryonic matter and dark matter) and after that there was a big change from matter dominated Universe to the present epoch in which dynamics of the Universe is dominated by mysterious form of energy. This unknown form of the energy called *dark energy*. The results of observation indicate that 70% of the total energy of the Universe come from dark energy [52], 30% of the total energy is from matter (baryonic matter and dark matter) and the remaining is in the form of radiation 10^{-4}%. Furthermore, remarkable fact that the energy densities of dark matter ρ_c and dark energy ρ_d are of the same order at present epoch that is $\rho_d/\rho_c \sim \mathcal{O}(1)$. This seems to indicate that we are living in the special moment of the cosmic history. In order to obtain the Universe which has the same order of the energy densities of dark matter and dark energy at present epoch, it requires specific initial conditions in the early Universe. The difference order of energy densities of dark matter and dark energy between early time and present time is so called *Cosmological Coincidence Problem* or CCP [25, 26].

Generally, there are many researches devoted to construct cosmological models for alleviating the cosmological coincidence problem for instance: quintessence model [53, 54], tracker field [55, 56], conformal gravity [57], the coupling between dark matter and dark energy model [29, 58, 59, 60, 61, 62], $f(R)$ model [63, 64, 65, 66], scalar-tensor theories [67, 68], MOND [69], TeVes [70], DGP [71], Gauss-Bonnet [72, 73] and Lovelock gravities [74], Horava-Lifshitz gravity [75], $f(T)$ gravity [76, 77], D-BIonic and DBI Scalar Field [78] and so on. However, there are many cosmological models that are ruled out because those models do not fit well with the observational data. In this research we study the coupling

between dark energy and dark matter via disformal transformations in which our analysis is based on scalar-tensor theory of gravitation.

2.1 Conformal transformation

It is generally known and accepted that Einstein theory of gravity is not only the theory which satisfies Einstein equivalent principle (EEP), and the general relativity theory cannot explain phenomena of gravity at the quantum level as well. Therefore, many physicists have been devoting to develop alternative theories of gravity instead of Einstein theory of gravity. One of the most important theories is the scalar-tensor theory of gravitation. An action of a scalar-tensor theory of gravitation in the Jordan frame can be written as

$$S = \int d^4x \sqrt{-g} \Big[\frac{F(\phi)R}{2} + P(\phi, X) \Big] + \int d^4x \sqrt{-g} \mathcal{L}_m(g_{\mu\nu}, \psi), \qquad (2.1)$$

where we have set $1/\sqrt{8\pi G} = 1$, g is the metric determinant, ϕ is the scalar field, X is the kinetic of scalar field, R is the Ricci scalar, F is a function depending on fields ϕ, $P(\phi, X)$ is the general Lagrangian density of the scalar field, $\mathcal{L}_m$ is the matter Lagrangian and ψ represents the matter fields. For convenience, we will use canonical scalar field with $P(\phi, X) = X - V(\phi)$, where $V(\phi)$ is the scalar field potential. The potential $V(\phi)$ is often inserted in the action when studying the early Universe or the late-time Universe or the accelerating Universe. One of the useful tools in order to study both interaction between dark energy and dark matter and relations between various theories of gravity and the Einstein theory of gravity is conformal transformations of metric tensor which can be written as,

$$\bar{g}_{\mu\nu} = C(\phi) g_{\mu\nu}, \qquad (2.2)$$

where $C(\phi)$ is the conformal factor. Under the conformal transformations given in equation (2.2), the light cones are not changed and also time-like and space-like vectors have the same character. The action in equation (2.1) can be transformed

into Einstein frame under the conformal transformations as

$$S = \int d^4x \sqrt{-\bar{g}} [\frac{\bar{R}}{2} - \frac{1}{2}\bar{\phi}_{;\mu}\bar{\phi}^{;\mu} - U(\bar{\phi})] + \int d^4x \sqrt{-\bar{g}}\bar{\mathcal{L}}_m(\bar{g}_{\mu\nu}, \psi), \qquad (2.3)$$

where $\bar{R}$ is calculated from $\bar{g}_{\mu\nu}$ given in equation (2.2) and ; is the covariant derivative. The relations between ϕ and $\bar{\phi}$, U and V are [79]

$$\frac{\partial \phi}{\partial \bar{\phi}} = \frac{F}{\sqrt{F + 3F_{,\phi}^2/2}}, \quad \text{and} \quad U(\bar{\phi}) = \frac{V(\phi)}{F^2(\phi)}\Big|_{\phi=\phi(\bar{\phi})}, \qquad (2.4)$$

where $F_{,\phi} = \frac{\partial F(\phi)}{\partial \phi}$. One can see that action for gravity in equation (2.3) is in the Einstein-Hilbert form. Thus, the action given in equation (2.3) relies in the Einstein frame. In this frame the conformal part enters the matter sector explicitly (the last term of this equation). Consequently there is a coupling between scalar field and the matter. In the original frame called *the Jordan frame*, a scalar degree of freedom in scalar-tensor theory modifies gravity via non-minimal coupling between scalar field and Ricci scalar. However, in the Einstein frame, scalar field affects the geodesic of matter via the direct coupling. In the next topic we study the coupling between dark matter and dark energy through disformal transformations which is a general form of the conformal transformations.

2.2   Disformal transformation

In order to alleviate coincidence problem we assume that there is a coupling between dark matter and dark energy. So as to study interaction between dark energy and dark matter, we consider action for gravity and scalar field in the Einstein frame (EF) and write the action for matter in other frame using a new metric as follows,

$$S = \int d^4x \sqrt{-g}[R + P(\phi, X)] + \int d^4x \sqrt{-\bar{g}}\mathcal{L}_m(\bar{g}_{\mu\nu}, \psi, \psi_{;\mu}), \qquad (2.5)$$

where R is the Ricci scalar, $P(\phi, X) \equiv X - V(\phi)$ is the Lagrangian of the scalar field, $\mathcal{L}_m$ is the Lagrangian of matter field and $X = -\frac{1}{2}\phi_{;\alpha}\phi^{;\alpha}$ is the kinetic energy of the scalar field. The metric in Einstein frame g and the metric $\bar{g}$ is related

through general disformal transformations as [80, 81, 82],

$$\bar{g}_{\mu\nu} = C(\phi, X)g_{\mu\nu} + D(\phi, X)\phi_{;\mu}\phi_{;\nu}, \qquad (2.6)$$

we use signature $(-, +, +, +)$. Noticed that this transformation will become the conformal transformation if $D(\phi, X) = 0$. Using the property of the metric $g_{\alpha\mu}g^{\beta\mu} = \delta^{\beta}_{\alpha}$, we determine the inverse metric $\bar{g}^{\mu\nu}$ which is given as

$$\bar{g}^{\mu\nu} = \frac{g^{\mu\nu}}{C(\phi, X)} + \frac{D(\phi, X)\phi^{;\mu}\phi^{;\nu}}{C(\phi, X)[C(\phi, X) - 2XD(\phi, X)]}. \qquad (2.7)$$

One can see that the inverse metric $\bar{g}^{\mu\nu}$ can exist as long as

$$C(\phi, X)[C(\phi, X) - 2XD(\phi, X)] \neq 0, \qquad (2.8)$$

From the relation between $g_{\mu\nu}$ and $\bar{g}_{\mu\nu}$, we can derive the determinant of $\bar{g}_{\mu\nu}$ as

$$g_{\mu\nu}\bar{g}^{\nu\alpha} = C\left(\delta^{\alpha}_{\mu} + \frac{D}{C}\phi^{;\alpha}\phi_{;\mu}\right), \qquad (2.9)$$

$$\frac{\bar{g}}{g} = C^3(C - 2XD), \qquad (2.10)$$

where $\bar{g}$ and g are the determinants of $\bar{g}_{\mu\nu}$ and $g_{\mu\nu}$ respectively. One can see that the transformation of the action for matter field in equation (2.5) into the Einstein frame (unbarred frame) leads to the interaction between dark energy and dark matter. In general, disformal transformations given in equation (2.6) may lead to Ostrogradski instability in a Jordan frame. In order to avoid this problem we will use coefficient C and D based on the result from literature which will be presented below.

The results from Ostrogradski's theorem in 1850 [83] show that linear instability in the Hamiltonian associated with a Lagrangian which depends on higher than first derivative cannot be eliminated by partial integration. This instability occur because the Hamiltonian is not bounded from below and hence large negative energy can exist in some configurations. This suggests that the realistic theories of nature should contain only first derivatives of the field in the Lagrangian.

After Ostrogradski proposed theorem of linear instability, there have been many studies on this theorem and have been found that the Lagrangian which has

second derivatives can be free from Ostrogradski instability for some combination of second derivative of the field. The important work is from G. W. Horndeski in 1974 [84] which has shown that in four dimensional space-time the general Lagrangian for scalar-tensor theory of gravity with second order derivative of scalar field can avoid the linear instability when the general Lagrangian is of the form

$$\mathcal{L}_H = \sum_{i=2}^{5} \mathcal{L}_i \,, \tag{2.11}$$

where

$$\mathcal{L}_2 = G_2(\phi, X) \,, \tag{2.12}$$

$$\mathcal{L}_3 = -G_3(\phi, X)\Box\phi \,, \tag{2.13}$$

$$\mathcal{L}_4 = G_4(\phi, X)R + G_{4,X}[(\Box\phi)^2 - \phi_{;\mu\nu}\phi^{;\mu\nu}] \,, \tag{2.14}$$

$$\mathcal{L}_5 = G_5(\phi, X)G_{\mu\nu}\phi^{;\mu\nu} - \frac{1}{6}G_{5,X}[(\Box\phi)^3 - 3(\Box\phi)\phi_{;\mu\nu}\phi^{;\mu\nu} + 2\phi_{;\mu}^{;\nu}\phi_{;\nu}^{;\lambda}\phi_{;\lambda}^{;\mu}] \,, \tag{2.15}$$

where $\Box$ is the d'Alembertian operator, $G_{\mu\nu}$ is the Einstein tensor and $\phi_{;\mu\nu} = \nabla_\nu\nabla_\mu\phi$. Horndeski Lagrangian is one of the important attempts to develop general form of scalar-tensor theory. It has been shown that the Horndeski action is structurally invariant under disformal transformations if C and D depend only on ϕ. For the appropiate functions of C and D the Horndeski action can be transformed into Einstein frame using disformal transformations [85]. The generalization of the Horndeski theory has been recently proposed in [86]. They have shown that the propagating degrees of freedom obey the second order equation of motion and therefore this theory is free from Ostrogradski instability. This theory is structurally invariant under disformal transformations where C depends on ϕ and D depends on both ϕ and X. Thus, if we use this disformal transformations to our analysis Ostrogradski instability will not occur. Therefore, in this work we study the interaction between dark energy and dark matter using disformal transformations as follows

$$\bar{g}_{\mu\nu} = C(\phi)g_{\mu\nu} + D(\phi, X)\phi_{;\mu}\phi_{;\nu} \,, \tag{2.16}$$

In the modern viewpoint, Horndeski theory can be constructed by covariantization

of Galileon theory of scalar field. Recently, however, it has been attempted to generalize Horndeski theory. An interesting work has been proposed in [86]. They have shown that one of the possible generalizations of Horndeski theory is to add some pieces of the Galileon action into the $\mathcal{L}_4$ and $\mathcal{L}_5$ of Horndeski Lagrangian given by equations (2.14) - (2.15) such as

$$\mathcal{L}_4^\phi \equiv G_4(\phi, X)^{(4)}R - 2G_{4,X}(\phi, X)(\Box\phi^2 - \phi^{;\mu\nu}\phi_{;\mu\nu})$$
$$+ F_4(\phi, X)\epsilon^{\mu\nu\rho}_\sigma \epsilon^{\mu'\nu'\rho'\sigma}\phi_{;\mu}\phi_{;\nu'}\phi_{;\nu\nu'}\phi_{;\rho\rho'}, \tag{2.17}$$
$$\mathcal{L}_5^\phi \equiv G_5(\phi, X)^{(4)}G_{\mu\nu}\phi^{\mu\nu} + \frac{1}{3}G_{5,X}(\phi, X)\left[(\Box\phi)^3 - 3\Box\phi\phi_{;\mu\nu}\phi^{;\mu\nu} + 2\phi_{;\mu\nu}\phi^{;\mu\sigma}\phi^{;\nu}_{;\sigma}\right]$$
$$+ F_5(\phi, X)\epsilon^{\mu\nu\rho\sigma}\epsilon^{\mu'\nu'\rho'\sigma'}\phi_{;\mu}\phi_{;\mu'}\phi_{;\nu\nu'}\phi_{;\rho\rho'}\phi_{;\sigma\sigma'}, \tag{2.18}$$

where $G_{4,X} = \partial G_4(\phi, X)/\partial X$ and $\epsilon_{\mu\nu\rho\sigma}$ is the totally antisymmetric Levi-Civita tensor. One can see that Horndeski theory is a subset of the above theory under the condition

$$F_4(\phi, X) = 0, \quad F_5(\phi, X) = 0, \tag{2.19}$$

It has been shown that the EOM of the extended Horndeski theories remains second order time derivatives. It is significant that this theory has one more degree of freedom higher than Horndeski theory. This extra degree of freedom may lead to Ostrogradski instability. Nevertheless, it has been shown that this extra degree of freedom does not propagate. Thus, this theory does not involve with Ostrogradski instability. Usually this theory is called Gleyzes-Langlois-Piazza-Vernizzi (GLPV) theory [86].

It is clear that the Horndeski action or GLPV action cannot be transformed into Einstein frame using conformal transformations. Therefore, conformal transformations must be extended to general form. The simplest extention of conformal transformations is called *disformal transformation* in which the transformation relation is shown in equation (2.6). The work of [87] have been already wrote that general Horndeski action or GLPV action is invariance under disformal transformation for the case where $C = C(\phi)$ and $D = D(\phi, X)$ which is the equation (2.16).

2.3 Disformal coupling between dark sectors

In this work we use disformal transformations equation (2.16) to study the coupling between dark energy and dark matter. In order to study the coupling between dark energy and dark matter, we write the action in the bi-metric form as shown in equation (2.5). The variation of the equation (2.5) with respect to the metric tensor $g_{\mu\nu}$ yields the Einstein equation as

$$G^{\mu\nu} = T_\phi^{\mu\nu} + T_m^{\mu\nu}\,, \tag{2.20}$$

where $G^{\mu\nu}$ is the Einstein tensor computed from $g_{\mu\nu}$. The energy momentum tensor for scalar field and matter are defined in unbarred frame as

$$T_\phi^{\mu\nu} = \frac{2}{\sqrt{-g}}\frac{\delta(\sqrt{-g}P(\phi,X))}{\delta g_{\mu\nu}}\,, \tag{2.21}$$

$$T_m^{\mu\nu} = \frac{2}{\sqrt{-g}}\frac{\delta(\sqrt{-g}\mathcal{L}_m)}{\delta g_{\mu\nu}}\,. \tag{2.22}$$

From the equation (2.20) and the definitions of energy momentum tensor in equations (2.21) and (2.22), we can use Bianchi identities to show the conservation of total energy momentum tensor $\nabla_\alpha(T_\phi^{\mu\nu} + T_m^{\mu\nu}) = 0$. However, the energy momentum tensor of dark energy and dark matter are not separately conserved. The variation of the action in equation (2.5) with respect to scalar field ϕ gives

$$\delta S|_{\delta\phi} = \int d^4x\sqrt{-g}\delta P|_{\delta\phi} + \int \delta(\sqrt{-g}\mathcal{L}_m)|_{\delta\phi} = 0 \tag{2.23}$$

$$= \delta S_\phi + \delta S_m\,. \tag{2.24}$$

The variation for the first term of the above equation is shown below

$$\delta S_\phi = \int d^4x\sqrt{-g}\delta\left[-\frac{1}{2}g^{\mu\nu}\phi_{;\mu}\phi_{;\nu} - V(\phi)\right]$$

$$= \int d^4x\sqrt{-g}\left[-\frac{1}{2}g^{\mu\nu}\left\{\phi_{;\mu}\frac{\partial(\phi_{;\nu})}{\partial(\phi_{;\lambda})} + \phi_{;\nu}\frac{\partial(\phi_{;\mu})}{\partial(\phi_{;\lambda})}\right\}\delta\phi_{;\lambda} - \frac{\partial V(\phi)}{\partial\phi}\delta\phi\right]$$

$$= \int d^4x\sqrt{-g}\left[-\frac{1}{2}g^{\mu\nu}\left(\delta_\nu^\lambda\phi_{;\mu} + \delta_\mu^\lambda\phi_{;\nu}\right)\delta\phi_{;\lambda} - V_{,\phi}\delta\phi\right]$$

$$= \int d^4x\sqrt{-g}\left[-\phi^{;\lambda}\delta\phi_{;\lambda} - V_{,\phi}\delta\phi\right]$$

$$= \int d^4x \sqrt{-g}(\phi^{;\lambda}_{;\lambda} - V_{,\phi})\delta\phi \,, \tag{2.25}$$

where the above equation we use integration by part and ignore surface term and $V_{,\phi} = \delta V/\delta\phi$. The variation for the second term of the equation (2.24) is shown below

$$\delta S_m = \int d^4x \delta(\sqrt{-\bar{g}}\mathcal{L}_m)|_{\delta\phi} = \int d^4x \frac{\delta(\sqrt{-\bar{g}}\mathcal{L}_m)}{\delta\bar{g}_{\alpha\beta}}\delta\bar{g}_{\alpha\beta}|_{\delta\phi} \,. \tag{2.26}$$

The energy-momentum tensor in barred frame is related to the unbared frame given in equation (2.22) as

$$T_m^{\alpha\beta} = \frac{\sqrt{-\bar{g}}}{\sqrt{-g}}\frac{\delta\bar{g}_{\rho\sigma}}{\delta g_{\alpha\beta}}\frac{2}{\sqrt{-\bar{g}}}\frac{\delta(\sqrt{-\bar{g}}\mathcal{L}_m)}{\delta\bar{g}_{\rho\sigma}} = \frac{\sqrt{-\bar{g}}}{\sqrt{-g}}\frac{\delta\bar{g}_{\rho\sigma}}{\delta g_{\alpha\beta}}\bar{T}_m^{\rho\sigma} \,, \tag{2.27}$$

where

$$\bar{T}_m^{\rho\sigma} = \frac{2}{\sqrt{-\bar{g}}}\frac{\delta(\sqrt{-\bar{g}}\mathcal{L}_m)}{\delta\bar{g}_{\rho\sigma}} \tag{2.28}$$

Using the equation (2.28), the equation (2.26) becomes

$$\delta S_m = \int d^4x \frac{\sqrt{-\bar{g}}}{2}\bar{T}_m^{\alpha\beta}\delta\bar{g}_{\alpha\beta}|_{\delta\phi} \,. \tag{2.29}$$

From the equation (2.16), we have

$$\begin{aligned}
\delta\bar{g}_{\alpha\beta}|_{\delta\phi} &= g_{\alpha\beta}\delta C(\phi) + \delta\left[D(\phi, X)\phi_{;\alpha}\phi_{;\beta}\right] \\
&= g_{\alpha\beta}\frac{\delta C(\phi)}{\delta\phi}\delta\phi + \left(\frac{\delta D(\phi, X)}{\delta\phi}\delta\phi + \frac{\delta D(\phi, X)}{\delta X}\delta X\right)\phi_{;\alpha}\phi_{;\beta} \\
&\quad + D(\phi, X)\frac{\delta(\phi_{;\alpha}\phi_{;\beta})}{\delta\phi_{;\lambda}}\delta\phi_{;\lambda} \\
&= g_{\alpha\beta}C_{,\phi}\delta\phi + (D_{,\phi}\delta\phi + D_{,X}\delta X)\phi_{;\alpha}\phi_{;\beta} + D\left(\phi_{;\alpha}\frac{\delta\phi_{;\beta}}{\delta\phi_{;\lambda}} + \phi_{;\beta}\frac{\delta\phi_{;\alpha}}{\delta\phi_{;\lambda}}\right)\delta\phi_{;\lambda} \\
&= g_{\alpha\beta}C_{,\phi}\delta\phi + (D_{,\phi}\delta\phi + D_{,X}\delta X)\phi_{;\alpha}\phi_{;\beta} + D\left(\phi_{;\alpha}\delta^\lambda_\beta + \phi_{;\beta}\delta^\lambda_\alpha\right)\delta\phi_{;\lambda} \quad (2.30)
\end{aligned}$$

Consider the third term of the above equation

$$\begin{aligned}
\delta X &= \delta(-\frac{1}{2}g^{\mu\nu}\phi_{;\mu}\phi_{;\nu}) = -\frac{1}{2}g^{\mu\nu}\delta(\phi_{;\mu}\phi_{;\nu}) \\
&= -\frac{1}{2}g^{\mu\nu}(\phi_{;\mu}\delta\phi_{;\nu} + \phi_{;\nu}\delta\phi_{;\mu}) = -\phi^{;\nu}\delta\phi_{;\nu} \,. \tag{2.31}
\end{aligned}$$

Using the above equation, then the equation (2.30) becomes

$$\delta\bar{g}_{\alpha\beta}|_{\delta\phi} = g_{\alpha\beta}C_{,\phi}\delta\phi + (D_{,\phi}\delta\phi - D_{,X}\phi^{;\nu}\delta\phi_{;\nu})\phi_{;\alpha}\phi_{;\beta} + D\left(\phi_{;\alpha}\delta^\lambda_\beta + \phi_{;\beta}\delta^\lambda_\alpha\right)\delta\phi_{;\lambda} \tag{2.32}$$

Inserting the equation (2.32) into the equation (2.29), we have

$$
\begin{aligned}
\delta S_m &= \int d^4x \frac{\sqrt{-\bar{g}}}{2} \bar{T}_m^{\alpha\beta} \left[g_{\alpha\beta} C_{,\phi} \delta\phi + \left(D_{,\phi} \delta\phi - D_{,X} \phi^{;\nu} \delta\phi_{;\nu} \right) \phi_{;\alpha} \phi_{;\beta} + 2D\phi_{;\alpha} \delta\phi_{;\beta} \right] \\
&= \int d^4x \sqrt{-g} \left[\frac{\sqrt{-\bar{g}}}{2\sqrt{-g}} \bar{T}_m^{\alpha\beta} \left(C_{,\phi} g_{\alpha\beta} + D_{,\phi} \phi_{;\alpha} \phi_{;\beta} \right) \delta\phi - \frac{\sqrt{-\bar{g}}}{2\sqrt{-g}} \bar{T}_m^{\alpha\beta} D_{,X} \phi^{;\nu} \delta\phi_{;\nu} \phi_{;\alpha} \phi_{;\beta} \right. \\
&\quad \left. + \frac{\sqrt{-\bar{g}}}{\sqrt{-g}} \bar{T}_m^{\alpha\beta} D\phi_{;\alpha} \delta\phi_{;\beta} \right] .
\end{aligned}
\tag{2.33}
$$

Using integration by part to the third and fourth terms and define $J = \sqrt{-\bar{g}}/\sqrt{-g}$, the equation (2.33) becomes

$$
\begin{aligned}
\delta S_m &= \int d^4x \sqrt{-g} \left[\frac{J}{2} \bar{T}_m^{\alpha\beta} \left(C_{,\phi} g_{\alpha\beta} + D_{,\phi} \phi_{;\alpha} \phi_{;\beta} \right) + \frac{1}{2} \nabla_\nu \left(J \bar{T}_m^{\alpha\beta} D_{,X} \phi^{;\nu} \phi_{;\alpha} \phi_{;\beta} \right) \right. \\
&\quad \left. - \nabla_\alpha \left(J \bar{T}_m^{\alpha\beta} D\phi_{;\beta} \right) \right] \delta\phi
\end{aligned}
\tag{2.34}
$$

where $\bar{T}_m^{\alpha\beta}$ is the energy momentum tensor in barred frame which is related to $T_m^{\alpha\beta}$ as

$$
T_m^{\alpha\beta} = \frac{\sqrt{-\bar{g}}}{\sqrt{-g}} \frac{\delta\bar{g}_{\rho\sigma}}{\delta g_{\alpha\beta}} \frac{2}{\sqrt{-\bar{g}}} \frac{\delta(\sqrt{-\bar{g}}\mathcal{L}_m)}{\delta\bar{g}_{\rho\sigma}} = \frac{\sqrt{-\bar{g}}}{\sqrt{-g}} \frac{\delta\bar{g}_{\rho\sigma}}{\delta g_{\alpha\beta}} \bar{T}_m^{\rho\sigma}
\tag{2.35}
$$

$$
= (C\delta_\rho^\alpha \delta_\sigma^\beta - \frac{1}{2} D_{,X} \phi^{;\alpha} \phi^{;\beta} \phi_{;\rho} \phi_{;\sigma}) J \bar{T}_m^{\rho\sigma} .
\tag{2.36}
$$

From the equations (2.25) and (2.34), we obtain the evolution equation for scalar field as

$$
\begin{aligned}
\phi^{;\alpha}_{;\alpha} - V_{,\phi} &= \nabla_\beta (J \bar{T}_m^{\alpha\beta} D\phi_{;\alpha}) - \frac{1}{2} J \bar{T}_m^{\alpha\beta} (C_{,\phi} g_{\alpha\beta} + D_{,\phi} \phi_{;\alpha} \phi_{;\beta}) \\
&\quad - \frac{J}{2} \nabla_\nu [\bar{T}_m^{\alpha\beta} D_{,X} \phi^{;\nu} \phi_{;\alpha} \phi_{;\beta}] \equiv Q .
\end{aligned}
\tag{2.37}
$$

We use the disformal transformations in equation (2.16) to calculate the evolution equation for scalar field in equation (2.37) and the relation between $T_m^{\alpha\beta}$ and $\bar{T}_m^{\alpha\beta}$. Then, we obtain the relation between $T_m^{\alpha\beta}$ and $\bar{T}_m^{\alpha\beta}$ as follows

$$
\bar{T}_m^{\alpha\beta} = \frac{T^{\alpha\beta}}{CJ} + \frac{D_{,X} \phi^{;\alpha} \phi^{;\beta}}{2CJ(C - 2D_{,X}X^2)} T_{mp},
\tag{2.38}
$$

where

$$T_m = g_{\alpha\beta}T_m^{\alpha\beta} = JCg_{\rho\sigma}\bar{T}_m^{\rho\sigma} + JD_{,X}X\phi_{;\rho}\phi_{;\sigma}\bar{T}_m^{\rho\sigma} , \tag{2.39}$$

$$T_{mp} \equiv \phi_{;\alpha}\phi_{;\beta}T_m^{\alpha\beta} = J(C - 2D_{,X}X^2)\phi_{;\rho}\phi_{;\sigma}\bar{T}_m^{\rho\sigma} , \tag{2.40}$$

and then

$$g_{\alpha\beta}\bar{T}_m^{\alpha\beta} = \frac{CT_m - D_{,X}X(T_{mp} + 2T_mX)}{CJ(C - 2D_{,X}X^2)} , \tag{2.41}$$

$$\phi_{;\alpha}\phi_{;\beta}\bar{T}_m^{\alpha\beta} = \frac{T_{mp}}{J(C - 2D_{,X}X^2))}. \tag{2.42}$$

From the conservation of the total energy momentum tensor, we get

$$\nabla_\alpha T_m^{\alpha\lambda} = -\nabla_\alpha T_\phi^{\alpha\lambda} = -Q\phi^{;\lambda}. \tag{2.43}$$

In order to obtain the coupling Q on the right hand side of the above equation, we multiply equation (2.37) by $\phi^{;\lambda}$ and rearrange the left hand side of the resulting equation in the form of the energy momentum tensor. Furthermore, for simplicity of the following calculation we write Q in the following expressions

$$\begin{aligned} FQ =& C[-2DF_1F_{1,\phi} + CF_1(F_{2,X\phi} - D_{,\phi}) + D_{,X}(C_{,\phi}F_1 - 2F_{1,\phi}F_2)X]T_{mp} \\ & - CC_{,\phi}F_1(C - 2D_{,X}X^2)T_m - CD_{,X}F_1F_2T_{mp} + 2CDF_1^2\Theta_1 \\ & + 2CD_{,X}F_1^2\Theta_2 + 2CDF_2^2\Theta_3 - CD_{,X}F_1F_2\Theta_4 - C(D_{,XX}F_1F_2 \\ & - D_{,X}F_{1,X}F_2 + D_{,X}F_1F_{2,X})T_{mp}\Theta_5, \tag{2.44} \end{aligned}$$

where $F_1 \equiv C - 2D_{,X}X^2, F_2 \equiv C + 2DX, F \equiv 2C^2F_1^2$ and

$$\Theta_1 = \phi_{;\alpha\beta}T_m^{\alpha\beta}, \quad \Theta_2 = \phi_{;\alpha}X_{;\beta}T_m^{\alpha\beta}, \quad \Theta_3 = \phi_{;\alpha}\nabla_\beta T_m^{\alpha\beta}, \tag{2.45}$$

$$\Theta_4 = \phi^{;\alpha}\nabla_\alpha T_{mp}, \quad \Theta_5 = \phi^{;\alpha}X_{;\alpha}. \tag{2.46}$$

Disformal coupling between dark energy and dark matter has been studied in [81, 82, 85, 88, 89, 90]. In those works they have studied the disformal transformation in the simple case in which both C and D depend only on ϕ. The results from [81] showed that the evolution of the background Universe in the disformal

coupling theory is nearly similar to that in ΛCDM model. This theory can address the coincidence problem and cosmological constant problems. It has been shown in [85] that the disformal coupling offers possibilities to construct models for cosmic acceleration. Furthermore, disformal coupling leads to a new fixed point of cosmic evolution and gives rise to the disformal screening mechanism. In [88], the authors study the effects of the interactions between dark energy and dark matter on the Universe using both conformal and disformal couplings. They discuss the background evolution, anisotropies in the cosmic microwave background and large scale structures. In our work we use the general disformal transformation, where D depends on both ϕ and X, to study the influence of disformal coupling between dark energy and dark matter on the background Universe and cosmological perturbations.

CHAPTER III

COSMOLOGICAL DYNAMICAL EQUATIONS

In order to understand and study evolution of the Universe from very early to late time. We need some tools to analyze the complex evolution of the Universe. One of the important tools for the cosmologist is the dynamical analysis. In the context of cosmology, we call *cosmological dynamical system*. In this chapter, we use the cosmological dynamical system in order to investigate the evolution of the Universe in the presence of the scalar field which is the presentation of dark energy and responds to the accelerating expansion of the Universe at late time. In this work, we are interested in *disformal* fixed point which occurs due to the disformal coupling that we have introduced in the equation (2.37). We use the cosmological dynamical system in order to find the fixed points of the system and use linear theory of stability to analyze the stability of each fixed point. In the next section, we will find evolution equation of the scalar field and then find the fixed points of the system and analyze the stability for each fixed point of the system.

3.1 Evolution equations for FLRW Universe

In this section, we study the influences of disformal coupling on the evolution of background Universe, based on the cosmological principle which states that the Universe is homogeneous and isotropic on large scale (no center or no special points exist in the Universe). We use the standard Friedmann–Lemaître–Robertson–Walker (FLRW) line element and perfect fluid model of matter. The spatially-flat FLRW line element takes the form

$$ds^2 = -a(\tau)^2 d\tau^2 + a(\tau)^2 dx_i dx^i, \tag{3.1}$$

here $a(\tau)$ is the scale factor and τ is the conformal time. The relation between cosmic time t and conformal time τ is $dt = ad\tau$. From the Einstein equation (2.20), we obtain the Friedmann equation as

$$\mathcal{H}^2 = \frac{1}{3M_p^2}\left[\frac{1}{2}\phi'^2 + a^2V(\phi) + a^2\rho_m\right]. \tag{3.2}$$

where $\mathcal{H} \equiv a'/a$ is the Hubble parameter and a prime denotes derivative with respect to the conformal time τ. Using the above line element in the equation (3.1), we can write the equations (2.45) - (2.46) as follows

$$a^2\Box\phi = \phi'' - 2\mathcal{H}\phi', \quad T_m = -\rho_m, \quad T_{mp} = 2\rho_m X,$$
$$a^2\Theta_1 = (\phi'' - \mathcal{H}\phi')\rho_m, \quad a^2\Theta_2 = 2(\phi'' - \mathcal{H}\phi')\rho_m X, \quad a^2\Theta_3 = \phi'(\rho_m' + 3\mathcal{H}\rho_m),$$
$$a^2\Theta_4 = \phi'(\rho_m' - 2\mathcal{H}\rho_m), \quad a^2\Theta_5 = -2\phi'\rho_m'X - 4(\phi'' - \mathcal{H}\phi')\rho_m X. \tag{3.3}$$

Inserting the above quantities into the equation (2.44), we obtain the interaction term for the background as,

$$FQ \Rightarrow F_cQ_0,$$
$$F_cQ_0 = 2C\phi'\rho_m'F_1(DF_1 + D_{,X}) + a^2C\rho_m[-4F_{1,\phi}X(DF_1 + D_{,X}F_2X)$$
$$+ CF_1(C,\phi + 2X(-D_{,\phi} + F_{2,X\phi}))] + 4C\phi'\mathcal{H}\rho_m[DF_1^2 - X(D_{,XX}F_1F_2X$$
$$+ D_{,X}(F_1^2 - F_{1,X}F_2X))] + 2C\phi''\rho_m[DF_1^2 + X(2D_{,XX}F_1F_2X$$
$$+ D_{,X}(2F_1^2 + 3F_1F_2 - 2F_{1,X}F_2X + 2F_1F_{2,X}))]. \tag{3.4}$$

We have used $X = \phi'^2/2a^2$ in the above equation. Inserting the above equation into the equation (2.43), then we can express ρ_m' as follows

$$F_m\rho_m' = a^2C\phi'\rho_m\left[-4F_{1,\phi}X(DF_1 + D_{,X}XF_2) + CF_1\left(C_\phi + 2(-D_{,\phi} + F_{2,X\phi})X\right)\right]$$
$$+ 2C\phi''\phi'\rho_m\left[DF_1^2 + X\left(2D_{,XX}F_1F_2X + D_{,X}(2F_1^2 + 3F_1F_2 - 2F_{1,X}F_2X\right.\right.$$
$$\left.\left. + 2F_1F_{2,X}X)\right)\right] - 2C\mathcal{H}\rho_m\left[3a^2CF_1^2 + 4a^2X\left(-DF_1^2 + X\left(D_{,XX}F_1F_2X\right.\right.\right.$$
$$\left.\left.\left. + D_X(F_1^2 - F_{1,X}F_2X + F_1F_{2,X}X)\right)\right)\right], \tag{3.5}$$

where $F_m = 2a^2 C F_1 [C F_1 - 2X(D F_1 + D_{,X} F_2 X)]$. From the equations (2.37) and (3.5), we obtain the equation of motion for the scalar field as

$$\partial_\alpha \partial^\alpha \phi + \Gamma^\alpha_{\alpha\beta} \phi^{,\beta} - V_{,\phi} = -Q, \tag{3.6}$$

$$\begin{aligned}
\phi'' + 2\mathcal{H}\phi' + V_{,\phi} a^2 &= F_\phi^{-1} \rho_m \Big[6\phi' \mathcal{H}(F_1^2 F_d + F_1 F_2 F_{d,X} X - 2D_{,X} F_{d3} X^2) \\
&\quad + a^2 C\{-C_{,\phi} F_1 + 2(D_{,\phi} F_1 - F_1 F_{2,X\phi} + 2F_{1,\phi} F_{d1})\} X \\
&\quad + 2a^2 V_\phi (F_1^2 F_d + F_1 F_2 F_{d,X} X - 2D_{,X} F_{d3} X^2) \Big], \\
&= F_\phi^{-1} \rho_m \Big[(6\phi' \mathcal{H} + 2a^2 V_\phi)(F_1^2 F_d + F_1 F_2 F_{d,X} X - 2D_{,X} F_{d3} X^2) \\
&\quad + a^2 C\{-C_{,\phi} F_1 + 2(D_{,\phi} F_1 - F_1 F_{2,X\phi} + 2F_{1,\phi} F_{d1})\} \Big] \equiv -Q_0,
\end{aligned} \tag{3.7}$$

where

$$F_\phi = 2\Big[C F_1 (F_1 - 2F_{d1} X) + \rho_m (F_1^2 F_d + F_1 F_2 F_{d,X} X - 2D_{,X} F_{d3} X^2) \Big], \tag{3.8}$$

and

$$F_d \equiv D + 2D_{,X} X, \qquad F_{d1} \equiv D + D_{,X} X,$$
$$F_{d2} \equiv D F_{1,X} + D_{,X} F_{2,X} X, \quad F_{d3} \equiv F_{1,X} F_2 - F_{2,X} F_1. \tag{3.9}$$

The equation of motion for energy density of matter ρ_m and radiation ρ_r can be computed from the equation (2.43) as

$$\rho'_m + 3H\rho_m = Q_0 \phi', \tag{3.10}$$

$$\rho'_r + 4H\rho_r = 0. \tag{3.11}$$

3.2 Cosmological dynamical systems

In this section, we discussed some aspects of cosmology in the context of dynamical systems. Alternative to [59], we suggest the readers that the work of [91] is also a good and simple example in order to deeply understand cosmological dynamical systems. In order to construct the models of cosmology which satisfy observational data, the series of cosmological epoch should contain the era

of inflation $\rightarrow$ radiation dominated $\rightarrow$ matter dominated $\rightarrow$ cosmological constant dominated respectively which could be dubbed *minimal cosmological model.*

We now use the results from the previous section to calculate the autonomous equations and evaluate fixed points which lead to the understanding the evolution of the background Universe for the existence of disformal coupling between dark energy and dark matter. We neglect the contribution from the radiation density in this work. We derive the autonomous equations using the conformal coefficient, disformal coefficient and the scalar field potential of the form

$$C = C_0 e^{\lambda_1 \phi}, \quad D = D_0 M^{-4(1+\lambda_3)} e^{\lambda_2 \phi} X^{\lambda_3}, \quad V = M_v^4 e^{\lambda_4 \phi}, \tag{3.12}$$

where $\lambda_1, \lambda_2, \lambda_3, \lambda_4$ and C_0 are dimensionless constant parameters whilst M and M_v are the constant parameters with the dimension of mass. So let us begin the analysis by defining the dimensionless variables as

$$\Omega_c = \frac{a^2 \rho_c}{3\mathcal{H}^2}, \quad \Omega_b = \frac{a^2 \rho_b}{3\mathcal{H}^2},$$
$$x_1^2 = \frac{\phi'^2}{6\mathcal{H}^2}, \quad x_2 = \frac{a^2 V}{3\mathcal{H}^2}, \quad x_3 = \frac{D\mathcal{H}^2}{a^2 C}, \tag{3.13}$$

where we set $1/\sqrt{8\pi G} = 1$ and Ω_c is the dark matter density parameter. It follows from the equation (3.2) that these quantities satisfy the constraint equation,

$$1 = x_1^2 + x_2 + \Omega_b + \Omega_c. \tag{3.14}$$

In order to compute the evolution equations for x_1, x_2 and x_3 we first differentiate the equation (3.2) to obtain

$$\frac{\mathcal{H}'}{\mathcal{H}^2} = \frac{1}{2}(3x_2 - 3x_1^2 - 1). \tag{3.15}$$

From the equation (3.15), we see that

$$\mathcal{H}' = \frac{d\mathcal{H}}{d\tau} = a\frac{d^2 a}{dt^2}, \tag{3.16}$$

$$\frac{d^2 a}{dt^2} = \frac{\mathcal{H}^2}{2a}(3x_2 - 3x_1^2 - 1), \tag{3.17}$$

where t is the cosmic time. Differentiating the variables x_1, x_2 and x_3 from the

equations (3.13) with respect to the number of e-folding $N = \ln a$ together with using the equation (3.15), we obtain the following autonomous equations,

$$x_{1,N} = \frac{dx_1}{dN} = \frac{\bar{K} + \bar{\Sigma}}{F_\phi}\,, \tag{3.18}$$

$$x_{2,N} = \frac{dx_2}{dN} = x_2[3(1 - x_2 + x_1^2) + \sqrt{6}\lambda_4 x_1]\,, \tag{3.19}$$

$$x_{3,N} = \frac{dx_3}{dN} = \frac{x_3}{x_1}[\sqrt{6}x_1^2(\lambda_2 - \lambda_1) + 2\lambda_3 x_{1,N} + 3x_1(1 + \lambda_3)(x_2 - x_1^2 - 1)]\,, \tag{3.20}$$

$$\Omega_{b,N} = \frac{d\Omega_b}{dN} = \Omega_b(3x_1^2 - 3x_2)\,. \tag{3.21}$$

where the $x_{1,N}$ means differentiation x_1 with respect to N and the new parameters from the equation (3.18) are expressed below

$$\begin{aligned} F_\phi =& 2C^3\Big[(1 - 6\lambda_3 x_3 x_1^2)\big(1 - 6x_3 x_1^2(1 + 2\lambda_3)\big) \\ &+ 3x_3(1 + \lambda_3)(1 - x_1^2 - x_2 - \Omega_b)\big(1 + 2\lambda_3(1 + 3x_3 x_1^2)\big)\Big], \end{aligned} \tag{3.22}$$

$$\begin{aligned} \bar{K} =& C^3\Big[3x_1^3 - \sqrt{6}\lambda_4 x_1 - 3x_1(1 + x_2)\Big]\Big[(1 - 6\lambda_3 x_3 x_1^2) \\ &\times \big(1 - 6x_3 x_1^2(1 + 2\lambda_3)\big) + 3x_3(1 + \lambda_3)(1 - x_1^2 - x_2 - \Omega_b) \\ &\times \big(1 + 2\lambda_3(1 + 3x_3 x_1^2)\big)\Big], \end{aligned} \tag{3.23}$$

$$\begin{aligned} \bar{\Sigma} =& \sqrt{3/2}C^3(1 - x_1^2 - x_2 - \Omega_b)\Big[\lambda_1\big(6x_3 x_1^2(2 + 3\lambda_3) - 1\big) \\ &+ 6x_3(1 + \lambda_3)(\sqrt{6}x_1 + \lambda_4 x_2)\big(1 + \lambda_3(2 + 6x_3 x_1^2)\big) \\ &- 6\lambda_2 x_3 x_1^2\big(1 + \lambda_3(2 + 6x_3 x_1^2)\big)\Big]. \end{aligned} \tag{3.24}$$

We can derive fixed points by solving the equation,

$$\frac{dx_1}{dN} = \frac{dx_2}{dN} = \frac{dx_3}{dN} = \frac{d\Omega_b}{dN} = 0, \tag{3.25}$$

and then we are able to analyze the stability of each fixed point using stability analysis in the later topic. The four autonomous equations (3.18) - (3.21) can completely describe the dynamics of this cosmological model in principle.

3.3 Fixed points and stability analysis

3.3.1 Fixed points

In this analysis we concentrate on the evolution of the Universe at late time. The fixed points of the system can be obtained by setting the left hand side of the equations (3.18) - (3.21) to be zero and then solving the resulting algebraic equations.

Potential dominated solution

Now we consider the phase of potential dominated Universe which corresponds to the fixed point $x_1 = 0$ and $x_2 = 1$. Inserting this fixed point into the equation (3.19) we obtain $\lambda_4 = 0$. Setting λ_4 and Ω_b to be zero, thus the equation (3.18) becomes

$$
\begin{aligned}
x_{1,N} =\frac{1}{4}x_{1f}\Bigg[&6(x_{1f}^2 - 2) - \bigg(\sqrt{6}x_{1f}\Big(-\lambda_1 + 36\lambda_3 x_{1f}^3 x_{3f}^2\big(-x_{1f}\lambda_2 + \sqrt{6}(\lambda_3 + 1)\big) \\
&+ 6x_{1f}x_{3f}\big(\sqrt{6}(1 + 3\lambda_3 + 2\lambda_3^2) + x_{1f}\big(-\lambda_2(1 + 2\lambda_3) + \lambda_1(2 + 3\lambda_3)\big)\big)\Big)\bigg) \\
&\times \Big(18x_{1f}^4\lambda_3\,(3\lambda_3 + 1)\,x_{3f}^2 - 3x_{1f}^2\,\big(2\lambda_3^2 + 9\lambda_3 + 3\big)\,x_{3f} + 1\Big)\Bigg] = 0. \quad (3.26)
\end{aligned}
$$

From the above equation, by taking limit $x_{1f} \to 0$, we obtain

$$
\lim_{x_{1f}\to 0}\left(\left.\frac{1}{x_{1f}}\frac{dx_{1f}}{dN}\right|_{x_1=x_{1f},x_2=0,\Omega_b=0}\right) = -3. \quad (3.27)
$$

Then, substituting the above result into the equation (3.20), we get

$$
-6\lambda_3 x_{3f} = 0. \quad (3.28)
$$

This equation suggests that the potential dominated solution can occur in two situations. First situation can occur when the disformal coefficient is much smaller than the conformal coefficient such that $x_{3f} \simeq 0$. Second situation exists when the disformal coefficient does not depend on kinetic energy of the scalar field, in other words $\lambda_3 = 0$.

Scaling and scalar field dominated solution

In this section we consider the case of $x_{1f}^2 + x_{2f} \leq 1$ and both x_{1f} and x_{2f} are not equal to zero. Then $\Omega_d = x_{1f}^2 + x_{2f} \geq 0$ at the fixed point. Let us begin our calculation by setting the equation (3.19) to be zero. We obtain

$$0 = x_{2f}[3(1 - x_{2f} + x_{1f}^2) + \sqrt{6}\lambda_4 x_{1f}]. \tag{3.29}$$

For this case x_{2f} is not zero, then we get

$$0 = 3(1 - x_{2f} + x_{1f}^2) + \sqrt{6}\lambda_4 x_{1f}, \tag{3.30}$$

$$x_{2f} = 1 + \sqrt{\frac{2}{3}}\lambda_4 x_{1f} + x_{1f}^2. \tag{3.31}$$

Inserting the equation (3.31) into the equation (3.20) and using the fact that at the fixed point both $x_{1,N}$ and $x_{3,N}$ are zero, we obtain

$$0 = \sqrt{6}[\lambda_2 - \lambda_1 + \lambda_4(1 + \lambda_3)]x_{1f}x_{3f}. \tag{3.32}$$

One can see that when $x_{3f} \neq 0$, the above equation gives

$$\lambda_2 = \lambda_1 - \lambda_4(1 + \lambda_3). \tag{3.33}$$

The equation (3.32) can also be satisfied when $x_{3f} = 0$, which implies that the disformal coefficient equals to zero at this fixed point. Then, this fixed point is the conformal scaling solution. It can be seen that for the case $x_{3f} \neq 0$, the fixed point corresponds to disformal scaling solution. We will consider the conformal and disformal fixed point in the following topics.

Conformal scaling solutions

In this section we consider the conformal fixed point where the disformal coefficient vanishes at the fixed point, that is $x_{3f} = 0$, but the conformal coefficient is not zero and still depends on the scalar field. So let us start the calculation by substituting the equation (3.31) into the equation (3.18) and setting $x_{3f} = 0$, we

obtain

$$0 = \frac{1}{2} \left[x_{1f} \left(\lambda_4 \lambda_1 - 2(\lambda_4^2 + 3) \right) + \sqrt{6} x_{1f}^2 \left(\lambda_1 - 2\lambda_4 \right) - \sqrt{6} \lambda_4 \right]. \tag{3.34}$$

From the above equation, we obtain the fixed point x_{1f} as

$$x_{1f} = -\frac{\lambda_4}{\sqrt{6}}, \quad \frac{\sqrt{6}}{\lambda_1 - 2\lambda_4}. \tag{3.35}$$

We can solve for fixed point x_{2f} by inserting the equation (3.35) into the equation (3.31), then we obtain

$$x_{2f} = 1 - \frac{\lambda_4^2}{6}, \quad \frac{\lambda_1^2 - 2\lambda_4 \lambda_1 + 6}{(\lambda_1 - 2\lambda_4)^2}. \tag{3.36}$$

From the equations (3.35) and (3.36), we obtain the conformal fixed points as

$$(x_{1f}, x_{2f}, x_{3f}) = \quad (-\tfrac{\lambda_4}{\sqrt{6}}, 1 - \tfrac{\lambda_4^2}{6}, 0), \tag{3.37}$$

$$(x_{1f}, x_{2f}, x_{3f}) = \quad (\tfrac{\sqrt{6}}{\lambda_1 - 2\lambda_4}, \tfrac{\lambda_1^2 - 2\lambda_4 \lambda_1 + 6}{(\lambda_1 - 2\lambda_4)^2}, 0). \tag{3.38}$$

One can see that the first fixed point given in equation (3.37) is the scalar field dominated solution due to $x_{1f}^2 + x_{2f} = 1$. This fixed point does not depend on λ_1 or conformal coupling term. Thus, this fixed point is similar to the field dominated fixed point in quintessence models. However, the stability of this fixed point is different from quintessence models that will be shown in section 3.3.2. The second fixed point given in equation (3.38) is the scaling solution, i.e. $(x_1^2 + x_2)/\Omega_m$ is a non-zero constant. Nevertheless, we note that in our consideration Ω_b vanishes at these fixed points.

Disformal scaling solutions

For this case, we consider fixed points where $x_{3f} \neq 0$ in which the disformal coefficient is not zero, then the equation (3.33) is satisfied. Consequently, these fixed points are disformal scaling solutions. We start to calculate by expressing the density parameter and the equation of state of dark energy in terms of x_{1f} and

x_{2f} at the fixed point as

$$\Omega_{df} = x_{1f}^2 + x_{2f}, \quad \omega_{df} = \frac{x_{1f}^2 - x_{2f}}{x_{1f}^2 + x_{2f}}, \tag{3.39}$$

where Ω_{df} and ω_{df} refer to the density parameter and the equation of state of dark energy at the fixed point respectively. In order to relate the calculation to the observable quantities, we also write x_{1f} and λ_4 in terms of Ω_{df} and ω_{df} by inserting the equation (3.31) into the equation (3.39). We obtain

$$\Omega_{df} = 2x_{1f}^2 + \sqrt{\frac{2}{3}}\lambda_4 x_{1f} + 1, \quad \omega_{df} = \frac{-1 - \sqrt{\frac{2}{3}}\lambda_4 x_{1f}}{2x_{1f}^2 + \sqrt{\frac{2}{3}}\lambda_4 x_{1f} + 1}. \tag{3.40}$$

Solving the above equations for x_{1f} and λ_4, we get

$$x_{1f} = \pm\frac{\sqrt{\Omega_{df}(1 + \omega_{df})}}{\sqrt{2}}, \quad \lambda_4 = \mp\frac{\sqrt{3}(1 + \omega_{df})}{\sqrt{(1 + \omega_{df})\Omega_{df}}}. \tag{3.41}$$

Inserting the above relations into the equation (3.31), we obtain

$$x_{2f} = \frac{1}{2}(1 - \omega_{df})\Omega_{df}. \tag{3.42}$$

It is noticed that we can choose the values of x_{1f}, x_{2f} and λ_4 by fixing Ω_{df} and ω_{df}. Next one, we calculate x_{3f} by inserting the equations (3.31) and (3.33) into the equation (3.18). We obtain the higher order polynomial equation as

$$\begin{aligned}
x_{1,N} = &-\frac{1}{2}\Big(2(\lambda_4^2 + 3)x_1 + 2\sqrt{6}\lambda_4 x_1^2 + \sqrt{6}\lambda_4\Big) \\
&- \frac{1}{4}\bigg[\sqrt{\frac{2}{3}}x_1\Big(\sqrt{6}\lambda_4 + 6x_1\Big)\Big(6x_3\Big(\lambda_4 + \sqrt{\frac{2}{3}}(3 + \gamma^2)x_1 + \lambda_4 x_1^2\Big)(\lambda_3 + 1) \\
&\times \Big(1 + (2 + 6x_3 x_1^2)\lambda_3\Big) + 6x_1^2 x_3(\lambda_4 - \lambda_1 + \lambda_4\lambda_3)\Big(1 + (2 + 6x_3 x_1^2)\Big) \\
&+ \lambda_1\Big(-1 + 6x_1^2 x_3(2 + 3\lambda_3)\Big)\Big)\bigg]\bigg[-x_1 x_3(\sqrt{6}\lambda_4 + 6x_1)(\lambda_3 + 1) \\
&\times \Big(\lambda_3(6x_1^2 x_3 + 2) + 1\Big) + \Big(1 - 6x_1^2\lambda_3 v_5\Big)\Big(1 - 6x_1^2(2\lambda_3 + 1)x_3\Big)\bigg]^{-1} = 0.
\end{aligned} \tag{3.43}$$

From the above equation, we then have a polynomial equation which has degree 2 of x_{3f} and degree 6 of x_{1f}. Therefore, it is difficult to solve this equation for x_{1f}.

For this reason, we will solve this equation for x_{3f} instead of x_{1f}. Consequently, we obtain solutions of x_{3f} as follows

$$x_{3f1} = \frac{1}{6x_1^2 \lambda_3}, \tag{3.44}$$

$$x_{3f2} = \frac{x_1 (2\lambda_4 - \lambda_1) + \sqrt{6}}{6x_1^2 \left(x_1 (4\lambda_4 \lambda_3 + 2\lambda_4 - \lambda_1) + \sqrt{6} (2\lambda_3 + 1) \right)}, \tag{3.45}$$

where x_{3f1} and x_{3f2} are the solutions of the polynomial equation of the fixed point. Substituting x_{1f} and λ_4 from the equation (3.41) into the above equation, we obtain the solutions of x_{3f} as

$$x_{3f1} = \frac{1}{3\lambda_3 \Omega_{df}(1 + \omega_{df})}, \tag{3.46}$$

$$x_{3f2} = \frac{2\omega_{df}\sqrt{3\Omega_{df}} + \lambda_1\sqrt{\omega_{df} + 1}}{3\Omega_{df}(\omega_{df} + 1)\left(2\sqrt{3\Omega_{df}}(2\lambda_3 + 1)\omega_{df} + \lambda_1\sqrt{\omega_{df} + 1}\right)}. \tag{3.47}$$

One can see from the equations (3.31), (3.41), (3.46) and (3.47) that there are two classes for the disformal scaling solutions as shown in Table 1. From the equation (3.46), it is remarkable that $x_{3f1} \to \infty$ when $\lambda_3 \to 0$. This implies that, the fixed point in the class I cannot occur when $\lambda_3 = 0$. In other words, this fixed point does not exist when disformal coefficient does not depend on kinetic terms of scalar field. In contrast, the fixed point in the equation (3.47) can occur when the parameter $\lambda_3 = 0$ discussed in [92]. We will discuss this case later. In the next section, we study linear stability theory and then use this theory to analyze the stability for each fixed point previously obtained from the cosmological dynamical analysis. Consequently, we can explain how the Universe evole and what are phases the Universe passed until present phase by the stability of fixed points.

3.3.2 Linear stability theory

In this section, we will give a brief detail of the linear stability theory. In the context of mathematics, this theory can address the stability of differential equation solutions. In the context of cosmology, this theory can use to analyze the stability of fixed points for each phase of cosmological dynamical system. Let us

Table 1 **The fixed points for the disformal scaling solutions in the fuction of ω_{df} and Ω_{df}. The fixed point class I cannot exist when $\lambda_3 = 0$**

class	x_{1f}	x_{2f}	x_{3f}
I	$\pm \frac{\sqrt{(1+\omega_{df})\Omega_{df}}}{\sqrt{2}}$	$\frac{1}{2}\left(1-\omega_{df}\right)\Omega_{df}$	x_{3f1}
II	$\pm \frac{\sqrt{(1+\omega_{df})\Omega_{df}}}{\sqrt{2}}$	$\frac{1}{2}\left(1-\omega_{df}\right)\Omega_{df}$	x_{3f2}

begin to study the linear stability theory by defining dynamical system in term of autonomous equation as $\dot{\mathbf{x}} = \mathbf{f}(\mathbf{x})$ where $\mathbf{f}(\mathbf{x}) = (f_1(x), ..., f_n(x))$. Using Taylor expansion around fixed point $\mathbf{x_0}$, we obtain

$$f_i(\mathbf{x}) = f_i(\mathbf{x}_0) + \sum_{j=1}^{n} \frac{\partial f_i}{\partial x_j}(\mathbf{x}_0)y_j + \frac{1}{2!}\sum_{j,k=1}^{n} \frac{\partial^2 f_i}{\partial x_j \partial x_k}(\mathbf{x}_0)y_j y_k + ..., \qquad (3.48)$$

where $\mathbf{y} = \mathbf{x} - \mathbf{x}_0$. Here, we consider only the first order partial derivative. Consequently, we obtain the Jacobian matrix of function $\mathbf{f}(\mathbf{x})$ as

$$J = \frac{\partial f_i}{\partial x_j}\bigg|_{\mathbf{x}=\mathbf{x}_0} = \begin{bmatrix} \frac{\partial f_1}{\partial x_1}\big|_{\mathbf{x}=\mathbf{x}_0} & \cdots & \frac{\partial f_1}{\partial x_n}\big|_{\mathbf{x}=\mathbf{x}_0} \\ \frac{\partial f_2}{\partial x_1}\big|_{\mathbf{x}=\mathbf{x}_0} & \cdots & \frac{\partial f_2}{\partial x_n}\big|_{\mathbf{x}=\mathbf{x}_0} \\ \vdots & \ddots & \vdots \\ \frac{\partial f_n}{\partial x_1}\big|_{\mathbf{x}=\mathbf{x}_0} & \cdots & \frac{\partial f_n}{\partial x_n}\big|_{\mathbf{x}=\mathbf{x}_0} \end{bmatrix}. \qquad (3.49)$$

The equation (3.49) contains the information about the stability of the system. Moreover, in the context of cosmology J can be used to determine the stability of the system. However, the linear stability theory cannot use to determine the stability of the system when the Jocobian matrix J equal to zero. For the case $J = 0$, the stability of the dynamical systems can be determined by changing variable, Lyapunov stability, centre manifold theory and etc. [93]. Although, we will consider this case in later topic.

Now, we consider a simple example of two dimensional dynamical system before returning to more complex cosmological dynamical system. Consider the

Table 2 The stability of the two dimensional dynamical system.

Eigenvalues	Explanation
$\mu_1 > 0, \mu_2 > 0$	unstable fixed point
$\mu_1 < 0, \mu_2 < 0$	stable fixed point
$\mu_1 < 0, \mu_2 > 0$	saddle fixed point
$\mu_1 > 0, \mu_2 < 0$	saddle fixed point

simple autonomous system given by

$$\dot{x}_1 = g(x_1, x_2), \tag{3.50}$$

$$\dot{x}_2 = h(x_1, x_2), \tag{3.51}$$

where g and h are functions of x_1 and x_2. At the fixed points (x_{10}, x_{20}) of the system $g(x_1, x_2)$ and $h(x_1, x_2)$ are equal to zero, that is

$$g(x_{10}, x_{20}) = 0, \quad \text{and} \quad h(x_{10}, x_{20}) = 0. \tag{3.52}$$

The Jacobian matrix of this system is given by

$$J_2 = \begin{bmatrix} \frac{\partial g}{\partial x_1} & \frac{\partial g}{\partial x_2} \\ \frac{\partial h}{\partial x_1} & \frac{\partial h}{\partial x_2} \end{bmatrix} = \begin{bmatrix} g_{,x_1} & g_{,x_2} \\ h_{,x_1} & h_{,x_2} \end{bmatrix}, \tag{3.53}$$

where J_2 is a 2×2 matrix. Thus, J_2 has 2 eigenvalues for this system that is $\mu_{1,2}$ as follows

$$\mu_1 = \frac{1}{2}(g_{,x_1} + h_{,x_2}) + \frac{1}{2}\sqrt{(g_{,x_1} - h_{,x_2})^2 + 4g_{x_2}h_{,x_1}}, \tag{3.54}$$

$$\mu_2 = \frac{1}{2}(g_{,x_1} + h_{,x_2}) - \frac{1}{2}\sqrt{(g_{,x_1} - h_{,x_2})^2 + 4g_{x_2}h_{,x_1}}. \tag{3.55}$$

The stability of the system depends on the values of eigenvalue. We express some possible cases and give a short explanation for each case in Table 2. In the next section, we use the linear stability theory to analyze each fixed point which is obtained from the previous section.

Potential dominated

The potential dominated fixed point corresponds to $(x_{1f}, x_{2f}) = (0, 1)$, $\lambda_1 = \lambda_4 = \Omega_b = 0$. As mentioned above and from the equation (3.49), we obtain the Jacobian matrix for the potential dominated fixed point as

$$J = \begin{bmatrix} \frac{\partial x_{1,N}}{\partial x_1} & \frac{\partial x_{1,N}}{\partial x_2} & \frac{\partial x_{1,N}}{\partial x_3} & \frac{\partial x_{1,N}}{\partial \Omega_b} \\ \frac{\partial x_{2,N}}{\partial x_1} & \frac{\partial x_{2,N}}{\partial x_2} & \frac{\partial x_{2,N}}{\partial x_3} & \frac{\partial x_{2,N}}{\partial \Omega_b} \\ \frac{\partial x_{3,N}}{\partial x_1} & \frac{\partial x_{3,N}}{\partial x_2} & \frac{\partial x_{3,N}}{\partial x_3} & \frac{\partial x_{3,N}}{\partial \Omega_b} \\ \frac{\partial \Omega_{b,N}}{\partial x_1} & \frac{\partial \Omega_{b,N}}{\partial x_2} & \frac{\partial \Omega_{b,N}}{\partial x_3} & \frac{\partial \Omega_{b,N}}{\partial \Omega_b} \end{bmatrix} = \begin{bmatrix} -3 & 0 & 0 & 0 \\ 0 & -3 & 0 & 0 \\ 0 & -3(-1 + 36x_3) & -6 & -108x_3^2 \\ 0 & 0 & 0 & -3 \end{bmatrix}.$$
(3.56)

From the above Jacobian matrix, we have four eigenvalues as follows

$$\mu_1 = -3, \quad \mu_2 = -3,$$

$$\mu_3 = -6, \quad \mu_4 = -3.$$
(3.57)

Then, the potential dominated solution is stable at fixed point because the all eigenvalues of the Jacobian matrix (3.57) are negative. This suggests that the Universe can evolve from other phase which is unstable or saddle phase to the stable phase of the potential dominated epoch.

Conformal scaling solutions

For the case of conformal scaling solutions, disformal coefficient vanishes $(D = 0)$ at the fixed points. This case we neglect the contributions for radiation. Once again, we write the eigenvalues of the fixed points in terms of density parameter Ω_{df} and the equation of state ω_{df} to reduce the complexity of the system. In order to calculate the stability of these fixed points, we begin the calculation by inserting the conformal fixed points from the equations (3.37) and (3.38) into the equation (3.39). Then we respectively get

$$\Omega_{df} = 1, \qquad \omega_{df} = \frac{\lambda_4^2}{3} - 1,$$
(3.58)

$$\Omega_{df} = \frac{\lambda_1^2 - 2\lambda_4\lambda_1 + 12}{(\lambda_1 - 2\lambda_4)^2}, \qquad \omega_{df} = -\frac{\lambda_1(\lambda_1 - 2\lambda_4)}{\lambda_1^2 - 2\lambda_4\lambda_1 + 12}.$$
(3.59)

The equation (3.58) for the fixed point in the equation (3.37) and the equation (3.59) for the fixed point in the equation (3.38). Solving the above equations for λ_1 and λ_4, we respectively obtain

$$\lambda_4 = \mp \sqrt{3(1 + \omega_{df})}, \quad \text{for the equation (3.58),} \tag{3.60}$$

$$\lambda_1 = \mp \frac{2\omega_{df}\sqrt{3\Omega_{df}}}{\sqrt{1 + \omega_{df}}}, \quad \lambda_4 = \mp \frac{\sqrt{3}(1 + \omega_{df})}{\sqrt{1 + \omega_{df}}\Omega_{df}}, \quad \text{for the equation (3.59).} \tag{3.61}$$

From the autonomous equations (3.18) - (3.20) and the equation (3.49), we obtain the Jacobian matrix for the conformal scaling solutions as

$$J = \begin{bmatrix} \frac{\partial x_{1,N}}{\partial x_1} & \frac{\partial x_{1,N}}{\partial x_2} & 0 & \frac{\partial x_{1,N}}{\partial \Omega_b} \\ 0 & \frac{\partial x_{2,N}}{\partial x_2} & 0 & 0 \\ 0 & 0 & \frac{\partial x_{3,N}}{\partial x_3} & \frac{\partial x_{3,N}}{\partial \Omega_b} \\ 0 & 0 & 0 & \frac{\partial \Omega_{b,N}}{\partial \Omega_b} \end{bmatrix}. \tag{3.62}$$

In order to determine eigenvalues for the conformal scaling solutions, we set $x_3 = 0$ and insert the equations (3.37) and (3.60) into the above Jacobian matrix. We have

$$J = \begin{bmatrix} 3\omega_{df} + \frac{\lambda_1}{2}\sqrt{3\alpha} & \frac{\sqrt{3}}{2\sqrt{2}}(\sqrt{3}\alpha + \lambda_1) & 0 & \frac{\sqrt{3}}{2\sqrt{2}}\lambda_1 \\ 0 & -\frac{3}{2}\alpha & 0 & 0 \\ 0 & 0 & -\sqrt{3\alpha}\left(\lambda_1 - \lambda_2 + \sqrt{3\alpha}(\lambda_3 + 1)\right) & 0 \\ 0 & 0 & 0 & 3\omega_{df} \end{bmatrix}, \tag{3.63}$$

where $\alpha = 1 + \omega_{df}$. We then obtain the eigenvalues for the conformal fixed point given in equation (3.37) as

$$\mu^+ = \left(3\omega_{df}, \frac{3(\omega_{df} - 1)}{2}, 3\omega_{df} + \frac{\lambda_1}{2}\sqrt{3\alpha},\right.$$
$$\left.\sqrt{\alpha}\left(\sqrt{3}(\lambda_2 - \lambda_1) - 3(1 + \lambda_3)\sqrt{\alpha}\right)\right), \tag{3.64}$$

$$\mu^- = \left(3\omega_{df}, \frac{3(\omega_{df} - 1)}{2}, 3\omega_{df} - \frac{\lambda_1}{2}\sqrt{3\alpha},\right.$$
$$\left.\sqrt{\alpha}\left(\sqrt{3}(\lambda_1 - \lambda_2) - 3(1 + \lambda_3)\sqrt{\alpha}\right)\right). \tag{3.65}$$

Similarly to the previous calculation, we set $x_3 = 0$ and insert the equations (3.38) and (3.61) into the Jacobian matrix given by equation (3.62). Then we obtain the

eigenvalues for the conformal fixed point given in equation (3.38) as follows

$$\mu^+ = \left(3\Omega_{df}\omega_{df}, \frac{3}{4}\left(\Omega_{df}\omega_{df} - 1 - \sqrt{\frac{\alpha\beta\omega_{df} - \gamma - 7}{\alpha}}\right),\right.$$

$$\frac{3}{4}\left(\Omega_{df}\omega_{df} - 1 + \sqrt{\frac{\alpha\beta\omega_{df} - \gamma - 7}{\alpha}}\right),$$

$$\left.\lambda_2\sqrt{3\Omega_{df}\alpha} - 3\lambda_3\left(1 - \Omega_{df}\omega_{df} + \lambda_3(1 + \Omega_{df}\omega_{df})\right)\right), \qquad (3.66)$$

$$\mu^- = \left(3\Omega_{df}\omega_{df}, \frac{3}{4}\left(\Omega_{df}\omega_{df} - 1 - \sqrt{\frac{\alpha\beta\omega_{df} - \gamma - 7}{\alpha}}\right),\right.$$

$$\frac{3}{4}\left(\Omega_{df}\omega_{df} - 1 + \sqrt{\frac{\alpha\beta\omega_{df} - \gamma - 7}{\alpha}}\right),$$

$$\left.- \lambda_2\sqrt{3\alpha\Omega_{df}} - 3\lambda_3\left(1 - \Omega_{df}\omega_{df} + \lambda_3(1 + \Omega_{df}\omega_{df})\right)\right), \qquad (3.67)$$

where $\beta = 9 + \Omega_{df}^2$ and $\gamma = 2\Omega_{df}(\omega_{df}^2 + 5\omega_{df} - 4)$. The stabilities of the fixed point in equations (3.37) and (3.38) have been already discussed in literature [94, 95]. Therefore, we are not going to discuss in detail here. However, the main conclusion can be summarize using equation (3.61) as following consideration.

For the conformal scaling solutions, we have $x_{1f} \neq 0$, so that $\omega_{df} > -1$ and then $\lambda_4 \neq 0$ as follows from the equation (3.60). This equation also suggests that the potential dominated fixed point, which corresponds to $\omega_d = -1$, occur when $\lambda_4 = 0$. We note that this fixed point describes de-Sitter expansion.

For the case $\lambda_4 < 0$, $\lambda_1 < \frac{-6\omega_{df}}{\sqrt{3(1+\omega_{df})}}$ and the values of λ_2 and λ_3 are chosen suitably, for example $\lambda_2 \sim \lambda_3 \sim \mathcal{O}(1)$, the Universe can evolve to the stable fixed point $(\omega_d, \Omega_d) = (\omega_{df}, 1)$ at late time. For the case $\lambda_4 > 0$, when $\lambda_1 > \frac{6\omega_{df}}{\sqrt{3(1+\omega_{df})}}$ the Universe evolve to the stable fixed point which is $(\omega_d, \Omega_d) = (\omega_{df}, 1)$.

Disformal scaling solutions

For the case of disformal fixed points, the fixed points can occur only when $x_{3f} \neq 0$ or $D \neq 0$. For this case, we set $\Omega_b = 0$. Then, determinant of the matrix

J for the disformal scaling solutions can be expressed as

$$
\begin{aligned}
\det J ={} & \frac{\partial x_{1,N}}{\partial x_3}\Big[3(1+\lambda_3)(\sqrt{6}\lambda_4 + 6x_{1f})x_{1f}x_{2f} + \Big(9x_{1f}^2(1+\lambda_3) \\
& + 2\sqrt{6}x_{1f}(\lambda_1 - \lambda_2) - 3(1+\lambda_3)(x_{2f}-1)\Big) \\
& \times \Big(\sqrt{6}\lambda_4 x_{1f} + 3x_{1f}^2 - 6x_{2f} + 3\Big)\Big]x_{3f}\,.
\end{aligned}
\tag{3.68}
$$

Inserting the fixed points from Table 1 into the above equation we obtain $J = 0$ for all fixed points. This suggests that one or more of the eigenvalues for each fixed points are zero. Consequently, we cannot use the linear stability theory to analyze the stability of the system for these fixed points. Fortunately, for the disformal fixed points, we have relation betweens λ_2 and $\lambda_1, \lambda_3, \lambda_4$ which is shown in the equation (3.33). From this relation, we can write x_3 in terms of x_1 and x_2 by using the relation in the equation (3.33), and the dimensionless variable in equation (3.13). We have

$$
\begin{aligned}
x_{3f} ={} & \frac{D\mathcal{H}^2}{a^2 C}\,, \\
x_{2f}x_{3f} ={} & \frac{D(\phi)V(\phi)}{C(\phi)} = \frac{D_0 e^{\lambda_2\phi}X^{\lambda_3}V_0 e^{\lambda_4\phi}}{3C_0 e^{\lambda_1\phi}} \\
={} & \frac{D_0 V_0 X^{\lambda_3}e^{(\lambda_2-\lambda_1+\lambda_4)\phi}}{3C_0} = \frac{D_0 V_0}{3C_0}X^{\lambda_3}e^{-\lambda_3\lambda_4\phi} \\
={} & \frac{D_0 V_0}{3C_0}\left(\frac{X}{e^{\lambda_4\phi}}\right)^{\lambda_3} = \frac{D_0 V_0^{1+\lambda_3}}{3C_0}\left(\frac{X}{V(\phi)}\right)^{\lambda_3}\,.
\end{aligned}
\tag{3.69}
$$

Using $X = \phi'^2/2a^2$ and define $r_0 = D_0 V_0^{1+\lambda_3}/3C_0$, we obtain

$$
\begin{aligned}
x_{2f}x_{3f} ={} & r_0\left(\frac{\phi'^2/2a^2}{3\mathcal{H}^2 x_{2f}/a^2}\right)^{\lambda_3} = r_0\left(\frac{\phi'^2}{6\mathcal{H}^2 x_{2f}}\right)^{\lambda_3} \\
={} & r_0\left(\frac{x_{1f}^2}{x_{2f}}\right)^{\lambda_3}\,,
\end{aligned}
\tag{3.70}
$$

$$
x_{3f} = r_0\frac{x_{1f}^{2\lambda_3}}{x_{2f}^{1+\lambda_3}}\,.
\tag{3.71}
$$

One can see that r_0 is a constant and controls magnitude of x_{3f} for a given value of x_{1f} and x_{2f}. Therefore, number of independent dimensionless variables or dimensions of phase space of this system reduced to two consisting of x_1 and x_2. Now we discuss the disformal fixed points in this two dimensional phase space.

Substituting the relations in equations (3.33) and (3.71) into the equation (3.18), we obtain a long polynomial equation as follows

$$
\begin{aligned}
x_{1f,N} =\frac{1}{4}\Bigg[& -\sqrt{\frac{2}{3}}x_{1f}(\sqrt{6}\lambda_4 + 6x_{1f})\Big(6\lambda_3 + r_0\Big(\sqrt{\frac{2}{3}}(\lambda_4^2+3)x_{1f} + \lambda_4 x_{1f}^2 + \lambda_4\Big)x_{1f}^{2\lambda_3} \\
& \times\Big(\sqrt{\frac{2}{3}}\lambda_4 x_{1f} + x_{1f}^2 + 1\Big)^{-(\lambda_3+1)}\Big(\lambda_3\Big(6r_0 x_{1f}^{2\lambda_3+2}(\sqrt{\frac{2}{3}}\lambda_4 x_{1f} + x_{1f}^2 + 1)^{-(\lambda_3+1)} \\
& +2\Big)+1\Big) - 6r_0\Big(\lambda_1 - (\lambda_3+1)\lambda_4\Big)x_{1f}^{2\lambda_3+2}\Big(\sqrt{\frac{2}{3}}\lambda_4 x_{1f} + x_{1f}^2 + 1\Big)^{-(\lambda_3+1)} \\
& \times(\lambda_3(6r_0 x_{1f}^{2\lambda_3+2}\Big(\sqrt{\frac{2}{3}}\lambda_4 x_{1f} + x_{1f}^2 + 1\Big)^{-(\lambda_3+1)} + 2) + 1) + \lambda_1\Big(6(3\lambda_3+2) \\
& \times r_0 x_{1f}^{2\lambda_3+2}\Big(\sqrt{\frac{2}{3}}\lambda_4 x_{1f} + x_{1f}^2 + 1\Big)^{-(\lambda_3+1)} - 1\Big)\Big(\Big(1 - 6\lambda_3 r_0 x_{1f}^{2\lambda_3+2} \\
& \times\Big(\sqrt{\frac{2}{3}}\lambda_4 x_{1f} + x_{1f}^2 + 1\Big)^{-(\lambda_3+1)}\Big)(1 - 6(2\lambda_3+1)r_0 x_{1f}^{2\lambda_3+2} \\
& \times\Big(\sqrt{\frac{2}{3}}\lambda_4 x_{1f} + x_{1f}^2 + 1\Big)^{-(\lambda_3+1)}) - (\lambda_3+1)r_0(\sqrt{6}\lambda_4 + 6x_{1f})x_{1f}^{2\lambda_3+1} \\
& \Big(\sqrt{\frac{2}{3}}\lambda_4 x_{1f} + x_{1f}^2 + 1\Big)^{-(\lambda_3+1)}\Big(\lambda_3(6r_0 x_{1f}^{2\lambda_3+2}\Big(\sqrt{\frac{2}{3}}\lambda_4 x_{1f} + x_{1f}^2 + 1\Big)^{-(\lambda_3+1)} \\
& +2) + 1)\Big)^{-1} - 2\Big(2(\lambda_4^2+3)x_{1f} + 2\sqrt{6}\lambda_4 x_{1f}^2 + \sqrt{6}\lambda_4\Big)\Big)\Bigg] = 0\,. \quad (3.72)
\end{aligned}
$$

It is noticed that, the highest degree of x_{1f} in the above equation is $6 + 4\lambda_3$. Since it is quite difficult to solve this polynomial equation for x_{1f}, we should solve this equation for r_0 instead of x_{1f}. However, in order to connect our results with the observational bound, we express r_0 in terms of Ω_{df} and ω_{df} by inserting the equation (3.41) into the equation (3.18). In such a way, we obtain

$$
r_0 = r_{01} = \frac{1}{6\lambda_3}\Big(\frac{1-\omega_{df}}{1+\omega_{df}}\Big)^{1+\lambda_3}, \quad (3.73)
$$

$$
r_0 = r_{0\pm} = \frac{1}{2\sqrt{3}}\Big(\frac{1-\omega_{df}}{1+\omega_{df}}\Big)^{1+\lambda_3} \times \frac{\lambda_1\sqrt{1+\omega_{df}} \pm 2\omega_{df}\sqrt{3\Omega_{df}}}{\lambda_1\sqrt{3(1+\omega_{df})} \pm 6(2\lambda_3+1)\omega_{df}\sqrt{\Omega_{df}}}. \quad (3.74)
$$

From the above equations, the fixed points in Table 1 can be expressed in terms of r_0 as shown in Table 3. It is noticed that when $\lambda_3 = 0$ the fixed points in the class II reduce to the fixed point in [96].

The fixed points in this case is quite complicate to perform the direct

Table 3 This table shows the fixed points of disformal scaling solutions in term of the observable parameters ω_d and Ω_d model which is separated into two class.

class	x_{1f}	x_{2f}	r_0
I^+	$\dfrac{\sqrt{(1+\omega_{df})\Omega_{df}}}{\sqrt{2}}$	$\dfrac{1}{2}\left(1 - \omega_{df}\right)\Omega_{df}$	r_{01}
I^-	$-\dfrac{\sqrt{(1+\omega_{df})\Omega_{df}}}{\sqrt{2}}$	$\dfrac{1}{2}\left(1 - \omega_{df}\right)\Omega_{df}$	r_{01}
II^+	$\dfrac{\sqrt{(1+\omega_{df})\Omega_{df}}}{\sqrt{2}}$	$\dfrac{1}{2}\left(1 - \omega_{df}\right)\Omega_{df}$	r_{0+}
II^-	$-\dfrac{\sqrt{(1+\omega_{df})\Omega_{df}}}{\sqrt{2}}$	$\dfrac{1}{2}\left(1 - \omega_{df}\right)\Omega_{df}$	r_{0-}
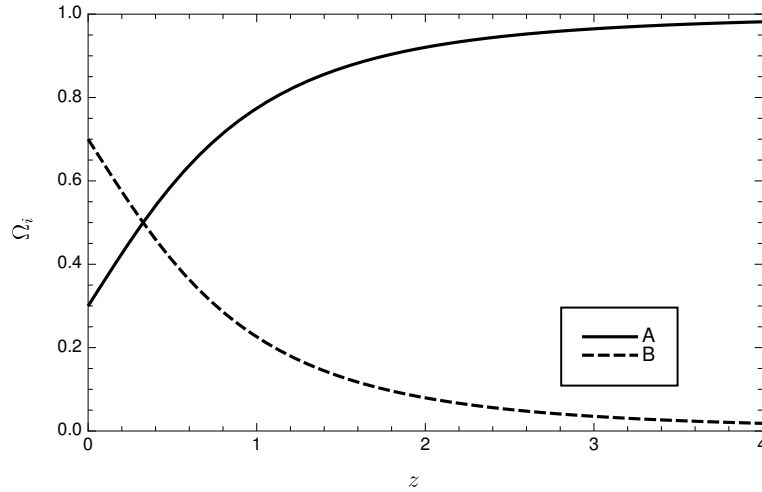
Figure 1 This figure shows the evolutions of dark matter and dark energy density parameters from the past to the present epoch which is computed from the ΛCDM model. Line A is the density parameter of the dark matter and line B is the density parameter of the dark energy

stability analysis analytically. Hence, we will operate the stability analysis by using numerical analysis instead of analytical analysis and show the regions of the stable and unstable of the fixed points which correspond to the observable parameters $(\Omega_{df}, \omega_{df})$. However, before going to the stability analysis, in order to compare our analysis with the standard model of cosmology, we show a plots of the evolution of the matter energy density parameter Ω_m and dark energy density parameter Ω_d from the ΛCDM model in Figure 1. This figure shows the value of Ω_m drops down from 1 to 0.3 and the value of Ω_d increases from ~ 0 to ~ 0.7 from the past to the present day and value of ω_d is ~ -0.99 from the past to present day. The

Figure 2 **The regions I** $(\lambda_3, \lambda_1) = (1, 100)$ **and II** $(\lambda_3, \lambda_1) = (20, 1)$ **are the stable regions of the fixed points for the class I$^+$. The fixed point is saddle out side these regions.**

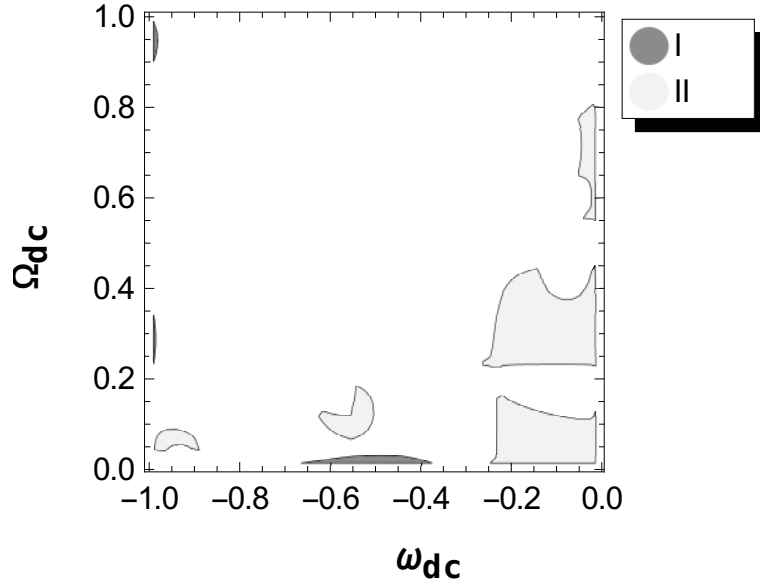standard model of cosmology (ΛCDM model) and the cosmological observations [97] suggest that the values of dark energy density parameter and the equation of state parameter are $(\Omega_d, \omega_d) \sim (0.69, -0.99)$. We use these values to connect our analysis with the observational bound by setting (Ω_d, ω_d) of the fixed point to be $\sim (0.69, -0.99)$.

Now, we analyze the case of the phase space which is dimension reduces to two by a relation given in equation (3.71) called *reduced phase space*. There exist two classes of the fixed points as shown in table 3. To perform stability analysis, we first linearlize the equation (3.72) and (3.19) around the fixed point and then compute corresponding eigenvalues. However, the expressions for the eigenvalues are very complicate. Thus, we evaluate the values of the eigenvalues numerically by inserting the numerical values of parameters and fixed points from Table 3 into the analytic expression of the eigenvalues. For the fixed points in class I, the fixed points are saddle and covers for entire region of the values of $-1 < \omega_{df} < 0$ and $0 < \Omega_{df} < 1$ when $\lambda_1 = \lambda_3 = 1$ (this class cannot exist when $\lambda_3 = 0$). We have shown the stable region for the class I$^+$ from the Table 3 in the $\Omega_{df} - \omega_{df}$ plane in Figure 2. For this plot, we use the values of $(\lambda_3, \lambda_1) = (1, 100)$ and $(20, 1)$. The regions I and II shown in Figure 2 are stable. However, the fixed points are saddle
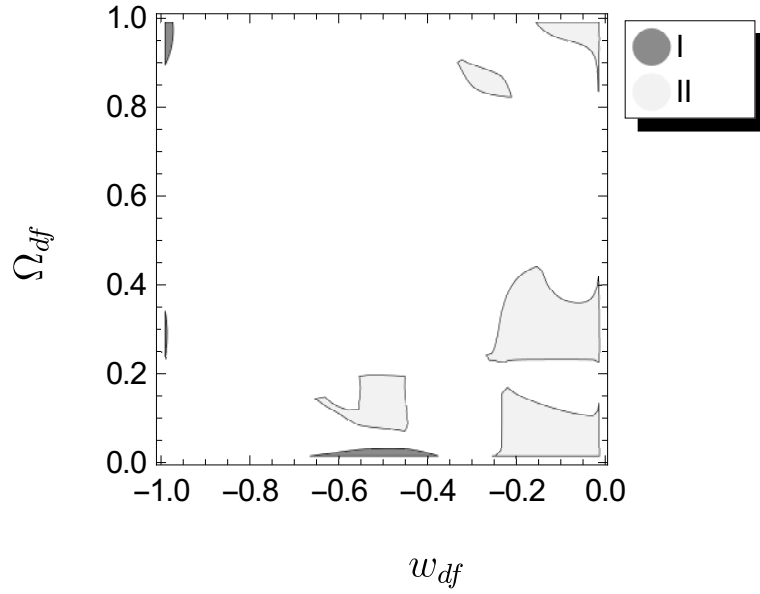
Figure 3 The regions I and II are the stable regions of the fixed points for the class I⁻. The fixed point is saddle out side these regions.

out side these regions. Similarly as class I⁺, we show the stable regions for the class I⁻ in Figure 3 and we set the values of $(\lambda_3, \lambda_1) = (1, 500)$ for region I and $(\lambda_3, \lambda_1) = (20, 1)$. The regions I and II in Figure 3 represent the regions of stable fixed points, so that the fixed points become saddle points out side these regions. According to the Figures 2 and 3, if λ_1 is large enough, the fixed points stable within the region $\Omega_{df} \in [0.7, 1)$ and $\omega_{df} \in (-0.99, -0.97)$.

Now we consider the case $\lambda_3 = 0$ which corresponds to the fixed points in class II. This class consists of two cases of the fixed points which are class II⁺ and II⁻. We consider class II⁺ which is saddle fixed point. We use the numerical calculation to perform the stability analysis and show the saddle regions in Figure 4. The saddle regions of this class are increasing when λ_1 increases. This figure shows the regions I, II and III which are saddle regions and set the values of $(\lambda_1, \lambda_3) = (2, 0), (5, 0), (10, 0)$. The fixed points are stable outside these regions and become saddle points within the region $\Omega_{df} \in [0.7, 1)$ and $\omega_{df} \in (-0.99, -0.97)$ when $\lambda_1 \gg 1$ and $\lambda_3 \gg 1$. The entire region II overlaps with a part of region III and the whole of region I overlaps with a part of region II.

Now we consider the case of $\lambda_3 \neq 0$, this case cannot exist for the fixed point in class I but occurs for the fixed points class II. We use the numerical method
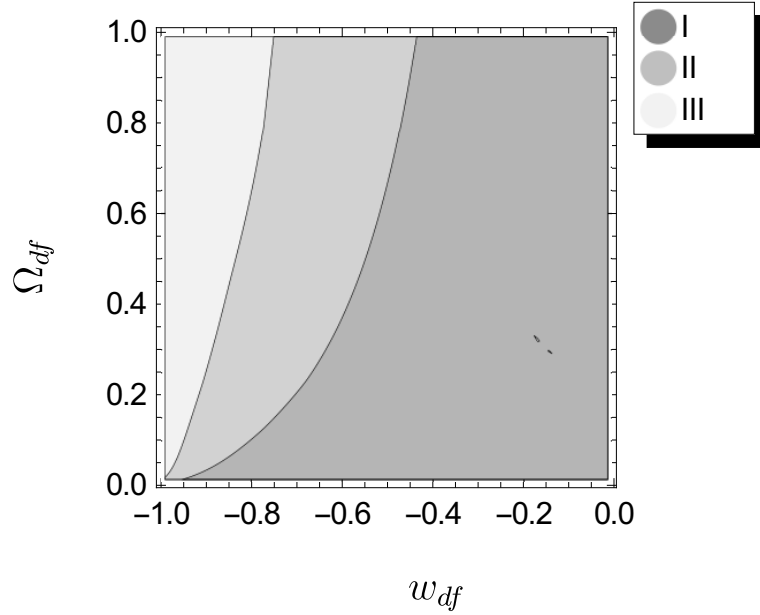
Figure 4 This figure show the saddle regions I, II and III of the fixed point class II$^+$. Out side these regions the fixed point is stable. In this numerical we have used $(\lambda_1, \lambda_3) = (2,0), (5,0), (10,0)$

to perform stability analysis for the fixed points class II$^+$ and II$^+$. Fixed points in this class are stable for a wide range of λ_1 when $-1 < \omega_{df} < 0$ and $0 < \Omega_{df} < 1$. Figures 5 and 6 show regions I, II and III which are saddle points. For these figure we set the values of $(\lambda_3, \lambda_1) = (1,1), (1,5), (5,1)$. It can be seen in the figures that the fixed points are stable outside these regions. For this case the same values of $\lambda_1, \lambda_2, \lambda_3$ can lead to different stable fixed points at late time.

Again, we consider for the case $\lambda_3 = 0$ the equation (3.74) becomes

$$r_{0\pm} = \frac{1 - \omega_{df}}{6(1 + \omega_{df})}. \tag{3.75}$$

One can see that, $r_{0\pm}$ or x_{3f} takes a single value for a given value of ω_{df}. From the equations (3.40) and (3.41) and a fixed value of λ_4, we obtain

$$\sqrt{\Omega_{df}} = \begin{cases} \dfrac{\lambda_4^2(\omega_{df}+1) + \sqrt{\lambda_4^2(\omega_{df}+1)\left(\lambda_4^2(\omega_{df}+1) - 12\omega_{df}\right)} - 6\omega_{df}}{6\omega_{df}^2} & \text{for negative } \lambda_4, \\[4mm] -\dfrac{-\lambda_4^2(\omega_{df}+1) + \sqrt{\lambda_4^2(\omega_{df}+1)\left(\lambda_4^2(\omega_{df}+1) - 12\omega_{df}\right)} + 6\omega_{df}}{6\omega_{df}^2} & \text{for positive } \lambda_4. \end{cases} \tag{3.76}$$

It is noticed that, Ω_{df} depends on λ_4 and takes a single value for a given λ_4 where $\omega_{df} = 0$. Nevertheless, the equation (3.76) shows that when $\omega_{df} \neq 0$, Ω_{df}

Figure 5 The regions I, II and III are the saddle regions of the fixed point for the class II$^+$. The fixed point is stable out side these regions.

exists two possible values for a given value of λ_4. One of the possible value of Ω_{df} is positive whilst another one is negative. We noticed that, λ_4 is a real value when $-1 < \omega_{df} < 0$. In addition, if $0 < \omega_{df} < 1$ and the values of λ_4 and ω_{df} are chosen as same as the first value of Ω_{df}, the value of Ω_{df} will be larger than one. Thus, for a given value of $\lambda_1, \lambda_2, \lambda_4$ and r_0 the only one fixed point lies inside the physical phase space when $\lambda_3 \neq 0$. Using similar analysis for the case where $\lambda_3 = 0$ and $-1 < \omega_{df} < 1$, the fixed points in the class I can takes a single physically relevant value for a given $\lambda_1, \lambda_2, \lambda_4$ and r_0.

For the fixed points class II, the equation which expresses the relation between ω_{df} and the parameters of the model $\lambda_1, \lambda_3, \lambda_4$ and r_0, can be computed by writing Ω_{df} in the equation (3.74) in terms of ω_{df} using the equations (3.41).
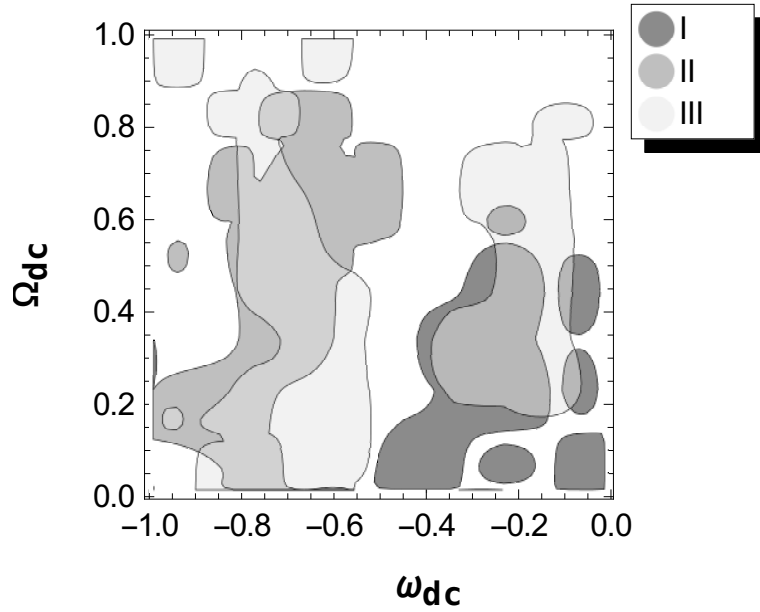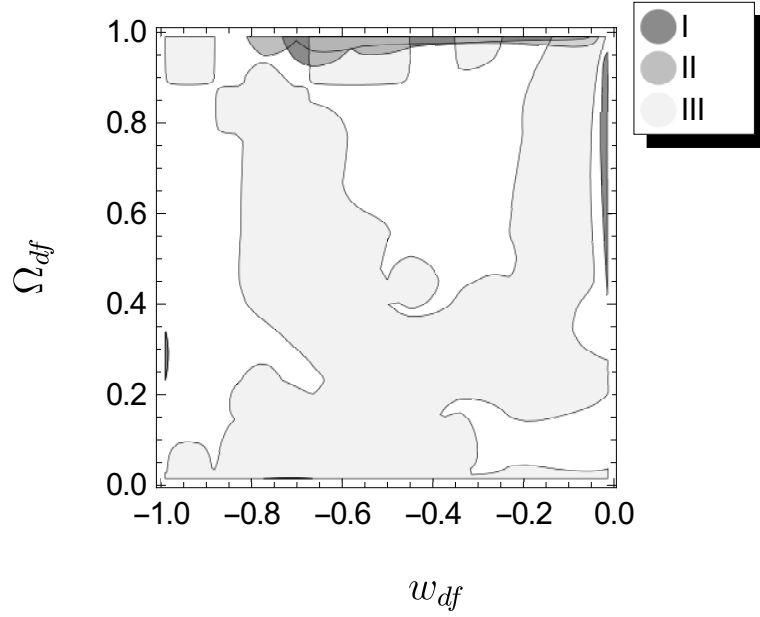
Figure 6 **The regions I, II and III are the saddle regions of the fixed points for the class II⁻. The fixed point is stable out side these regions.**

The result is

$$
\begin{aligned}
E_{w_{df}} =&\sqrt{3}\Big[(1-\omega_{df})^{2(1+\lambda_3)}\Big(12\omega_{df}+\lambda_1^2(1+\omega_{df})-2\lambda_1\lambda_4(1+\omega_{df})\Big) \\
&+36r_0^2(1+\omega_{df})^{2(1+\lambda_3)}\Big(12(1+2\lambda_3)^2\omega_{df}+\lambda_1^2(1+\omega_{df}) \\
&-2\lambda_1\lambda_4(1+2\lambda_3)(1+\omega_{df})\Big)-12r_0(1-\omega_{df}^2)^{1+\lambda_3}\Big(\lambda_1^2(1+\omega_{df}) \\
&-2\lambda_1\lambda_4(1+\lambda_3)(1+\omega_{df})+12\omega_{df}(1+2\lambda_3)\Big)\Big]=0\,.
\end{aligned}
\tag{3.77}
$$

The values of ω_{df} which correspond to $E_{w_{df}}=0$ are the value of the ω_d at the fixed point for a given value of $\lambda_1,\lambda_3,\lambda_4$ and r_0. We first choose the value of ω_{df} and Ω_{df} according to the observational bound, and select values of λ_1 and λ_3 to compute λ_4 and r_0 from the equations (3.41) and (3.74). Substituting the selected value of λ_1 and λ_3 and the computed value of λ_4 and r_0 into the equation (3.77), we see that $E_{w_{df}}=0$ can be satisfied by the value ω_{df} other than the value of Ω_{df} that is chosen at first time from the observational bound. This suggests that for the fixed points class II, the same value of the parameters of the model can yield two stable physically relevant fixed points.

In the Figures (7) and (8), we plot the equation (3.77) where r_0 and λ_4

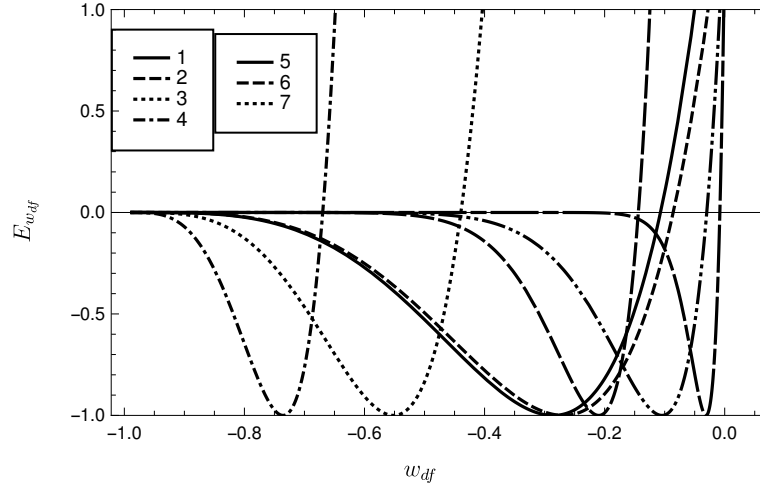**Figure 7** The plot show $E_{w_{df}}$ from the equation (3.77) be a function of w_{df} **for the fixed points class II$^+$. For lines 1 - 7, we set** $(\lambda_1, \lambda_3) = (1,1),(1,1),(5,1),(10,1),(5,5),(1,5)$ **and** $(1,20)$ **respectively.**

are calculated from the equation of state of dark energy $\omega_{df} = \omega_{df}^* = -0.99, -0.98$ and $\Omega_{df} = \Omega_{df}^* = 0.9$. The plots show that the values of ω_{df} are in a range $\omega_{df} = \omega_{df}^s \in (-0.98, 0.15)$. In the cases of $\lambda_1 \sim \mathcal{O}(1)$ and $\lambda_3 \sim \mathcal{O}(1)$, $\omega_{df}^s \in (0, 0.15)$ for the fixed points in the class II$^+$ and $\omega_{df}^s \in (-0.98, 0)$ for the fixed points in the class II$^-$. Inserting ω_{df}^s into the equation (3.41), we obtain the values of Ω_{df} associated with ω_{df}^s. The values of Ω_{df} lies within the range between 0 to 1. Using the stability analysis mentioned above, we have found that both of the fixed points are stable fixed points. This suggests that in the case of $\lambda_3 > 0$, the fixed points class II$^+$ and II$^-$ can take two different physically relevant values and both fixed points are stable for same values of the parameters of the model.

We now consider Figures 7 and 8 which refer to the fixed points class II$^+$ and II$^-$. For $E_{\omega_{df}} = 0$, the solutions of ω_{df}^s shifts to the lower value when λ_1 increases. In contrast, the solution of ω_{df}^s shifts to the larger value when λ_3 increases. We have found that the equation of state ω_{df}^s converges to 0 when λ_3 increases. However, ω_{df}^s does not exist when $\lambda_1 \gtrsim 30$. This suggests that when $\lambda_1 \gtrsim 30$ the fixed points in the class II$^+$ take only one physically relevant value. From Figure 8, one can see that when λ_3 increases the equation of state ω_{df}^s shifts toward 0. From our numerical analysis for the fixed point class II$^-$, we have found that when $\lambda_1 \gtrsim 1$ the value of Ω_{df} which is associated with ω_{df}^s becomes larger than 1. However, we can reduce the value of Ω_{df} by increasing the value of λ_3,
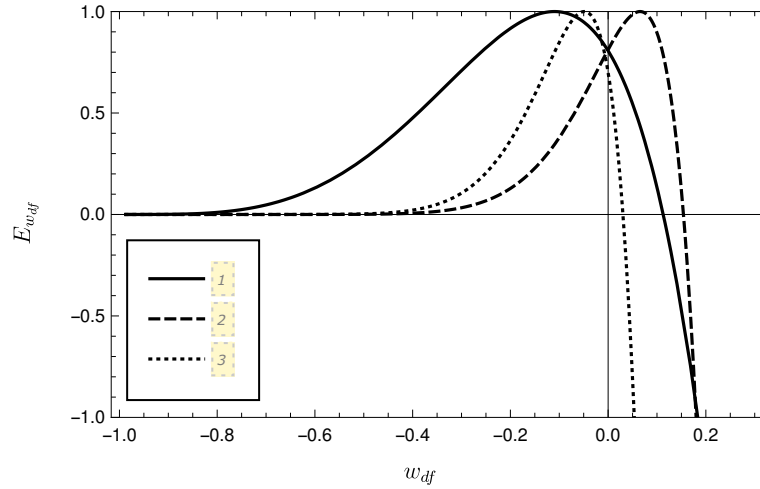
Figure 8 The plot show $E_{w_{df}}$ from the equation (3.77) be a function of w_{df} for the fixed points class II$^-$. For lines 1-3, we have setting $(\lambda_1, \lambda_3)=(1,1)$, (5,1), and (5,5) respectively.

for instance, $\Omega_{df} < 1$ when $\lambda_1 = \lambda_3 = 5$. Moreover, the fixed points in both class II$^+$ and II$^-$, if $\Omega_{df}^* \gtrsim 0.9$, the solution ω_{df}^s cannot exist. From the above analysis, we can summarize that, if the value of r_0 and λ_4 correspond to $\Omega_{df}^* \gtrsim 0.9$ or λ_1 is sufficiently larger than one, the fixed points correspond to ω_{df}^s cannot occur. Now we consider the situation that the same value of the parameters of the model gives rise to the different fixed points. We start by solving numerically the equations (3.18) - (3.20) and setting the density parameter of each species by $\Omega_c, \Omega_b, \Omega_r, \Omega_d$ and ω_d to be $0.27, 0.03, 10^{-4}, 0.7 - 10^{-4}$ and -0.99 respectively. Then we plot the evolution of Ω_d and ω_d shown in Figure 9 for the case $\lambda_1 = \lambda_3 = 1$ where r_0 and λ_4 are computed from $(\Omega_{df}, \omega_{df}) = (\Omega_{df}^*, \omega_{df}^*) = (0.9, -0.99)$.

One can see that, if we chose the initial conditions such that the initial value of ω_d larger than ω_{df}^*, the Universe can evolve toward the fixed points corresponding to the solution ω_{df} as displayed in Figures 7 and 8. Nevertheless, if the Universe evolves toward this fixed point, the present value of ω_d lies outside the observational bound. Thus, the existence of this solution seems to encounter with the problem. However, this problem can be avoided by setting the values of r_0 and λ_4 to match up with $\Omega_{df}^* \gtrsim 0.9$ or setting λ_1 to be sufficiently larger than 1.
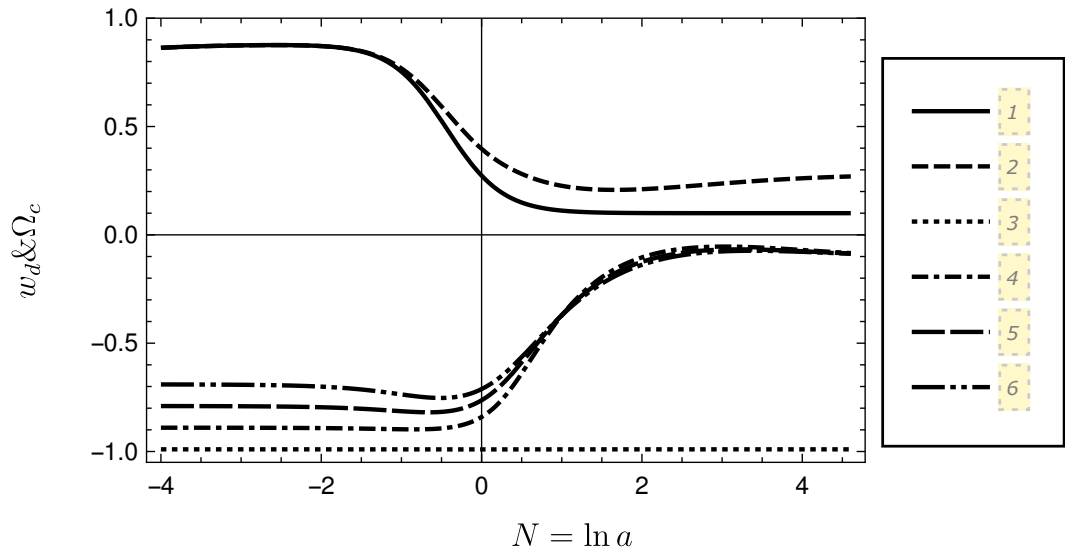
Figure 9 This plot show the evolution of Ω_c and ω_d. For the line 1-2, represent the evolution of Ω_c and set the initial condition for ω_d same as the line **3** and **4**. For the line **3-6**, we set the value of initial condition as $\omega_d = \omega_{df}^* = -0.89, -0.79$ and -0369 respectively.

CHAPTER IV

NON-LINEAR PERTURBATION AND SPHERICAL COLLAPSE MODEL

The evidences from the observational data indicate that currently our Universe is in the accelerating expansion phase. In principle we can suppose that the accelerating expansion of the Universe is driven by dark energy. One of the most important observation in order to encourage the existence and influence of dark energy on the structure formation is the growth of linear perturbations, for example the ISW effect [102], the Dark Energy Survey [103], the galaxy redshift survey [104]. The simple and useful tool for study influence of dark energy on structure formations is the spherical collapse model. This model describes the evolution of radius of the overdense regions using non-linear growth of matter perturbations inside the regions. In this chapter, we study effect of disformal coupling between dark energy and dark matter on large scale structure using spherical collapse model. The essential process in the spherical collapse model are as follows:

In the matter dominated epoch, density contrast of matter which is the ratio of density perturbation to background energy density grows propotional to scale factor inside the Hubble radius. As a result, in some regions of the Universe energy density of matter is higher than the other regions. These regions are overdense regions During the initial phase of matter dominated epoch, the radius of regions defining from fixed total mass of matter inside the regions expands along hubble expansion. However, due to the gravitational attraction of the overdensity inside the regions, the radius of regions expand slower than the hubble expansion rate. Consequently, magnitude of the overdensity inside the regions grows non-linearly inside the regions, and therefore the radius of region stops expanding when gravitational attraction from overdensity is sufficiently strong. At this phase, the radius of regions reaches the maximum value and start to collapse. This is the turn around phase. Nevertheless, the regions will not collapse down to an extremely small radius due to the balance of kinetic energy and the gravitational attraction

of matter inside the region which is the virialisation process.

From the virial theorem [106], we can express relation between the average over time of the total kinetic energy $< K >$ and the average over time of potential energy $< W >$ of the spherical collapse regions at steady state (constant moment of inertia) as

$$< K >= - < W > /2, \tag{4.1}$$

The virial theorem was first derived in the kinetic theory of gases and using the vis-viva equation [107] in the nineteenth century by Rudolf Clausius. The virial theorem was first applied to cosmology on the study of galaxies cluster [108, 109].

In this chapter we study linear and non-linear perturbation in the dark energy model disformally couple to dark matter where the coupling term is obtained from the Chapter III. We calculate evolution equations for the perturbations in the Newtonian limit. From these evolution equations for perturbation, the evolution equations for the spherical collapse can be derived. We use spherical collapse model and cluster number counts to investigate the influence of dark energy on the growth of structure and structure formation of the overdense regions. Based on the results from the spherical collapse model, we compute cluster number counts of the virialization haloes in order to distinguish the influence of disformally, conformally coupled, non-coupled and ΛCDM models.

4.1 Density and Velocity perturbation

In this section, we review the calculation of the evolution equations for the perturbations in matter. In the calculation, we use a new operator which is introduced in [50] as $\lambda^{-2} \equiv -\mathcal{H}^{-2}\nabla^2$. Hence in Fourier space we have $\lambda = \mathcal{H}/k$. Furthermore, we also use Newtonian limit or small scales limit $\lambda \ll 1$ in this calculation. In this limit we can neglect time derivative of $\delta\phi$ and the metric potential Φ compare with their spatial derivative, because time derivative are proportional to λ^2.f The reason why we can neglect these terms that is the time scale of the Universe is very large compare to the spatial variation of the perturbations $\delta\phi$ and Φ. We now rederive the non-linear evolution equations for matter perturbation $\delta\rho_m$ and velocity perturbation v_m^i where the subscript m refers

to matter. So let us start the calculation by using the FLRW line element equation (3.1) and the equation (2.43). We obtain

$$\dot{\bar{\rho}}_m = -3H\bar{\rho}_m + \bar{Q}\dot{\phi}. \tag{4.2}$$

where bar refers to the background quantities of the Universe. In this calculation we consider the case $C = C(\phi)$ and $D = D(\phi)$. The coupling term Q from the equation (2.44) becomes

$$\bar{Q} = -\frac{4C_{,\phi}DX - C\left[C_{,\phi} - 2D(3\dot{\phi}H + V_{,\phi}) + 2D_{,\phi}X\right]}{2C\left[C + D(\bar{\rho}_m - 2X)\right]}\bar{\rho}_m. \tag{4.3}$$

We define density contrast as $\delta_m = \delta\rho_m/\bar{\rho}_m$. We compute the perturbation equations for the matter from the equation (2.43) as

$$\delta(\nabla_\alpha T^\alpha_\beta) = -\delta(Q\phi_{,\beta}). \tag{4.4}$$

Here we neglect subscript m to avoid confuse between the subscript m and the indices. In this calculation, we use line element in the Newtonian gauge also known as the longitudinal gauge. It was advocated by V. F. Mukhanov et. al. as [110]

$$ds^2 = -(1 + 2\Psi)dt^2 + a^2(t)(1 - 2\Phi)\delta_{ij}dx^i dx^j, \tag{4.5}$$

where Ψ and Φ are scalar quantities. So let us begin the calculation of the equation (4.4) by setting $\beta = 0$ and using

$$\nabla_\gamma T^\alpha_\beta = \partial_\gamma T^\alpha_\beta + \Gamma^\alpha_{\gamma\rho}T^\rho_\beta - \Gamma^\rho_{\gamma\beta}T^\alpha_\rho, \tag{4.6}$$

where $\Gamma^\alpha_{\beta\gamma}$ is the Christoffel symbol. The equation (4.4) becomes

$$\delta(\nabla_\alpha T^\alpha_0) = \delta(\partial_\alpha T^\alpha_0) + \delta(\Gamma^\alpha_{\alpha\lambda}T^\lambda_0) - \delta(\Gamma^\lambda_{\alpha 0}T^\alpha_\lambda) = -\delta(Q\phi_{,0}). \tag{4.7}$$

In this analysis, we neglect the anisotropic stress contribution in the field equation, hence $\Psi = \Phi$. Using the Newtonian limit, we can neglect the terms proportional to $\dot{\Phi}$ and $\delta\dot{\phi}$. Thus, we can write the perturbation of the right hand side of equation

(4.7) as

$$\phi_{,\gamma}Q = (\bar{\phi}_{,\gamma} + \delta\phi_{,\gamma})(\bar{Q} + \delta Q)$$

$$= \bar{\phi}_{,\gamma}\bar{Q} + \bar{\phi}_{,\gamma}\delta Q + \bar{Q}\delta\phi_{,\gamma} + \delta\phi_{,\gamma}\delta Q, \tag{4.8}$$

$$\delta(\phi_{,\gamma}Q) = \bar{\phi}_{,\gamma}\delta Q + \bar{Q}\delta\phi_{,\gamma} + \delta\phi_{,\gamma}\delta Q, \tag{4.9}$$

$$\delta(\phi_{,0}Q) = \bar{\phi}_{,0}\delta Q + \bar{Q}\delta\phi_{,0} + \delta\phi_{,0}\delta Q = \dot{\bar{\phi}}\delta Q, \tag{4.10}$$

where we neglect the term $\delta\dot{\phi}$. The equation (4.7) becomes

$$\delta(\nabla_\alpha T_0^\alpha) = \underbrace{\delta(\partial_\alpha T_0^\alpha)}_{K1} + \underbrace{\delta(\Gamma_{\alpha\lambda}^\alpha T_0^\lambda)}_{K2} - \underbrace{\delta(\Gamma_{\alpha 0}^\lambda T_\lambda^\alpha)}_{K3} = -\dot{\bar{\phi}}\delta Q. \tag{4.11}$$

We calculate the term $K1$ from the above equation using the energy-momentum tensor as follows

$$T_\beta^\alpha \equiv (\bar{\rho}_m + \delta\rho_m)U^\alpha U_\beta = \rho_m U^\alpha U_\beta, \tag{4.12}$$

$$\delta(\partial_\alpha T_\beta^\alpha) = \partial_\alpha \delta T_\beta^\alpha = \partial_\alpha \delta(\rho_m U^\alpha U_\beta) = \partial_\alpha(U^\alpha U_\beta \delta\rho_m) + \partial_\alpha[\rho_m \delta(U^\alpha U_\beta)], \tag{4.13}$$

$$\delta(\partial_\alpha T_0^\alpha) = \partial_\alpha \delta T_0^\alpha = \partial_\alpha \delta(\rho_m U^\alpha U_0) = \partial_\alpha(U^\alpha U_0 \delta\rho_m) + \partial_\alpha[\rho_m \delta(U^\alpha U_0)]. \tag{4.14}$$

We define the four-velocity of matter as $U^\alpha = (\bar{U}^0 - \delta U^0, \delta U^i) = (1 - \Phi, v^i)$ and $U^i = \delta U^i$, then we obtain the first and second terms of the equation (4.14) as

$$U^\alpha U_\beta \delta\rho_m = U^\alpha U_0 \delta\rho_m = U^\alpha(-1)\delta\rho_m = -U^\alpha \delta\rho_m, \tag{4.15}$$

$$\partial_\alpha(U^\alpha U_0 \delta\rho_m) = -\partial_\alpha(U^\alpha \delta\rho_m) = -(\partial_\alpha U^\alpha)\delta\rho_m - U^\alpha \partial_\alpha \delta\rho_m$$

$$= -(\partial_0 U^0)\delta\rho_m - (\partial_i U^i)\delta\rho_m - U^0 \partial_0 \delta\rho_m - U^i \partial_i \delta\rho_m$$

$$= -[\partial_0(1 - \Phi)]\delta\rho - \partial_i v^i \delta\rho_m - \delta\dot{\rho}_m - v^i \partial_i \delta\rho_m$$

$$= -\partial_i v^i \delta\rho_m - \delta\dot{\rho}_m - v^i \partial_i \delta\rho_m, \tag{4.16}$$

where $1 - \Phi \sim 1$ compare to the perturbation of coupling term δQ,

$$\partial_\alpha[\bar{\rho}_m\delta(U^\alpha U_0)] = (\partial_\alpha\bar{\rho}_m)\delta(U^\alpha U_0) + \bar{\rho}_m\partial_\alpha[\delta(U^\alpha U_0)] = A_3 + A_4 \,, \tag{4.17}$$

$$A_3 = (\partial_\alpha\bar{\rho}_m)\delta(U^\alpha U_0) = (\partial_\alpha\bar{\rho}_m)[U^\alpha\delta U_0 + U_0\delta U^\alpha]$$

$$= (\partial_\alpha\bar{\rho}_m)[\cancel{-U^\alpha\Phi} + U_0\delta U^\alpha]$$

$$= (\partial_\alpha\bar{\rho}_m)U_0\delta U^\alpha = (\partial_\alpha\bar{\rho}_m)U_0\delta U^\alpha = (\partial_\alpha\bar{\rho}_m)(-1-\Phi)\delta U^\alpha$$

$$= -(\partial_\alpha\bar{\rho}_m)\delta U^\alpha - (\partial_\alpha\bar{\rho}_m)\Phi\delta U^\alpha = -(\partial_0\bar{\rho}_m)\delta U^0 - (\partial_i\bar{\rho}_m)\delta U^i$$

$$= -\dot{\rho}\Phi - v^i\partial_i\bar{\rho}_m = 0 \,, \tag{4.18}$$

where we neglect the term Φ and $\partial_i\bar{\rho}_m = 0$,

$$A_4 = \bar{\rho}_m\partial_\alpha[\delta(U^\alpha U_0)] = \bar{\rho}_m\partial_\alpha[\cancel{U^\alpha\delta U_0} + U_0\delta U^\alpha]$$

$$= \bar{\rho}_m\partial_\alpha(U_0\delta U^\alpha)$$

$$= \bar{\rho}_m[(\partial_\alpha U_0)\delta U^\alpha + U_0\partial_\alpha\delta U^\alpha]$$

$$= \bar{\rho}_m[(\partial_0 U_0)\delta U^0 + (\partial_i U_0)\delta U^i + U_0\partial_0\delta U^0 + U_0\partial_i\delta U^i]$$

$$= \bar{\rho}_m[\Phi\partial_0(1+\Phi) - v^i\partial_i(1+\Phi) - (1+\Phi)(-\partial_0\Phi + \partial_i v^i)]$$

$$= -\bar{\rho}_m(1-\Phi)\partial_\alpha\delta U^\alpha = -\bar{\rho}_m\partial_\alpha\delta U^\alpha = -\bar{\rho}_m[\partial_0\delta U^0 + \partial_i\delta U^i]$$

$$= -\bar{\rho}_m[\partial_0(-\Phi) + \partial_i v^i]$$

$$= -\bar{\rho}_m\partial_i v^i \,, \tag{4.19}$$

where $1+\Phi \sim 1$ and $\dot{\Phi} \sim 0$ compare to the perturbation of coupling term δQ. We obtain the term $K1$ as

$$\delta(\partial_\alpha T_0^\alpha) = -\delta\dot{\rho}_m - (\partial_i v^i)\delta\rho_m - v^i\partial_i\delta\rho_m - \bar{\rho}_m\partial_i v^i \,, \tag{4.20}$$

We calculate the term $K2$ from the equation (4.11) as follows

$$\delta(\Gamma^\alpha_{\alpha\lambda}T_0^\lambda) = \bar{\Gamma}^\alpha_{\alpha\rho}\delta T_0^\rho + \bar{T}_0^\rho\delta\Gamma^\alpha_{\rho\alpha} \,,$$

$$\bar{\Gamma}^\alpha_{\alpha\rho}\delta T_0^\rho = \bar{\Gamma}^\alpha_{\alpha0}\delta T_0^0 + \cancel{\bar{\Gamma}^\alpha_{\alpha i}\delta T_0^i}^{\overset{\displaystyle\bar{\Gamma}^\alpha_{\alpha i}=0}{}} = -3H\delta\rho_m \,, \tag{4.21}$$

$$\bar{T}_0^\rho\delta\Gamma^\alpha_{\rho\alpha} = \bar{T}_0^0\delta\Gamma^\alpha_{0\alpha} = \bar{\rho}_m\delta\Gamma^\alpha_{0\alpha} \,. \tag{4.22}$$

The non-zero components of Christoffel connection are $\bar{\Gamma}^0_{ij} = H\bar{g}_{ij}$ and $\bar{\Gamma}^i_{0j} = H\delta^i_j$. Using the perturbation of Christofel symbol as

$$\delta\Gamma^\lambda_{\mu\nu} = -\bar{g}^{\lambda\beta}h_{\beta\gamma}\bar{\Gamma}^\gamma_{\mu\nu} + \frac{1}{2}\bar{g}^{\lambda\alpha}(\partial_\mu h_{\alpha\nu} + \partial_\nu h_{\alpha\mu} - \partial_\alpha h_{\mu\nu})\,, \tag{4.23}$$

where $h_{\alpha\beta}$ is the metric perturbation. Then, the equation (4.22) becomes

$$\bar{T}^\rho_0\delta\Gamma^\alpha_{\rho\alpha} = \bar{\rho}_m\delta\Gamma^\alpha_{0\alpha}\,, \tag{4.24}$$

$$\delta\Gamma^\alpha_{0\alpha} = \frac{1}{2}\bar{g}^{\alpha\beta}(\partial_0 h_{\beta\alpha} + \partial_\alpha h_{0\beta} - \partial_\beta h_{0\alpha}) - \bar{g}^{\alpha\beta}h_{\beta\gamma}\bar{\Gamma}^\gamma_{0\alpha}$$

$$= S_1 - S_2\,, \tag{4.25}$$

$$S_1 = \frac{1}{2}\bar{g}^{\alpha\beta}(\partial_0 h_{\beta\alpha} + \partial_\alpha h_{0\beta} - \partial_\beta h_{0\alpha})$$

$$= \frac{1}{2}[(\bar{g}^{00}\partial_0 h_{00} + \bar{g}^{ij}\partial_0 h_{ij}) + \bar{g}^{\alpha 0}\partial_\alpha h_{00} - \bar{g}^{0\beta}\partial_\beta h_{00}]$$

$$= \frac{1}{2}\bar{g}^{00}\partial_0 h_{00} + \frac{1}{2}\bar{g}^{ij}\partial_0 h_{ij} = -\frac{1}{2}\partial_0\Phi + \frac{\delta^{ij}}{2a^2}\partial_0(-2a^2\Phi\delta_{ij})$$

$$= -2H\Phi\delta^i_i\,, \tag{4.26}$$

$$S_2 = \bar{g}^{\alpha\beta}h_{\beta\gamma}\bar{\Gamma}^\gamma_{0\alpha} = \bar{g}^{jk}h_{ki}\bar{\Gamma}^i_{0j} = \frac{\delta^{jk}}{a^2}(-2a^2\Phi\delta_{ki})H\delta^i_j$$

$$= -2\Phi H\delta^i_i\,, \tag{4.27}$$

$$\delta\Gamma^\alpha_{0\alpha} = 0\,, \tag{4.28}$$

where $\dot{\Phi} \sim 0$ compare to the perturbation of coupling term δQ. Thus, we obtain the term $K2$ as

$$\delta(\Gamma^\alpha_{\alpha\lambda}T^\lambda_0) = -3H\delta\rho_m\,. \tag{4.29}$$

We calculate the term $K3$ from the equation (4.11) as follows

$$\delta(\Gamma^\lambda_{\alpha 0}T^\alpha_\lambda) = \bar{\Gamma}^\lambda_{\alpha 0}\delta T^\alpha_\lambda + \bar{T}^\alpha_\lambda\delta\Gamma^\lambda_{\alpha 0} \tag{4.30}$$

$$\bar{\Gamma}^\lambda_{\alpha 0}\delta T^\alpha_\lambda = \bar{\Gamma}^\lambda_{00}\delta T^0_\lambda + \bar{\Gamma}^\lambda_{i0}\delta T^i_\lambda = \bar{\Gamma}^\lambda_{i0}\delta T^i_\lambda \quad;\quad \bar{\Gamma}^\lambda_{00} = 0\,,$$

$$= \bar{\Gamma}^0_{i0}\delta T^i_0 + \bar{\Gamma}^j_{i0}\delta T^i_j = \bar{\Gamma}^j_{i0}\delta T^i_j \quad;\quad \bar{\Gamma}^j_{i0} = 0\,,$$

$$T^i_j = \rho_m U^i U_j = (\bar{\rho}_m + \delta\rho_m)(\bar{U}^i + \delta U^i)(\bar{U}_j + \delta U_j)$$

$$= (\bar{\rho}_m + \delta\rho_m)\delta U^i\delta U_j\,,$$

$$\delta T^j_i = (\bar{\rho}_m + \delta\rho_m)v^i v_j = \rho_m v^i v_j\,, \tag{4.31}$$

$$\bar{\Gamma}^\lambda_{\alpha 0}\delta T^\alpha_\lambda = H\delta^i_j\rho_m v^i v_j = \rho_m H v^i v_i\,, \tag{4.32}$$

$$\bar{T}^\alpha_\lambda \delta\Gamma^\lambda_{\alpha 0} = \bar{T}^0_0 \delta\Gamma^0_{00} = \bar{\rho}_m\delta\Gamma^0_{00} \tag{4.33}$$

From the equation (4.23), we obtain

$$\delta\Gamma^0_{00} = -\bar{g}^{0\beta}h_{\beta\gamma}\bar{\Gamma}^\gamma_{00} + \frac{1}{2}\bar{g}^{0\alpha}(\partial_0 h_{\alpha 0} + \partial_0 h_{0\alpha} - \partial_\alpha h_{00})$$
$$= \frac{1}{2}\bar{g}^{00}\partial_0 h_{00} = \frac{1}{2}(\frac{-1}{a^2})\partial_0(-2a^2\Phi) = \dot{\Phi} + 2H\Phi\,. \tag{4.34}$$

We neglect the above equation compare to the coupling term δQ. Then, we obtain the term $K3$ as

$$\delta(\Gamma^\lambda_{\alpha 0}T^\alpha_\lambda) = \rho_m H v^i v_i \tag{4.35}$$

From the equations (4.20), (4.29), (4.35), the equation (4.11) becomes

$$\delta(\nabla_\alpha T^\alpha_0) = -\delta\dot{\rho}_m - (\partial_i v^i_m)\delta\rho_m - v^i_m\partial_i\delta\rho_m - \bar{\rho}_m\partial_i v^i_m - 3H\delta\rho_m - \rho_m H v^i v_i$$
$$= -\dot{\phi}\delta Q\,, \tag{4.36}$$

$$\delta\dot{\rho}_m = -(\partial_i v^i_m)\delta\rho_m - v^i_m\partial_i\delta\rho_m - \bar{\rho}_m\partial_i v^i_m - 3H\delta\rho_m - \rho_m H v^i v_i + \dot{\phi}\delta Q\,, \tag{4.37}$$

where $\rho_m = \bar{\rho}_m + \delta\rho_m$. Dividing the above equation by $\bar{\rho}_m$ and using

$$\delta_m = \frac{\delta\rho_m}{\bar{\rho}_m} \quad \text{and} \quad \frac{\delta\dot{\rho}_m}{\bar{\rho}_m} = \dot{\delta}_m + \frac{\dot{\bar{\rho}}_m\delta\rho_m}{\bar{\rho}_m^2}\,, \tag{4.38}$$

then the equation (4.37) becomes

$$\dot{\delta}_m = -(1+\delta_m)\partial_i v^i_m - v^i_m\partial_i\delta_m - \frac{\dot{\bar{\rho}}_m}{\bar{\rho}_m}\delta_m - 3H\delta_m - (1+\delta_m)H v^i v_i + \frac{\dot{\phi}\delta Q}{\bar{\rho}_m}\,. \tag{4.39}$$

Using $\dot{\bar{\rho}}_m = -3H\bar{\rho}_m + \bar{Q}\dot{\phi}$, we obtain

$$\dot{\delta}_m = -(1+\delta_m)\partial_i v^i - v^i\partial_i\delta_m - (1+\delta_m)H v^i v_i - \frac{\bar{Q}\dot{\phi}\delta_m}{\bar{\rho}_m} + \frac{\dot{\phi}\delta Q}{\bar{\rho}_m}\,. \tag{4.40}$$

From the above equation, we obtained the first-order differential equation for the density perturbation. Now, we consider the equation (4.4) for $\beta = i$, we get

$$\delta(\nabla_\alpha T_i^\alpha) = \delta(\partial_\alpha T_i^\alpha) + \delta(\Gamma_{\rho\alpha}^\alpha T_i^\rho) - \delta(\Gamma_{i\alpha}^\rho T_\rho^\alpha) = -\delta(\phi_{,i} Q)$$

$$= L_1 + L_2 + L_3 = -\delta(\phi_{,i} Q) \,. \tag{4.41}$$

We calculate the term L_1 from the above equation as follows

$$\delta(\partial_\alpha T_i^\alpha) = \partial_0 \delta T_i^0 + \partial_j \delta T_i^j \,, \tag{4.42}$$

$$\delta T_i^0 = \delta(\rho_m U^0 U_i) = \delta(\rho_m U_i) = U_i \delta\rho_m + \bar{\rho}_m \delta U_i = v_i \delta\rho_m + \bar{\rho}_m v_i \tag{4.43}$$

$$= v_i(\bar{\rho}_m + \delta\rho_m) = v_i \rho_m \,, \tag{4.44}$$

$$\partial_0 \delta T_i^0 = \partial_0(v_i \rho_m) = \dot{v}_i \rho_m + v_i \dot{\rho}_m \,, \tag{4.45}$$

$$T_i^j = \rho_m U^j U_i = (\bar{\rho}_m + \delta\rho_m)(\bar{U}^j + \delta U^j)(\bar{U}_i + \delta U_i)$$

$$= (\bar{\rho}_m + \delta\rho_m)\delta U^j \delta U_i \,, \tag{4.46}$$

$$\delta T_i^j = (\bar{\rho}_m + \delta\rho_m)v^j v_i = \rho_m v^j v_i \,, \tag{4.47}$$

$$\partial_j \delta T_i^j = \partial_j(\rho_m v^j v_i) = v^j v_i \partial_j \delta\rho_m + \rho_m \partial_j(v^j v_i) \,. \tag{4.48}$$

From the equations (4.45) and (4.48), we obtain the term L_1 as

$$\partial_\alpha \delta T_i^\alpha = v_i \dot{\rho}_m + \dot{v}_i \rho_m + v_i v^j \partial_j \delta\rho_m + \rho_m \partial_j(v^j v_i) \,, \tag{4.49}$$

where $\rho_m = \bar{\rho}_m + \delta\rho_m$ and we neglect the subscript m for v_i and v^i to avoid confusion of the subscript m and i. Consider the term L_2 from the equation (4.41), we have

$$\Gamma_{\rho\alpha}^\alpha T_i^\rho = (\bar{\Gamma}_{\rho\alpha}^\alpha + \delta\Gamma_{\rho\alpha}^\alpha)(\bar{T}_i^\rho + \delta T_i^\rho)$$

$$= \underbrace{\bar{\Gamma}_{\rho\alpha}^\alpha \bar{T}_i^\rho}_{\text{background}} + \bar{\Gamma}_{\rho\alpha}^\alpha \delta T_i^\rho + \overset{\text{pressureless}}{\cancel{\bar{T}_i^\rho \delta\Gamma_{\alpha\rho}^\alpha}} + \delta\Gamma_{\alpha\rho}^\alpha \delta T_i^\rho \,,$$

$$= \bar{\Gamma}_{\rho\alpha}^\alpha \delta T_i^\rho + \delta\Gamma_{\alpha\rho}^\alpha \delta T_i^\rho \tag{4.50}$$

$$\delta(\Gamma_{\rho\alpha}^\alpha T_i^\rho) = \bar{\Gamma}_{\rho\alpha}^\alpha \delta T_i^\rho + \delta\Gamma_{\alpha\rho}^\alpha \delta T_i^\rho \tag{4.51}$$

$$\bar{\Gamma}_{\rho\alpha}^\alpha \delta T_i^\rho = \bar{\Gamma}_{0\alpha}^\alpha \delta T_i^0 + \bar{\Gamma}_{j\alpha}^\alpha \delta T_i^j$$

$$= \cancel{\bar{\Gamma}_{00}^0 \delta T_i^0} + \bar{\Gamma}_{0j}^j \delta T_i^0 + \cancel{\bar{\Gamma}_{j0}^0 \delta T_i^j} + \cancel{\bar{\Gamma}_{jk}^k \delta T_i^j}$$

$$= \bar{\Gamma}_{0j}^j \delta T_i^0 = 3H \rho_m v_i \,. \tag{4.52}$$

$$\delta\Gamma^\alpha_{\alpha\rho}\delta T^\rho_i = \delta\Gamma^\alpha_{\alpha 0}\delta T^0_i + \delta\Gamma^\alpha_{\alpha j}\delta T^j_i \tag{4.53}$$

$$= \delta\Gamma^0_{0j}\delta T^j_i + \delta\Gamma^k_{kj}\delta T^j_i$$

$$\sim 0\,, \tag{4.54}$$

where we neglect the terms $\delta\Gamma^0_{0j}$ and $\delta\Gamma^k_{kj}$ compare to the coupling term δQ. We compute the term L_3 from the equation (4.41) as follows

$$\Gamma^\rho_{i\alpha} T^\alpha_\rho = \underbrace{\bar\Gamma^\rho_{i\alpha}\bar T^\alpha_\rho}_{\text{background}} + \bar\Gamma^\rho_{i\alpha}\delta T^\alpha_\rho + \bar T^\alpha_\rho\delta\Gamma^\rho_{i\alpha} + \delta\Gamma^\rho_{i\alpha}\delta T^\alpha_\rho\,,$$

$$\delta(\Gamma^\rho_{i\alpha} T^\alpha_\rho) = \bar\Gamma^\rho_{i\alpha}\delta T^\alpha_\rho + \bar T^\alpha_\rho\delta\Gamma^\rho_{i\alpha} + \delta\Gamma^\rho_{i\alpha}\delta T^\alpha_\rho\,, \tag{4.55}$$

$$\bar\Gamma^\rho_{i\alpha}\delta T^\alpha_\rho = \bar\Gamma^\rho_{i0}\delta T^0_\rho + \bar\Gamma^\rho_{ij}\delta T^j_\rho$$

$$= \bar\Gamma^0_{i0}\delta T^0_0 + \bar\Gamma^j_{i0}\delta T^0_j + \bar\Gamma^0_{ij}\delta T^j_0 + \bar\Gamma^k_{ij}\delta T^j_k \qquad \overset{\bar\Gamma^0_{i0}=0}{} \qquad \overset{\bar\Gamma^k_{ij}=0}{}$$

$$= \bar\Gamma^j_{i0}\delta T^0_j + \bar\Gamma^0_{ij}\delta T^j_0 = (H\delta^j_i)(v_j\rho_m) + (\frac{\dot a}{a}\bar g_{ij})(-\rho_m v^j)$$

$$= \rho_m H v_i - \rho_m H v_i = 0\,, \tag{4.56}$$

$$\bar T^\alpha_\rho\delta\Gamma^\rho_{i\alpha} = \bar T^0_0\delta\Gamma^0_{i0} = -\rho_m\delta\Gamma^0_{i0} = -\rho_m\left(\frac{1}{2}\bar g^{00}\partial_i h_{00}\right) = -\rho_m\partial_i\Phi\,, \tag{4.57}$$

$$\delta(\Gamma^\rho_{i\alpha} T^\alpha_\rho) = -\rho_m\partial_i\Phi\,. \tag{4.58}$$

Consider right hand side of the equation (4.41) and using the equation (4.9), we have

$$Q\phi_i = (\bar Q + \delta Q)\delta\phi_{,i},$$

$$\delta(\phi_{,i}Q) = Q\partial_i\delta\phi\,. \tag{4.59}$$

From the equations (4.49), (4.52), (4.58) and (4.59), the equation (4.41) becomes

$$\delta(\nabla_\alpha T^\alpha_i) = \rho_m\dot v_i + v_i\dot\rho_m + v^i v_j\partial_j\delta\rho_m + \rho_m\partial_j(v^i v_j) + 3H\rho_m v_i + \rho_m\partial_i\Phi \tag{4.60}$$

$$= -Q\partial_i\delta\phi\,, \tag{4.61}$$

$$\rho_m\dot v_i = -v_i\dot\rho_m - v^i v_j\partial_j\delta\rho_m - \rho_m\partial_j(v^i v_j) - 3H\bar\rho_m v_i - \rho_m\partial_i\Phi - Q\partial_i\delta\phi\,. \tag{4.62}$$

Using the equation (4.2) and (4.36), we obtain

$$\dot{\rho}_m = \dot{\bar{\rho}}_m + \delta\dot{\rho}_m = -3H\bar{\rho}_m + \bar{Q}\dot{\bar{\phi}} - (\bar{\rho}_m + \delta\rho_m)\partial_j v^j - v^j\partial_j\delta\rho_m - 3H\delta\rho_m + \dot{\bar{\phi}}\delta Q$$
$$= -3H\rho_m - \rho_m\partial_j v^j - v^j\partial_j\delta\rho_m + \dot{\bar{\phi}}Q\,. \tag{4.63}$$

Inserting the equation (4.63) into the equation (4.62), we get

$$\rho_m\dot{v}_i = -v_i[-3H\rho_m - \rho_m\partial_j v^j - v^j\partial_j\delta\rho_m + \dot{\bar{\phi}}Q]$$
$$- \rho_m\partial_j(v^j v_i) - v_i v^j\partial_j\delta\rho_m - 3H\rho_m v_i + \rho_m\partial_i\Phi - Q\partial_i\delta\phi$$
$$= -\rho_m v^j\partial_j v_i - \rho_m\partial_i\Phi - v_i Q\dot{\bar{\phi}} - Q\partial_i\delta\phi\,. \tag{4.64}$$

Substituting $v_i = a^2 v^i$ and

$$\dot{v}_i = a^2\dot{v}_i + 2a\dot{a}v^i = a^2\dot{v}^i + 2a^2\frac{\dot{a}}{a}v^i$$
$$= a^2(\dot{v}^i + 2Hv^i) \tag{4.65}$$

into the equation (4.64) and divided by $\bar{\rho}_m$, we get

$$\dot{v}^i = -\Big(2H + \frac{Q\dot{\bar{\phi}}}{\bar{\rho}_m}\Big)v^i - v^j\partial_j v^i - \frac{1}{a^2}\Big(\partial_i\Phi + \frac{Q}{\bar{\rho}_m}\partial_i\delta\phi\Big)$$
$$= -(2H + \widetilde{Q}_0\dot{\bar{\phi}})v^i - v^j\partial_j v^i - \frac{1}{a^2}\Big(\partial_i\Phi + \widetilde{Q}_0\partial_i\delta\phi\Big)\,, \tag{4.66}$$

where $\widetilde{Q}_0 = Q/\bar{\rho}_m$. From the equations (4.40) and (4.66), we then have the first order differential equations for non-linear density and velocity perturbations. We show results of the calculation for perturbation of the coupling term Q from the equations (2.44) - (2.46) as follows

$$\delta T_m = -\delta\rho_m, \quad \delta T_{mp} = 2\bar{X}\delta\rho_m, \tag{4.67}$$
$$\delta(T_{mp}\Box\phi) = -2\bar{X}\delta\rho_m(\ddot{\bar{\phi}} + 3H\dot{\bar{\phi}}) + 2\bar{X}\bar{\rho}_m\nabla^2\delta\phi\,, \tag{4.68}$$
$$\delta\theta_1 = \ddot{\bar{\phi}}\delta\rho_m - \dot{\bar{\phi}}H\rho v^i v_k, \quad \delta\theta_2 = -8\bar{\rho}_m\bar{X}\ddot{\bar{\phi}}\Phi + 2\bar{X}\ddot{\bar{\phi}}\delta\rho_m\,, \tag{4.69}$$
$$\delta\theta_3 = \dot{\bar{\phi}}[\delta\dot{\rho}_m + \partial_i(v^i\delta\rho_m) + \bar{\rho}_m\partial_i v^i + 3H\delta\rho_m]\,, \tag{4.70}$$
$$\delta\theta_4 = 8\Phi\bar{X}(2\ddot{\bar{\phi}}\dot{\bar{\rho}}_m) - \dot{\bar{\phi}}(\dot{\bar{\phi}}\ddot{\bar{\phi}}\delta\rho_m + \bar{X}\delta\dot{\rho}_m)\,, \tag{4.71}$$
$$\delta(T_{mp}\theta_5) = 4\bar{X}^2\ddot{\bar{\phi}}(6\bar{\rho}_m\Phi - \delta\rho_m)\,. \tag{4.72}$$

However, we express the explicit calculation for the perturbations of T_m, T_{mp}, $T_{mp}\Box\phi$ and $\theta_1 - \theta_5$ in appendix A.

Next section, we use Newtonian limit and the assumption of top hat model to derived the second order differential equation of the non-linear density perturbation and the relation between matter density contrast and its radius.

4.2   Evolution equations for the perturbation on small scales

In order to calculate the perturbations of the coupling term Q from the equation (3.7), we consider the case where $C = C(\phi)$ and $D = D(\phi)$. From the metric perturbation in Newtonian gauge given in the equation (4.5) the Einstein theory converges to Newtonian limit on small scales, such that component $\mu\nu = 00$ of the perturbed Einstein equation becomes

$$\partial_i\partial^i\Phi \equiv \nabla^2\Phi \simeq \frac{1}{2}\delta\rho_m. \tag{4.73}$$

On sufficiently small scales we have $\nabla^2\delta\phi \gg \delta\ddot{\phi}, H\delta\dot{\phi}$, where $\delta\phi$ is the perturbation of ϕ. Then, the equation (2.37) becomes

$$\nabla^2\delta\phi = \delta Q\,. \tag{4.74}$$

The perturbation of coupling term δQ appears in the equations (4.74) and (4.40) can be computed by applying the small scales limit to the equation (2.44). Then we obtain

$$\frac{\delta Q}{\bar{\rho}_m} = \frac{D\dot{\phi}}{C}[\dot{\delta}_m + (1 + \delta_m)\partial_i v_m^i + v_m^i\partial_i\delta_m] + \widetilde{Q}_0\delta_m\,. \tag{4.75}$$

Substituting the equation (4.75) into the equation (4.40), we then have

$$\dot{\delta}_m = -(1 + \delta_m)\partial_i v_m^i - v_m^i\partial_i\delta_m\,. \tag{4.76}$$

Inserting the equation (4.76) into the equation (4.40), we get

$$\frac{\delta Q}{\bar{\rho}_m} = \widetilde{Q}_0\delta_m\,. \tag{4.77}$$

One can see from the above equation that, the $\dot{\delta}_m$ can be eliminated and therefore the equation (4.74) becomes

$$\nabla^2 \delta\phi = \widetilde{Q}_0 \delta\rho_m \,. \tag{4.78}$$

We use the evolution of top hat model in order to obtain a correct explanation of the spherical collapse model (see the detail in appendix B and [105]). Applying the assumption of top hat model to the equations (4.66) and (4.76), then differentiating both equations with respect to time t, the term $\partial_i v_m^i$ can be eliminated. We obtain

$$\ddot{\delta}_m = -(2H + \widetilde{Q}_0\dot{\phi})\dot{\delta}_m + \frac{4}{3}\frac{\dot{\delta}_m^2}{1+\delta_m} + (1+\delta_m)(\nabla^2\Phi + \widetilde{Q}_0\nabla^2\delta\phi) \,. \tag{4.79}$$

Here we use the assumptions that mass of dark matter particles in the collapsing regions and the conservation of the number of dark matter particles in the overdense regions do not differ from the background. In order to connect the equation (4.79) to the evolution of the radius r of the region which contains dark matter overdensity δ_m, these assumptions are applied. Hence, we get [105]

$$1 + \delta_m = (1 + \delta_{m,in})\Big(\frac{a}{r}\Big)^3 \,, \tag{4.80}$$

where $\delta_{m,in}$ is the density contrast of matter in the collpase regions and we set the initial conditions as $r = a$ and $\delta_m = \delta_{m,in} \ll 1$. The above relation implies that the overdense regions of radius r will collapse when $\delta_m \to \infty$.

4.2.1 Spherical collapse

In order to study evolution of spherical collapse regions, we use

$$C = e^{\lambda_1\phi}, \quad D = M_d^{-4}e^{\lambda_2\phi}, \quad V = M_v^4 e^{\lambda_3\phi} \,, \tag{4.81}$$

where λ_1, λ_2 and λ_3 are the dimensionless constant parameters, while M_d and M_v are the constant parameters with dimension of mass. In this computation, we define the dimensionless variables as

$$x_1^2 \equiv \frac{\dot{\phi}^2}{6H^2} \,, \quad x_2 \equiv \frac{V}{3H^2} \,, \quad x_3 \equiv \frac{DH^2}{C} \,. \tag{4.82}$$

From [96, 111], we can write the evolution equations for the background Universe in the form of autonomous equations show below

$$x_1' = \frac{1}{2}\left[x_1(3x_1^2 - 3x_2 + 1) - 2(\sqrt{3/2}\lambda_3 x_2 + 2x_1)\right]$$
$$- \frac{\sqrt{3}}{2\sqrt{2}}(x_1^2 + x_2 - 1)\frac{\lambda_1(12x_1^2 x_3 - 1) - 6x_3(\lambda_2 x_1^2 - \sqrt{6}x_1 - \lambda_3 x_2)}{1 - 3x_3(3x_1^2 + x_2 - 1)} \quad (4.83)$$
$$x_2' = x_2(\sqrt{6}\lambda_3 x_1 + 3x_1^2 - 3x_2 + 3)\,, \quad (4.84)$$
$$x_3' = -x_3[3x_1^2 + \sqrt{6}(\lambda_1 - \lambda_2)x_1 - 3x_2 + 3]\,, \quad (4.85)$$

where a prime denotes derivative with respect to number of e-folding $N = \ln a$. The equations (4.83) - (4.85) can completely describe the evolution of the background Universe in principle. We have used the relation between density parameter of dark matter Ω_m and dimensionless parameters x_1 and x_2 in the derivation of the equations (4.83) - (4.85) as

$$1 = x_1^2 + x_2 + \Omega_m\,. \quad (4.86)$$

From the equation (4.82), we can write x_3 in terms of x_2 as

$$\begin{aligned}
x_3 &= \frac{DM_p^2 H^2}{C} = \frac{M_p^2 H^2}{M_d^4}\mathrm{e}^{(\lambda_2 - \lambda_1)\phi/M_p} \\
&= \frac{M_p^2 H_0^2 E^2}{M_d^4}\mathrm{e}^{(\lambda_2 - \lambda_1)\phi/M_p} = \frac{M_p^2 H_0^2 E^2}{M_d^4}\exp\left[\frac{(\lambda_2 - \lambda_1)}{\lambda_3}\frac{\lambda_3\phi}{M_p}\right] \\
&= \frac{M_p^2 H_0^2 E^2}{M_d^4}\left(e^{\lambda_3\phi/M_p}\right)^{(\lambda_2 - \lambda_1)/\lambda_3} \\
&= \frac{M_p^2 H_0^2 E^2}{M_d^4}\left(\frac{3M_p^2 H_0^2}{M_v^4}E^2 x_2\right)^{(\lambda_2 - \lambda_1)/\lambda_3}\,, \quad (4.87)
\end{aligned}$$

where $E \equiv H/H_0$ and H_0 is the current value of the Hubble parameter. In order to avoid confusion, reduced planck mass is restored into the equation (4.87). We have chosen $M_d = M_v \simeq 1/0.55 meV$ [27]. From the observations, we have $M_p^2 H_0^2 \simeq 2.7 \times 10^{-47} GeV^4 \simeq 27 meV^4$. The equations (4.83) - (4.85), (4.87) and evolution equation for E form complete set of evolution equations for the background Universe, so that the evolution of the background Universe is described by x_1, x_2 and E. Since the evolution of E is required to calculate cluster number

counts in the next section, we solve the evolution equations for x_1, x_2 and E instead of x_1, x_2 and x_3. In this calculation, we use cosmic time t instead of conformal times τ. Then, we have

$$H^2 \equiv (\frac{\dot{a}}{a})^2 = \frac{1}{3}[\rho_m + \frac{1}{2}\dot{\phi}^2 + V(\phi)]. \tag{4.88}$$

In order to compute the evolution equation for E, we differentiate the equation (4.88) with respect to N to yield

$$\frac{E'}{E} = \frac{\dot{H}}{H^2} = \frac{3}{2}(x_2 - 1 - x_1^2). \tag{4.89}$$

To numerically solve evolution equations for the background Universe, we set initial conditions for dark energy ω_d by requiring that the equation of state parameter of dark energy to lies within the range $-1 < \omega_d < -0.9$ and $\Omega_d = x_1^2 + x_2$ takes value 0.7. The initial values for E is set such that $E = 1$ at present. We now turn to discuss the evolution of the background Universe. From the equation (4.82), we can write the coupling term $\widetilde{Q}_0$ in terms of dimensionless variables as

$$\widetilde{Q}_0 = \frac{\lambda_1 - 6\left(2\lambda_1 - \lambda_2\right) x_3 x_1^2 - 6\lambda_3 x_2 x_3 - 6\sqrt{6}x_3 x_1}{6\left(1 - 3x_1^2 - x_2\right) x_3 + 2}. \tag{4.90}$$

Inserting the equation (4.90) into the equation (4.2), we have

$$\dot{\rho}_m + 3H\left(1 - \sqrt{\frac{2}{3}}\widetilde{Q}_0 x_1\right)\rho_m = 0. \tag{4.91}$$

It can be seen from the equation (4.86) that during the matter dominated epoch, we have $x_1, x_2 \ll 1$. Hence the equation (4.90) becomes

$$\widetilde{Q}_0 = \frac{\lambda_1}{2 + 6x_3}. \tag{4.92}$$

This equation suggests that during the matter dominated epoch, the influence of conformal coupling which is quantified by λ_1 is suppressed by the amplitude of disformal coupling which is quantified by x_3. The equation (4.87) gives $x_3 \sim E \gg 1$ during the matter dominated epoch when $0 < \lambda_1, |\lambda_2|, |\lambda_3| \lesssim 1$ and $M_d \sim 1 meV$. The effect of conformal coupling can be strongly suppressed by disformal coupling

Table 4 This table shows values of parameters λ_1, λ_2 and λ_3 for each model.

Model λ_i	A	B	C	D	E	F
λ_1	0.1	0.1	0.1	0.1	0	-
λ_2	0	0	-2	-1	0	-
λ_3	-1	-1	-1	-0.1	-1	-
	conformal	disformal			uncoupling	ΛCDM

as same as the magnitude of coupling during the matter dominated epoch. In addition to the suppression due to the disformal coupling, when dark energy slowly evolves, i.e., $x_1 \ll 1$ the effect of coupling term in the equation (4.91) can be reduced. The magnitude of x_1 depends on λ_3 which mainly controll potential slope of dark energy. The disformal coupling can lead to a large magnitude of the coupling compared with conformal coupling at late time while the coupling can be negligible during the matter dominated epoch. From the equation (4.90), for the case $\lambda_3 < 0$ when $x_2 \sim 0.7$ and $x_3 \sim 1$ the third term in the numerator can enhance the magnitude of coupling at late time. During dark energy and dark matter dominated epoch, for the pure conformally coupled model the equation (4.90) becomes $\widetilde{Q_0} = \lambda_1/2$. Thus, if $\lambda_1 \sim 1$, the evolution of the Universe during the matter dominated epoch may become unphysical. If $\lambda_1 \sim 1$ and $\rho_d \ll \rho_m$ where ρ_d is the energy density of the dark energy, the last two terms on the LHS of the equation (2.37) will be smaller than the coupling term on the RHS of this equation. Therefore, the *external force* Q_0 will strongly drive the dark energy field ϕ, consequently matter dominated epoch will stop quickly and the acceleration epoch cannot start as it should be. However, even though $\lambda_1 > 1$, the universe still evolve suitably if ρ_d is not too small compared with ρ_m during the matter dominated epoch. This situation exists when dark energy starts scaling solution during the matter dominated epoch in the quintessence model with the exponential potential [112]. For this case, the dark energy in the matter dominated epoch can contribute to the spherical collapse and cluster number counts [113]. In this work, we assume that the dark energy slowly evolve through the whole evolution of the Universe. Hence, $\rho_d \ll \rho_m$ during the matter dominated era.
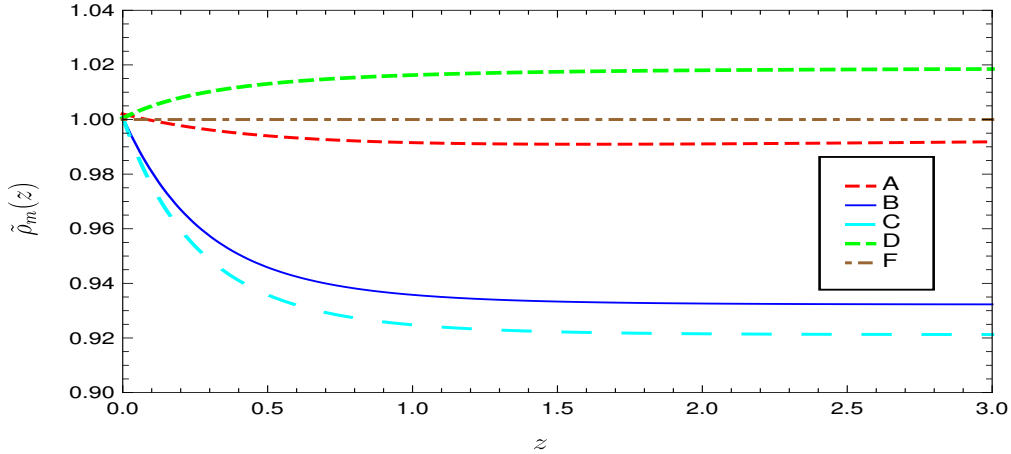
Figure 10 Plots of $\tilde{\rho}_m \equiv a^3 \rho_m / \rho_{m0}$ as a function of redshift z. The lines A, B, C, D, and F represent the models A, B, C, D and F in table 4 respectively.

In order to study the influences of the coupling term $\widetilde{Q_0}$ on the evolution of ρ_m, we plot the evolution of $\tilde{\rho}_m / \rho_{m0} \equiv a^3 \rho_m / \rho_{m0}$ in Figure 10 where ρ_{m0} is the present value of ρ_m. One can see from the plot that $\rho_m \propto 1/a^3$ when coupling disappears. For a fixed ρ_{m0}, ρ_m decreases when λ_1 and $-\lambda_2$ increase for $\lambda_3 = -1$ at a given redshift because the coupling term $\widetilde{Q_0}$ increases in this situation. It can be seen that the coupling term $\widetilde{Q_0}$ increases when λ_1 increases. Corresponding to the equation (4.87) that for negative λ_2, λ_3 can enhance x_3 because $3M_p^2 H_0^2 E^2 x_2 / M_v^4 > 1$ at late time. It follows from the equation (4.90), for the case $\lambda_3 = -1$ the third term in the numerator of this equation can give a dominant contribution due to an enhancement of x_3 when $-\lambda_2$ increases. From the equation (4.87), the coupling term $\widetilde{Q_0}$ can become negative because a large contribution of the fourth term in the numerator of the equation (4.90). x_3 can enhance by increasing λ_3 from negative value toward zero at late time. In the Figure 10, when $\widetilde{Q_0}$ becomes negative, ρ_m decay faster than a^{-3} as shown by line D. The values of parameters λ_1, λ_2 and λ_3 for each model show in table (4).

Now we turn to study the effect of the disformally and conformally coupled models on the growth of density perturbations. Inserting the equations (4.73) and (4.78) into the equation (4.79) and using the equation (4.82), we obtain second order differential equation of the matter density contrast in terms of dimensionless
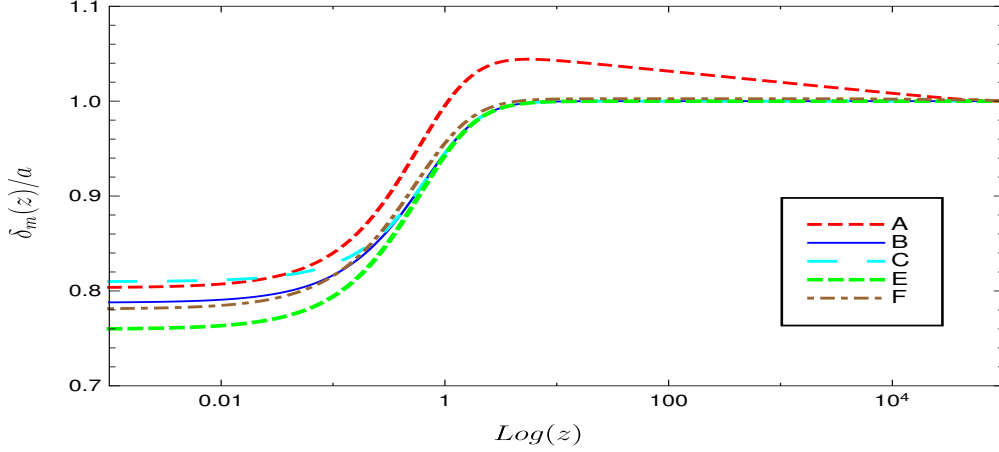
Figure 11 **Plots of δ_m/a as a function of redshift z. The values of λ_1, λ_2 and λ_3 for each line are similar to those of the Figure (10). We set $\delta_m/a = 1$ initially for all cases.**

variables x_1, x_2, δ_m and $\widetilde{Q_0}$ as follows

$$
\begin{aligned}
\delta_m'' &= -\left(\frac{1}{2}(1 + 3x_2 - 3x_1^2) + \sqrt{6}\widetilde{Q_0}x_1\right)\delta_m' + \frac{4}{3}\frac{(\delta_m')^2}{1 + \delta_m} \\
&\quad + \frac{3}{2}(1 - x_1^2 - x_2)(1 + \delta_m)(1 + 2\widetilde{Q_0}^2)\delta_m\,,
\end{aligned}
\tag{4.93}
$$

and the linearized version of the above equation is

$$
\begin{aligned}
\delta_m'' &= -\left(\frac{1}{2}(1 + 3x_2 - 3x_1^2) + \sqrt{6}\widetilde{Q_0}x_1\right)\delta_m' \\
&\quad + \frac{3}{2}(1 - x_1^2 - x_2)(1 + 2\widetilde{Q_0}^2)\delta_m\,.
\end{aligned}
\tag{4.94}
$$

Since $\widetilde{Q_0}$ during the matter dominated epoch obeys the estimation given in the equation (4.92), for the case where $x_3 = 0$, i.e. the case of pure conformally coupled, we obtain the growing solution of the equation (4.94) as

$$
\delta_m \propto e^{pN}\,, \quad \text{where} \quad p = -\frac{1}{4} + \frac{1}{4}\sqrt{25 + 12\lambda_1^2}\,.
\tag{4.95}
$$

This equation shows that during the matter dominated epoch the conformally coupled model can enhance the growth of δ_m. In contrast, for the case of disformally coupled model the enhancement disappear as shown in Figure 11. It can be seen in this plot that the ratios δ_m/a are not different for disformally coupled and uncoupled models during matter dominated epoch, because $\widetilde{Q}$ is suppressed by disformal
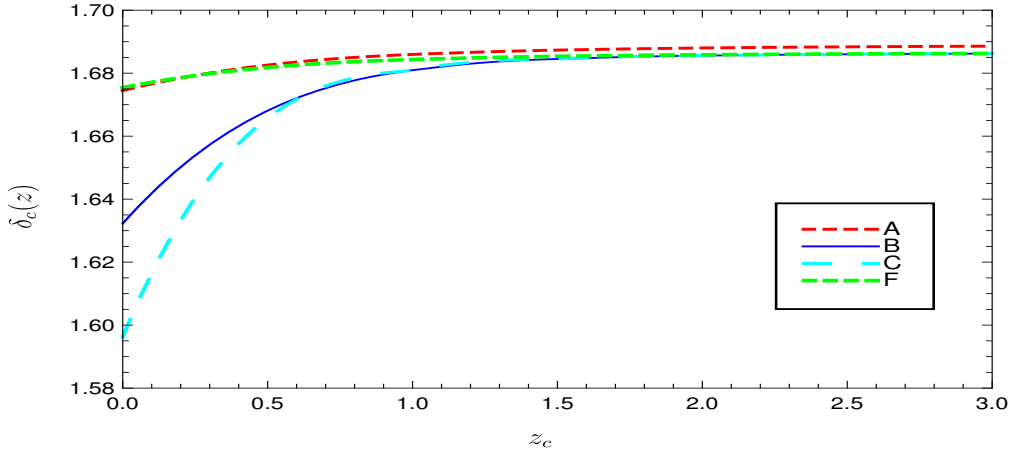
Figure 12 Plots of δ_c as a function of collapsing redshift z_c. The values of λ_1, λ_2 and λ_3 for each line are similar to those of the Figure (10).

coupling in the disformally coupled models. However, the ratio δ_m/a for the conformally coupled is larger than the uncoupled model at any given redshifts during the matter dominated epoch. At late time, the ratio δ_m/a for the disformally coupled models can decrease slower than that of the uncoupled and pure conformally coupled models, which agrees with [27]. For the coupled models at late time, the decreasing rate of the ratio δ_m/a depends on the coupling term $\widetilde{Q_0}^2$ which controls the *growing rate* of δ_m in the equation (4.94). One can see in the Figure 11 that at late time the decreasing rate of the ratio δ_m/a depends on λ_1, λ_2 and λ_3.

In order to study spherical collapse in the disformally coupled models, we define δ_c which is extrapolated linear density contrast at collapse redshifts. We compute this quantity by numerically solving the equation (4.93), and then finding the relation between collapse redshifts (the value of redshift at $\delta_m \to \infty$) and the initial conditions for δ_m which lead to collapse at that redshift. For this computation, we vary the initial value of δ_m within the range $\delta_m \lesssim 10^{-3}$ and fix the initial redshift at 10^5. Therefore, we can assume that δ_m obeys the linear evolution equation given in the equation (4.94). Hence, to calculate δ_c, we can set $\delta_m' = \delta_m$ at the initial time. Solving the equation (4.94) from the initial redshift to the collapsing redshift z_c using the initial value of δ_m that leads to the collapse of the overdense regions at redshift z_c. We obtain the extrapolated linear density contrast at collapsing redshift z_c. We also plot δ_c as a function of redshift z in

Figure 12. It can be seen in the plot that the enhancement of decay rate of δ_c at late time is a result of increasing disformal coupling term and the higher growth rate of density perturbation of dark matter for the model of disformally coupled. The less amount of density perturbation is needed for collapse when the growth rate is large. This suggests that the overdense regions are able to efficiently collapse due to the disformally coupled at late time. Using the approximation $\omega_d = -1$, the gravitational potential for dark energy is given by [114]

$$U_d = -\frac{4\pi G M \rho_d}{5} r^2 \,, \tag{4.96}$$

where $M \equiv 4\pi \rho_m r^3/3$ is the total mass of dark matter inside spherical collapsing regions. For a system with potential of the form $U \propto r^p$ and the kinetic energy K, the virial theorem can be expressed in the general form as $K = pU/2$ [115]. Thus, we can compute overdensity for dark matter at virialization phase δ_{vir} using nonlinear overdensity of dark matter as a function of redshift to compute maximum radius and redshift at turn around. Then, combining the virial theorem and the conservation of energy, we obtain a relation between potential energies of the overdense regions at turn-around phase and at the time when virialization is reached as follows

$$U_{m,ta} + U_{d,ta} = \frac{1}{2} U_{m,vir} + 2U_{d,vir} \,, \tag{4.97}$$

where subscript ta refers to turn around, $U_m = -\frac{3}{5}\frac{GM^2}{r}$ is the gravitational potential energy of dark matter. From the equation (4.97), we have used the fact that at turn around kinetic energy of the overdense regions $K_{m,ta}$ equal to zero. We have also used $K_{m,vir} = -U_{m,vir}/2$ and $K_{d,vir} = U_{d,vir}$ to obtain the equation (4.97). From the equation (4.97) and the gravitational potential for dark energy given in equation (4.96), we obtain

$$\rho_m r_{ta}^2 + \rho_d r_{ta}^2 = \frac{1}{2} \rho_m r_{vir}^2 + 2\rho_d r_{vir}^2 \,. \tag{4.98}$$

The overdensity of the forming cluster at turn around is $\zeta = \left(\frac{\rho_m}{\rho_{bg}}\right)_{ta}$ where ρ_{bg} is the matter energy density of the background universe. To calculate the overdensity

for dark matter at virialization, we defined

$$\eta = \frac{r_{vir}}{r_{ta}} \quad \text{and} \quad \theta = \left(\frac{\rho_d}{\rho_m}\right)_{ta}. \tag{4.99}$$

To obtain a relation between η and θ, we used

$$\left(\frac{\rho_d}{\rho_m}\right)_{vir} = \theta\eta^3. \tag{4.100}$$

From the equation (4.98) and the above relation, we obtain

$$4\theta\eta^3 - 2\eta(1+\theta) + 1 = 0. \tag{4.101}$$

Therefore, we obtain the overdensity for dark matter at virialization [114] as follows

$$\delta_{vir} = \frac{\rho_{m,vir}}{\rho_{bg,vir}} = \frac{\zeta}{\eta^3}\left(\frac{1+z_{ta}}{1+z_{coll}}\right)^3. \tag{4.102}$$

We also plot the overdensity for dark matter at virialization in Figure 13. It can be seen in this plot that there is no significant difference between the conformally coupled and uncoupled models and the overdensity for both cases are larger than that for the disformal coupling and ΛCDM models. The overdensity can be suppressed in the disformally coupled models compared with the conformally coupled and uncoupled models at virialization. This is a result of the low overdensity at turn around for the disformally coupled model.

4.2.2 Cluster number counts

As mentioned in the introduction, cluster number counts can be used to study influence of dark energy to spherical collapse of overdense regions. In this section, we use Press-Schechter/Sheth-Torman formalism to estimate cluster number counts and study influence of the disformally coupled on the collapse of overdense regions. Let us begin the calculation by using the volume fraction as [112]

$$f = \int_{\delta_L}^{\infty} P(\delta_L, R)d\delta_L = \frac{1}{2}\text{erfc}[\frac{\delta_c}{\sqrt{2}\sigma}], \tag{4.103}$$

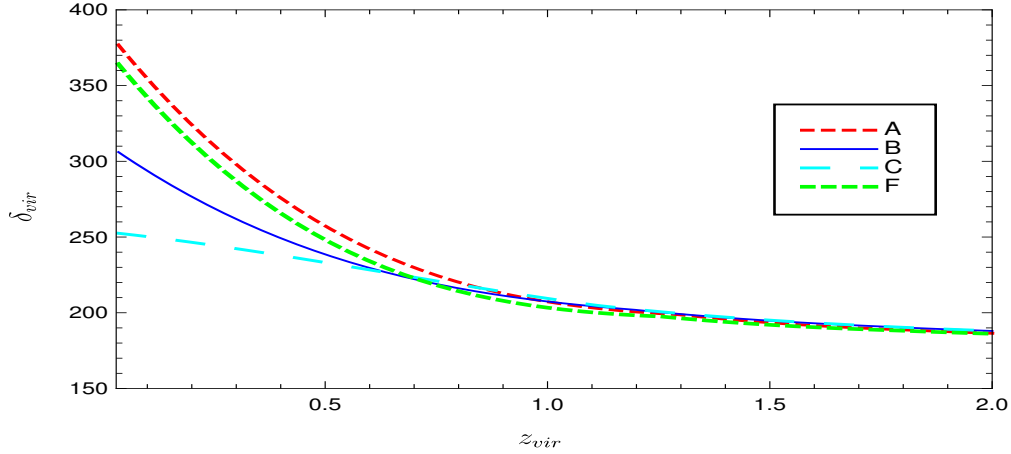**Figure 13** **Plots of δ_{vir} as a function of virialized redshift z_{vir}. The values of λ_1, λ_2 and λ_3 for each line are similar to those of the Figure (10).**

where Gaussian distribution $P(\delta_L, R) = e^{-\sigma_L^2/2\sigma^2}/\sqrt{2\pi}\sigma$, δ_L is linear density contrast and both σ and δ_L are redshift dependent. Differentiating the equation (4.103) with respect to the σ, we obtain

$$\frac{df}{d\sigma} = \frac{1}{2}\frac{d}{d\sigma}\text{erfc}\Big[\frac{\delta_c}{\sqrt{2}\sigma}\Big]$$

$$= \frac{-1}{\sigma\sqrt{2\pi}}\Big(\frac{\delta_c}{\sigma}\Big)\exp\Big(\frac{\delta_c^2}{2\sigma^2}\Big). \tag{4.104}$$

For the Press-Schechter formalism, the mass function describing the comoving number density of the collapse regions with range of mass between M to $M + dM$ is given by

$$n(M)dM = 2\frac{\bar{\rho}}{M}\frac{df}{d\sigma}\frac{d\sigma}{dM}dM$$

$$= -\sqrt{\frac{2}{\pi}}\bar{\rho}_m\Big(\frac{\delta_c}{\sigma}\Big)\frac{d\ln\sigma}{d\ln M}\exp\Big[-\frac{\delta_c^2}{2\sigma^2}\Big]\frac{dM}{M^2}, \tag{4.105}$$

where parameter σ is the variance in spheres of radius R. The parameter σ can be approximately calculated from [116]

$$\sigma(R, z) = \sigma_8\Big(\frac{R}{8h^{-1}Mpc}\Big)^{-\gamma(R)}D(z). \tag{4.106}$$
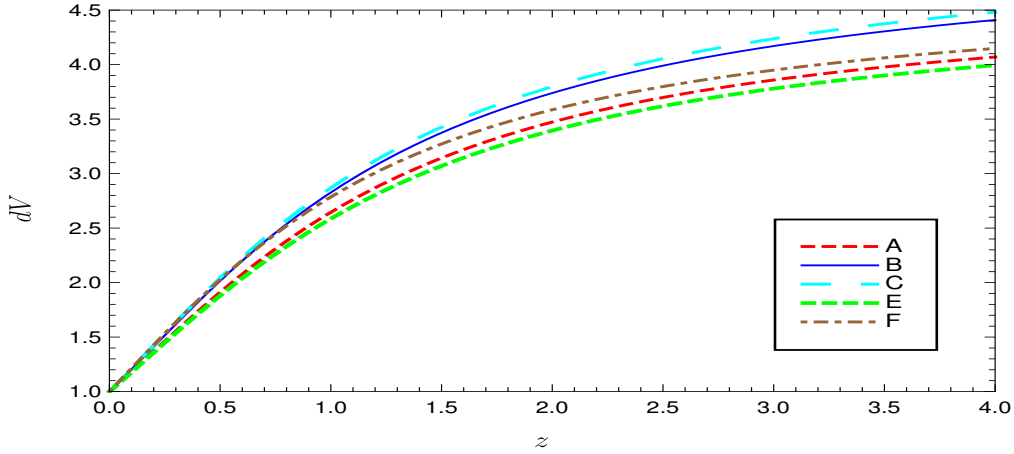
Figure 14 **Plots of $dV \equiv (dV/dZ)/(dV/dZ)_{ES}$ as a function of redshift z. The values of λ_1, λ_2 and λ_3 for each line are similar to those of the Figure (10).**

Here, the growth factor $D(z) \equiv \delta_m(z)/\delta(0)$ and $\delta(0)$ is the linear density contrast of matter perturbation at present and γ in the above equation is

$$\gamma(R) = (0.3\Omega_m h + 0.2)\Big[2.92 + \log_{10}\Big(\frac{R}{8h^{-1}Mpc}\Big)\Big]. \qquad (4.107)$$

However, using the assumption of ellipsoidal collapse of halo, the obtained mass function can fit well with N-body simulation for ΛCDM model compared with the assumption of spherical collapse of halo in Press-Schechter formalism. From the work [117], the authors have derived the mass function called *Sheth-Tormen mass function* which is given by

$$n(M)dM = -0.2709\sqrt{\frac{2}{\pi}}\bar{\rho}_m\frac{d\ln\sigma}{d\ln M}\Big[1 + 1.1096\Big(\frac{\delta_c}{\sigma}\Big)^{0.6}\Big]\exp\Big[-\frac{0.707}{2}\Big(\frac{\delta_c}{\sigma}\Big)^2\Big]\frac{dM}{M^2}. \qquad (4.108)$$

From the equation (4.108), we can compute cluster number counts per redshift with mass $M \geq M_{min}$ as

$$\frac{dN}{dz} = f_{sky}\frac{dV_e}{dz}\int_{M_{min}}^{\infty}n(M)dM, \qquad (4.109)$$

where f_{sky} is the observed sky fraction, $dV_e/dz \equiv 4\pi r^2(z)/H_0E(z)$ is the comoving volume element per unit redshift and $r(z)$ is the comoving distance.

To study the influence of disformal coupling term on the cluster number counts, we plot $(dV_e/dz)/(dV_e/dz)_{EdS}$ and $\delta_c/\sigma D(z)$ in Figures 14 and 15 respec-
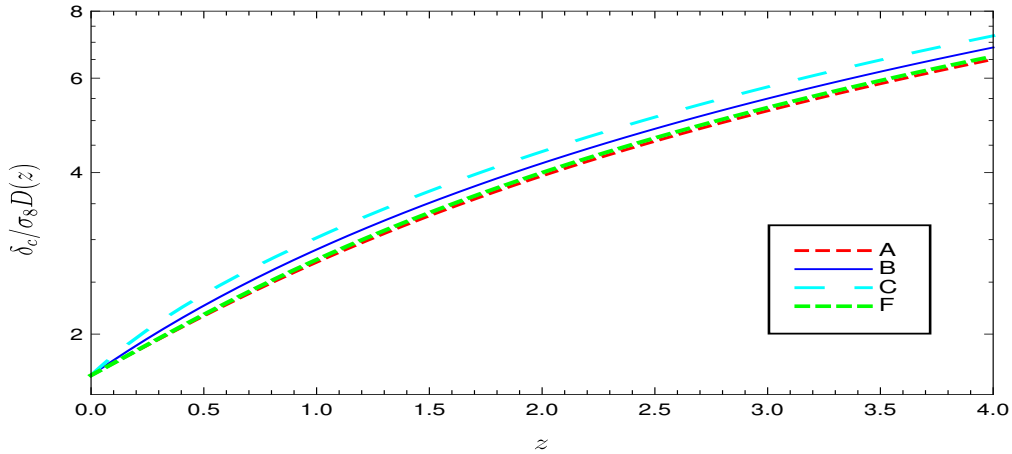
Figure 15 **Plots of $\delta_c/(\sigma_8 D(z))$ as a function of redshift z. The values of λ_1, λ_2 and λ_3 for each line are similar to those of the Figure (10).**

tively. Here, $(dV_e/dz)_{EdS}$ is the comoving volume element per unit redshift for the model of Einstein-de Sitter. It can be seen from the Figure 14 that due to large magnitude of the coupling term $\widetilde{Q_0}$, dV_e/dz for the disformally coupled model is larger than the pure conformally coupled and uncoupled models at all redshifts. However, dV_e/dz for the uncoupled model is lowest at all redshifts. In the Figure 15, we plot $\delta_c/\sigma_8 D(z)$ in order to study the influence of disformal coupling on $\delta_c/\sigma D(z)$. In this plot, we set $\sigma_8 = 0.83$ [97] for ΛCDM model and for each model, σ_8 is set such that the ratio $\delta_c/\sigma_8 D(z)$ equal to ΛCDM model at redshift $z = 0$. Based on this setting, the value of σ_8 for all models lie within the $2 - \sigma$ bound from the result of [97]. Due to high growth rate of linear density perturbation and low δ_c at late time for the disformally coupled model and $\delta_c/\sigma_8 D(z)$ equals to that for ΛCDM, the ratio $\delta_c/\sigma_8 D(z)$ for the disformally coupled model is larger than the pure conformally coupled and uncoupled models. The ratio $\delta_c/\sigma_8 D(z)$ for the uncoupled model is lowest compared with the disformally coupled and pure conformally coupled models. We now plot cluster number counts with mass $M \geq M_{min}$ as a function of redshifts in Figure 16, to see the effects of disformally coupling on the collapse regions. In this plot, we use Sheth-Tormen mass function to compute and plot the cluster number counts as a function of redshifts for each model. We also connect the results with the galaxy surveys by using the method as presented in [98, 99, 100] to compute $M_{min}(z)$ from limiting flux of the surveys. We set
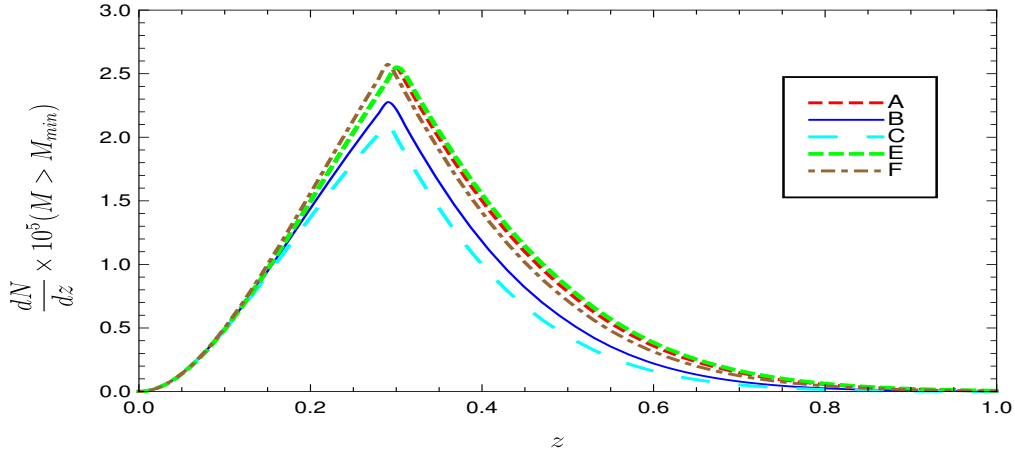
Figure 16 Plots of dN/dz **with mass** $M \geq M_{min} = 10^{14} M_\odot h^{-1}$ **as a function of redshift** z**. The values of** λ_1**,** λ_2 **and** λ_3 **for each line are similar to those of the Figure (10).**

the limiting flux $F_{lim} = 3.3 \times 10^{-14} \mathrm{ergs}^{-1}\mathrm{cm}^{-2}$ and use $f_{sky} \simeq 0.485$ according to eROSITA surveys [101] to the plot of cluster number counts in Figure 16. One can see in the Figure 16 that, due to the large $\delta_c/\sigma_8 D(z)$ for the disformally coupled model, this model can strongly suppress cluster number per redshift compared with the uncoupled model. There is not a significant difference between the conformally coupled and uncoupled models in this plot. The limiting mass $M_{min}(z)$ which depends on $E(z)$, luminosity distance d_L, limit flux F_{lim} controls shape of the graph of cluster number counts. The graph of cluster number counts seem to deviate from the bell shape because the limiting mass increases with redshift. For more detail about the investigation of the effect of disformal coupling on cluster number counts, we plot the difference ratio $\Delta_{dN} \equiv (dN/dz)/(dN/dz)_f - 1$ in Figure 17 for the disformally and conformally coupled models. Here, $(dN/dz)_f$ is dN/dz for either ΛCDM or uncoupled model. In this plot, we defined the label of each line as follows.

Lines A1, A2, B1, B2 and EL are the difference ratio between conformally coupled model A and ΛCDM model, the difference ratio between conformally coupled model A and uncoupled model, the difference ratio between disformally coupled model B and ΛCDM model, the difference ratio between disformally coupled model B and uncoupled model, the difference ratio between uncoupled and ΛCDM respectively. It can be seen from the Figure 17 that at high redshifts the difference ratio

Δ_{dN} of disformally coupled model B1 and B2 are negative and become positive at late time. The difference ratio Δ_{dN} of conformally coupled model A1 is negative and A2 is positive at high redshifts. It can be seen in the plot that at late time the line A1 converges to zero and the line A2 drops down from positive to small negative values and rapidly increases to positive values again at redshifts closed to zero. Similarly as line A2, at high redshifts the value of difference ratio for line EL are positive values. As mentioned above, this suggests that the conformally and disformally coupled models can suppress the cluster number counts at high redshifts and the strongly suppression exists in disformally coupled model. For the coupled models, the enhancement of the cluster number counts at low redshift is mainly effect by a large values of dV/dz. In addition, at high redshifts the cluster number counts does not significantly depend on the chosen value of σ_8. From the Figures 16 and 17, we have found that the difference of clusters between pure conformally coupled and ΛCDM models is ~ 6800 at $z \simeq 0.3$ and ~ 160 at $z \sim 1$. The difference number of clusters between disformally coupled and ΛCDM models is ~ 26000 at $z = 0.3$ and ~ 240 at $z = 1$. These difference number of clusters yield the uncertainties which are computed from the Poisson error of the dN/dz as $\Delta N \sim 470$ and $\Delta N \sim 14$ at redshifts 0.3 and 1 respectively. The difference of cluster number counts from the disformally coupled models are larger than the estimated in eROSITA uncertainty, $\Delta N \sim 500$ [101].
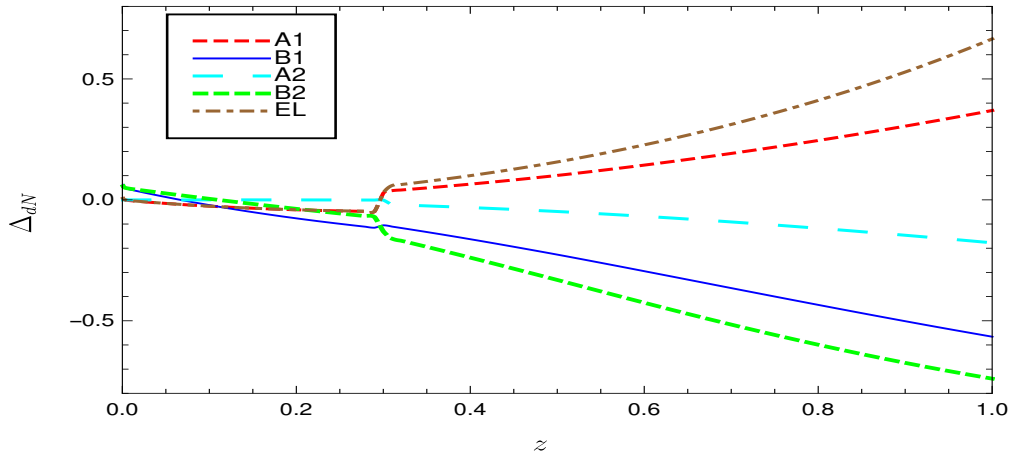
Figure 17 **Plots of different ratio $\Delta_{dN} \equiv (dN/dz)/(dN/dz)_f - 1$ from dN/dz presented in the Figure (16). Here, lines A1 and A2 represent the different ratio of line A in the Figure (16) with ΛCDM and uncoupled models respectively. Lines B1 and B2 represent the different ratio of line B in the Figure (16) with ΛCDM and uncoupled models respectively. Line E corresponds to the different ratio of uncoupled model with ΛCDM model.**

CHAPTER V

CONCLUSIONS

In this work, we study the influence of disformally coupled on the evolution of the Universe and cluster number counts of the overdense regions. We have found that when the disformal coefficient depends on the kinetic terms of scalar field, there exist two classes of fixed points. The fixed points in the first class are saddle points, and exist only when disformal coefficient depends on the kinetic terms. The fixed points in the second class can be stable when we set the parameters corresponding to the accelerating expansion of the Universe. The fixed points in this class can take different physically relevant values for the same value of the parameters of the model. The two difference values of the fixed point for the same value of the parameters can be avoided if λ_1 is larger than one or the values of r_0 and λ_4 are set from the fixed point $w_{df} \sim -0.99$ and $\Omega_{df} \gtrsim 0.9$.

In addition to the background evolution of the Universe, we also study effects of the disformal coupling between dark energy and dark matter on large scale structure using spherical collapse model and the Press-Schechter/Sheth-Torman mass function to compute cluster number counts. We have found that during matter dominated epoch, the disformally coupled models have no significant effect on the growth rate of dark matter density perturbation. Then, collapsing properties of overdense regions are not altered by disformally coupled model.

For the disformally coupled model, at late time, the growth rate of dark matter density perturbation can be enhanced due to the large coupling between dark matter and dark energy. Thus, at late time, overdense regions can collapse more efficiently indicating by low δ_c at low redshifts. In addition, comparing the conformally coupled and uncoupled models, the overdensity at virialization phase in the disformally coupled model can be suppressed at low redshifts.

Based on the Press-Schechter and Sheth-Torman mass functions, we have

found that the estimated cluster number counts per redshift strongly suppressed compared with uncoupled model at redshifts larger than 0.3 by the disformally coupled model because of a large $\delta_c/\sigma_8 D(z)$. Furthermore, increasing the disformal coupling between dark matter and dark energy at late time, the predicted cluster number counts can be increased compared with the conformally coupled and uncoupled models at low redshifts by disformally coupled because of a large comoving volume element per redshift.

REFERENCES

REFERENCES

[1] Magnan, C. (2007). Complete calculations of the perihelion precession of Mercury and the deflection of light by the Sun in General Relativity. *arXiv:0712.3709 [gr-qc]*.

[2] Biswas, A., & Mani, K. (2008). Relativistic Perihelion Precession of Orbits of Venus and the Earth. *Central European Journal of Physics*, 6, 754-758.

[3] Barone-Nugent, R. L., Wyithe, J. S. B, Trenti M., Treu, T., Oesch, P., Bouwens, R., Illingworth, G. D., & Schmidt, K. B. (2015). The Impact of Strong Gravitational Lensing on Observed Lyman-Break Galaxy Numbers at 4<z<8 in the GOODS and the XDF Blank Fields. *Monthly Notices of the Royal Astronomical Society*, 450, 2.

[4] Kaiser, N., Squires, G., & Broadhurst, T. (1995). A Method for Weak Lensing Observations. *The Astrophysical Journal*, 449, 460-475.

[5] Luppino, G. A., & Kaiser, N. (1997). Detection of Weak Lensing by a Cluster of Galaxies at z = 0.83. *The Astrophysical Journal*, 475, 20.

[6] Clifford, M. Will (2015). The 1919 measurement of the deflection of light. Classical and Quantum Gravity, 32, 124001.

[7] Titov, O., & Girdiuk, A. (2015). The deflection of light induced by the Sun's gravitational field and measured with geodetic VLBI. *Proc. of "Journees-2014" meeting (edited by Z. Malkin and N. Capitaine)*, 75-78.

[8] Giné, J. (2005). On the origin of the deflection of light. *Chaos Solitons Fractals*, 35, 1-6.

[9] Peebles, P. J. E., & Ratra, B. (2003). The Cosmological Constant and Dark Energy. *Reviews of Modern Physics*, 75, 559-606.

[10] Carroll, S. M. (2001). The Cosmological Constant. *Living Reviews in Relativity*, 4, 1.

[11] Perlmutter, S., Aldering, G., Della Valle, M., Deustua, S., Ellis, R. s., ... & Walton, N. (Supernova Cosmology Project Collaboration) (1998). Discovery of a Supernova Explosion at Half the Age of the Universe and its Cosmological Implications. *Nature*, 391, 51.

[12] Perlmutter, S., Aldering, G., Goldhaber, G., Knop, R.A., Nugent, ... & Couch, W.J. (Supernova Cosmology Project Collaboration) (1999). Measurements of Omega and Lambda from 42 High-Redshift Supernovae. *The Astrophysical Journal*, 517, 565.

[13] Riess, A. G., Filippenko, A. V., Challis, P., Clocchiattia, A., Diercks, ... & Tonry, J. (Supernova Search Team Collaboration) (1998). Observational Evidence from Supernovae for an Accelerating Universe and a Cosmological Constant. *The Astrophysical Journal*, 116, 1009.

[14] Planck Collaboration: Ade, P. A. R., Aghanim, N., Arnaud, M., Ashdown, M., Aumont, J., ... & Zonca A. (2016). Planck 2015 results. XIII. Cosmological parameters. *Astronomy & Astrophysics*, 594, A13.

[15] Komatsu, E., Smith, K. M., Dunkley, J., Bennett, C. L., Gold, B., ... & Wright, E. L. (2011). Seven-Year Wilkinson Microwave Anisotropy Probe (WMAP) Observations: Cosmological Interpretation, *The Astrophysical Journal Supplement*, 192, 18.

[16] D. Larson, Dunkley, J., Hinshaw, G., Komatsu, E., M. R. Nolta, Bennett, C. L., ... & Wright, E. L. (2011). Seven-Year Wilkinson Microwave Anisotropy Probe (WMAP) Observations: Power Spectra and WMAP-Derived Parameters. *The Astrophysical Journal Supplement*, 192, 16.

[17] Comparat, J., Delubac T., Jouvel, S., Raichoor, A., Kneib. J-P., ... & Zhang, Y. (2016). SDSS-IV eBOSS emission-line galaxy pilot survey. *Astronomy & Astrophysics*, 592, A121.

[18] Fukugita, M., Ichikawa, T., Gunn, J. E., Doi, M., Shimasaku, K., & Schneider, D. P. (1996). The Sloan Digital Sky Survey Photometric System. *Astronomical Journal*, 111, 1748.

[19] Scranton, R., Connolly, A. J., Nichol, R. C., Stebbins, A., & Szapudi, I. (2003). Physical Evidence for Dark Energy. *arXiv:astro-ph/0307335*.

[20] Sahni, V., & Starobinsky, A. (2000). The Case for a Positive Cosmological Lambda-term, *International Journal of Modern Physics D*, 9, 373-444.

[21] Carroll, S. M., Press, W. H., & Turner, E. L. (1992). The Cosmological Constant, *Annual Review of Astronomy and Astrophysics*, 30, 499-542.

[22] Riess, A. G., Filippenko, A. V., Challis, P., Clocchiattia, A., Diercks, A., ... & Tonry, J. (1998). Observational Evidence from Supernovae for an Accelerating Universe and a Cosmological Constant. *Astronomical Journal*, 116, 3.

[23] Padmanabhan, T. (2003). Cosmological Constant-the Weight of the Vacuum. *Physics Reports*, 380, 235.

[24] Sahni, V. (2002). The Cosmological Constant Problem and Quintessence. *Classical and Quantum Gravity*, 19, 3435-3448.

[25] Velten, H. E. S., vom Marttens, R. F., & Zimdahl, W. (2014). Aspects of the cosmological *coincidence problem. The European Physical Journal C*, 74, 3160.

[26] Dodelson, S., Kaplinghat, M., & Stewart, E. (2000). Solving the coincidence problem: tracking oscillating energy. *Physical Review Letters*, 85, 5276.

[27] Mifsud, J., & van de Bruck, C. (2017). Probing the imprints of generalized interacting dark energy on the growth of perturbations. *Journal of Cosmology and Astroparticle Physics*, 11, 1 (2017).

[28] He, J. H., & Wang, B. (2010). The interaction between dark energy and dark matter. *Journal of Physics: Conference Series*, **222**, 1.

[29] He, J. H., & Wang, B. (2008). Effects of the interaction between dark energy and dark matter on cosmological parameters. *Journal of Cosmology and Astroparticle Physics*, 0806, 010.

[30] Bolotin, Y. L., Kostenko, A., Lemets, O. A., & Yerokhin, D. A. (2015). Cosmological Evolution With Interaction Between Dark Energy And Dark Matter. *International Journal of Modern Physics D*, 24, 1530007 (2015).

[31] Boehmer, D. G., Caldera-Cabral, G., Lazkoz, R., & Maartens, R. (2008). Dynamics of dark energy with a coupling to dark matter. *Physical Review D*, 78, 023505.

[32] Frieman, J., Turner, M., & Huterer, D. (2008). Dark Energy and the Accelerating Universe. *Annual Review of Astronomy and Astrophysics*, 46, 385-432.

[33] Armendariz-Picon, C., Mukhanov, V. F. , & Steinhardt, P. J. (2000). A Dynamical Solution to the Problem of a Small Cosmological Constant and Late-time Cosmic Acceleration. *Physical Review Letters*, 85, 4438-4441.

[34] de Putter, R., & Linder, E. V. (2007). Kinetic k-essence and Quintessence. *Astroparticle Physics*, 28, 263-272.

[35] Myrzakul, S., Myrzakulov, R., & Sebastiani, L. (2016). K-essence in Horndeski models. *Astrophysics and Space Science*, 361, 254.

[36] Carlberg, R. G. (2018). Globular Clusters in a Cosmological N-body Simulation. *The Astrophysical Journal*, 861, 1.

[37] Adamek, J., Daverio, D., Durrer, R., & Kunz, M. (2016). gevolution: a cosmological N-body code based on General Relativity. *Journal of Cosmology and Astroparticle Physics*, 1607, 053.

[38] Pace, F., Waizmann, J. C., & Bartelmann, M. (2010). Spherical collapse model in dark energy cosmologies. *Monthly Notices of the Royal Astronomical Society*, 406, 1865-1874.

[39] N. J. Nunes, N. J., & Mota, D. F. (2006). Structure Formation in Inhomogeneous Dark Energy Models. *Monthly Notices of the Royal Astronomical Society*, 368, 751-758.

[40] Peacock, J. A., & Dodds, S. D. (1996). Non-linear evolution of cosmological power spectra. *Monthly Notices of the Royal Astronomical Society*, 280, 3, L19.

[41] Angrick, C., & Bartelmann, M. (2010). Triaxial collapse and virialisation of dark-matter haloes. *Astronomy & Astrophysics*, 518, A38.

[42] Gunn, J. E., Gott, I., & Richard, J. (1972). On the Infall of Matter Into Clusters of Galaxies and Some Effects on Their Evolution. *The Astrophysical Journal*, 176, 1.

[43] Lima, J. A. S., Zanchin, V., & Brandenberger, R. (1997). On the Newtonian Cosmology Equations with Pressure. *Monthly Notices of the Royal Astronomical Society*, 291, L1-L4.

[44] Malekjani, M., Basilakos, S., & Heidari, N. (2017). Spherical collapse model and cluster number counts in power law $f(T)$ gravity. *Monthly Notices of the Royal Astronomical Society*, 466, 3488.

[45] Chamseddine, A. H., & Mukhanov, V. F. (2016). Inhomogeneous Dark Energy, *Journal of Cosmology and Astroparticle Physics*, 1602, 02, 040.

[46] Faraoni, V., Dent, J. B., & Saridakis, E. N. (2014). Covariantizing the interaction between dark energy and dark matter. *Physical Review D*, 90, 063510.

[47] Ferreira, E. G. M., Quintin, J., Costa, A. A., Abdalla, E., & Wang, B. (2017). Evidence for interacting dark energy from BOSS. *Physical Review D*, 95, 043520.

[48] Salvatelli, V., Said, N., Bruni, M., Melchiorri, A., & Wands, D. (2014). Indications of a late-time interaction in the dark sector. *Physical Review Letters*, 113, 181301.

[49] Amendola, L., & Quercellini, C. (2003). Tracking and coupled dark energy as seen by WMAP. *Physical Review D*, 68, 023514.

[50] Amendola, L. (2004). Linear and non-linear perturbations in dark energy models. *Physical Review D*, 69, 103524 (2004).

[51] van de Bruck, C., & Mifsud, J. (2018). Searching for dark matter - dark energy interactions: going beyond the conformal case, *Physical Review D*, 97, 023506 (2018).

[52] Perlmutter, S., Aldering, G., Goldhaber, G., Knop, R. A., Nugent, P., ... & Couch, W. J. (1999). Measurements of Omega and Lambda from 42 High-Redshift Supernovae. *The Astrophysical Journal*, 517, 565-586.

[53] Chimento, L. P., Jakubi, A. S., Pavon, D., & Zimdahl, W. (2003). Interacting quintessence solution to the coincidence problem. *Physical Review D*, 67, 083513.

[54] Zlatev, I., Wang, L., & Steinhardt, P. J. (1999). Quintessence, Cosmic Coincidence, and the Cosmological Constant. *Physical Review Letters*, 82, 896-899.

[55] Johri, V. B. (2002). Search for Tracker Potentials in Quintessence Theory. *Classical and Quantum Gravity*, 19, 5959-5968.

[56] Tsujikawa, S. (2013). Quintessence: A Review, *Classical and Quantum Gravity*, 30, 214003.

[57] Mannheim, P. D. (2006). Alternatives to Dark Matter and Dark Energy. *Progress in Particle and Nuclear Physics*, 56, 340.

[58] Karwan, K. (2008). The Coincidence Problem and Interacting Holographic Dark Energy. *Journal of Cosmology and Astroparticle Physics*, 0805, 011.

[59] Copeland, E. J., Sami, M., & Tsujikawa, S. (2006). Dynamics of dark energy. *International Journal of Modern Physics D*, 15, 1753-1936.

[60] Amendola, L. (2000). Coupled Quintessence, *Physical Review D*, 62, 043511.

[61] Mangano, G., Miele, G., & Pettorino, V. (2003). Coupled quintessence and the coincidence problem. *Modern Physics Letters A*, 18, 831-842.

[62] Boehmer, C. G., Caldera-Cabral, G., Lazkoz R., & Maartens, R. (2008). Dynamics of dark energy with a coupling to dark matter. *Physical Review D*, 78, 023505.

[63] Bisabr, Y. (2010). Coincidence Problem in $f(R)$ Gravity Models. *Physical Review D*, 82, 124041.

[64] Bisabr, Y. (2012). A comparison of search templates for gravitational waves from binary inspiral - 3.5PN update. *Gravitation and Cosmology*, 18, 151.

[65] Carroll, S. M., Duvvuri, V., Trodden, M., Turner, M. S. (2004). Is Cosmic Speed-Up Due to New Gravitational Physics?. *Physical Review D*, 70, 043528.

[66] Buchdahl, H. A. (1970). Non-linear Lagrangians and cosmological theory. *Monthly Notices of the Royal Astronomical Society*, 150, 1.

[67] Brans, C., & Dicke, R. H. (1961). Mach's Principle and a Relativistic Theory of Gravitation. *Physical Review*, 124, 925.

[68] Amendola, L. (1999). Scaling solutions in general nonminimal coupling theories. *Physical Review D*, 60, 043501.

[69] Milgrom, M. (1983). A modification of the Newtonian dynamics as a possible alternative to the hidden mass hypothesis, *The Astrophysical Journal*, 270, 365.

[70] Bekenstein, J. D. (2004). Relativistic gravitation theory for the modified Newtonian dynamics paradigm. *Physical Review D*, 70, 083509.

[71] Dvali, G. R., Gabadadze, G., & Porrati, M. (2000). 4D Gravity on a Brane in 5D Minkowski Space. *Physics Letters B*, 485, 208.

[72] B. Zwiebach, B. (1985). Curvature squared terms and string theories. *Physics Letters B*, 156, 315.

[73] Nojiri, S., Odintsov, S. D., & Sasaki, M. (2005). Gauss-Bonnet dark energy, *Physical Review D*, 71, 123509.

[74] Lovelock, D. (1971). The Einstein Tensor and Its Generalizations. *Journal of Mathematical Physics*, 12, 498.

[75] Horava, P. (2009). Quantum Gravity at a Lifshitz Point. *Physical Review D*, 79, 084008.

[76] Bengochea, G. R. & Ferraro, R. (2009). Dark torsion as the cosmic speed-up. *Physical Review D*, 79, 124019.

[77] Linder, E. V. (2010). Einstein's other gravity and the acceleration of the Universe. *Physical Review D*, 81, 127301.

[78] Panpanich, S., Maeda, K., & Mizuno, S. (2017). Cosmological dynamics of D-BIonic and DBI scalar field and coincidence problem of dark energy. *Physical Review D*, 95, 103520.

[79] Amendola, L., and Tsujikawa, S. (2010). *Dark Energy: Theory and observations* (1st ed.). Cambridge University Press.

[80] Bekenstein, J. D. (1993). Relation between physical and gravitational geometry. *Physical Review D*, 48, 3641.

[81] Koivisto, T. S., Mota, D. F. & Zumalacarregui, M. (2012). Screening Modifications of Gravity through Disformally Coupled Fields. *Physical Review Letters*, 109, 241102.

[82] Zumalacarregui, M., & García-Bellido, J. (2014). Transforming gravity: from derivative couplings to matter to second-order scalar-tensor theories beyond the Horndeski Lagrangian. *Physical Review D*, 89, 064046.

[83] Ostrogradski, M. (1850). Memoires sur les equations differentielles relatives au probleme des isoperimetres. *Mémoires de l'Académie Impériale des Sciences de St. Pétersbourg*, VI, 385.

[84] Horndeski, G. W. (1974). Second-order scalar-tensor field equations in a four-dimensional space. *International Journal of Theoretical Physics*, 10, 363.

[85] Zumalacarregui, M., Koivisto, T. S. & Mota, D. F. (2013). DBI Galileons in the Einstein Frame: Local Gravity and Cosmology. *Physical Review D*, 87, 083010.

[86] Gleyzes, J., Langlois, D., Piazza, F., & Vernizzi, F. (2015). Healthy theories beyond Horndeski. *Physical Review Letters*, 114, 211101.

[87] Tsujikawa, S. (2015). Disformal invariance of cosmological perturbations in a generalized class of Horndeski theories. *Journal of Cosmology and Astroparticle Physics*, 1504, 043.

[88] van de Bruck, C., & Morrice, J. (2015). Disformal couplings and the dark sector of the Universe. *Journal of Cosmology and Astroparticle Physics*, 04, 036.

[89] Deruelle, N., & Rua, J. (2014). Disformal Transformations, Veiled General Relativity and Mimetic Gravity. *Journal of Cosmology and Astroparticle Physics*, 09, 002.

[90] Fujita, T., Gao, X., & Yokoyama, J. (2016). Spatially covariant theories of gravity: disformal transformation, cosmological perturbations and the Einstein frame. *Journal of Cosmology and Astroparticle Physics*, 02, 014.

[91] Boehmer, D. G., & Chan, N. (2014). Dynamical systems in cosmology. *arXiv:1409.5585 [gr-qc]*.

[92] Wetterich, C. (1995). The cosmon model for an asymptotically vanishing time-dependent cosmological *constant. Astronomy & Astrophysics*, 301, 321.

[93] Bahamonde, S., Boehmer, C. G., Carloni, S., Copeland, E. J., Fang, w., & Tamanini, N. (2017). Dynamical systems applied to cosmology: dark energy and modified gravity. *arXiv:1712.03107 [gr-qc]*.

[94] Holden, D. J., & Wands, D. (2000). Self-similar cosmological solutions with a non-minimally coupled scalar field. *Physical Review D*, 61, 043506.

[95] Jamil, M., Momeni, D., & Myrzakulov, R. (2012). Stability of a non-minimally conformally coupled scalar field in $F(T)$ cosmology. *The European Physical Journal C*, 72, 2075.

[96] Sakstein, J. (2015). Towards Viable Cosmological Models of Disformal Theories of Gravity. *Physical Review D*, 91, 024036.

[97] Ade, P. A. R., Aghanim, N., Arnaud, M., Ashdown, M., Aumont, J., Baccigalupi, C., ... & Zonca, A. (2016). Planck 2015 results. XIII. Cosmological parameters. *Astronomy & Astrophysics*, 594, A13.

[98] Basilakos, S., Plionis, M., & Lima, J. A. S. (2010). Confronting Dark Energy Models using Galaxy Cluster Number Counts. *Physical Review D*, 82, 083517.

[99] Fedeli, C., Moscardini, L., & Matarrese, S. (2009). The clustering of galaxy clusters in cosmological models with non-Gaussian initial conditions: Predictions for future surveys. *Monthly Notices of the Royal Astronomical Society*, 397, 1125.

[100] Devi, N. C., Gonzalez, J. E., & Alcaniz, J. S. (2014). Constraining thawing and freezing models with cluster number counts. *Journal of Cosmology and Astroparticle Physics*, 1406, 055.

[101] Merloni, A., Predehl, P., Becker, W., Böhringer, H., Boller, T., Brunner, H., ... & German eROSITA Consortium. (2012). eROSITA Science Book: Mapping the Structure of the Energetic Universe. *arXiv:1209.3114 [astro-ph.HE]*.

[102] Corasaniti, P. S., Bassett, B. A., Ungarelli, C., & Copeland, E. J. (2003). Model-Independent Dark Energy Differentiation with the Integrated Sachs-Wolfe Effect. *Physical Review Letters*, 90, 091303.

[103] Parkinson, D., Riemer-Sorensen, S., Blake, D., Poole, G. B., Davis, T. M., ... & Yee, H. K. C. (2012). The WiggleZ Dark Energy Survey: Final data release and cosmological results. *Physical Review D*, 86, 103518.

[104] Hawkins, E., Maddox, S., Cole, S., Lahav, O., Madgwick, D., Norberg, P., ... & Taylor, K. (The 2dFGRS Team). (2003). The 2dF Galaxy Redshift Survey: correlation functions, peculiar velocities and the matter density of the Universe. *Monthly Notices of the Royal Astronomical Society*, 346, 78.

[105] Wintergerst, N., & Pettorino, V. (2010). Clarifying spherical collapse in coupled dark energy cosmologies. *Physical Review D*, 82, 103516.

[106] Ryden, B. (2003). *Introduction to Cosmology*. Addison-Wesley.

[107] Logsdon, T. (1998). *Orbital Mechanics: theory and applications*. John Wiley & Sons.

[108] Collins, G. W. (1978). *The Virial Theorem in Stellar Astrophysics*. Pachart Publishing House, 1978.

[109] Colless, M., & Dunn, A. M. (1996). Structure and Dynamics of the Coma Cluster. *The Astrophysical Journal*, 458, 435.

[110] Mukhanov, V. F., Feldman, H. A. & Brandenberger, R. H. (1992). Theory of cosmological perturbations. *Physics Reports*, 215, 203-333.

[111] Karwan, K., & Sapa, S. (2017). Dynamics of the universe with disformal coupling between the dark sectors. *The European Physical Journal C*, 77, 352.

[112] Manera M., & Mota, D. F. (2006). Cluster number counts dependence on dark energy inhomogeneities and coupling to dark matter. *Monthly Notices of the Royal Astronomical Society*, 371, 1373.

[113] Bartelmann, M., Doran, M., & Wetterich, C. (2006). Non-linear Structure Formation in Cosmologies with Early Dark Energy. *Astronomy & Astrophysics*, 454, 27-36.

[114] Horellou, C., & Berge, J. (2005). Dark energy and the evolution of spherical overdensities. *Monthly Notices of the Royal Astronomical Society*, 360, 1393-1400.

[115] Landau, L. D., & Lifshitz E. M. (1960). *Mechanics*. Pergamon Press, Oxford.

[116] Viana, P., & Liddle, A. (1999). Galaxy clusters at $0.3 < z < 0.4$ and the value of Ω_0. *Monthly Notices of the Royal Astronomical Society*, 303, 535.

[117] Sheth, R. K., & Tormen, G. (1999). Large scale bias and the peak background split. *Monthly Notices of the Royal Astronomical Society*, 308, 119.

APPENDIX

APPENDIX A PERTURBATION OF Q

In this appendix we explicitly show the computation for perturbation of the coupling term Q from the equations (2.45) and (2.46). We begin the calculation using the energy-momentum tensor for perfect fluid as

$$T^{\alpha\beta} = \begin{bmatrix} \rho_m & 0 & 0 & 0 \\ 0 & p & 0 & 0 \\ 0 & 0 & p & 0 \\ 0 & 0 & 0 & p \end{bmatrix}, \tag{A.1}$$

where we set $c = 1$. From the metric perturbation in Newtonian gauge given in equation (4.5), we can write components 00 and ij of the metric perturbation and also the inverse metric perturbation as

$$g_{00} = \bar{g}_{00} + \delta g_{00} = -1 - 2\Phi, \quad g_{ij} = \bar{g}_{ij} + \delta g_{ij} = a^2(1 - 2\Phi)\delta_{ij}, \tag{A.2}$$

$$g^{00} = \bar{g}^{00} + \delta g^{00} = -1 + 2\Phi, \quad g^{ij} = \bar{g}^{ij} + \delta g^{ij} = \frac{1}{a^2}(1 + 2\Phi)\delta^{ij}. \tag{A.3}$$

We use the metric perturbation in Newtonian gauge, small scales limit and use the energy-momentum tensor for perfect fluid given in equation (A.1) to compute the perturbation for the coupling term Q. From the equation (2.39)

$$T_m = g_{\alpha\beta}T^{\alpha\beta} = g_{\alpha\beta}g^{\rho\beta}T^{\alpha}_{\rho}, \tag{A.4}$$

the perturbation of the above equation is

$$\begin{aligned} \delta T_m &= (\delta g_{\alpha\beta})\bar{g}^{\rho\beta}\bar{T}^{\alpha}_{\rho} + \bar{g}_{\alpha\beta}(\delta g^{\rho\beta})\bar{T}^{\alpha}_{\rho} + \bar{g}_{\alpha\beta}\bar{g}^{\rho\beta}\delta T^{\alpha}_{\rho} \\ &= (\delta g_{00})\bar{g}^{00}\bar{T}^{0}_{0} + \bar{g}_{00}(\delta g^{00})\bar{T}^{0}_{0} + \bar{g}_{00}\bar{g}^{00}\delta T^{0}_{0} + \bar{g}_{ij}\bar{g}^{ij}\delta T^{i}_{j} \\ &= 2\Phi\rho_m - 2\Phi\rho_m - \delta\rho_m \\ &= -\delta\rho_m. \end{aligned} \tag{A.5}$$

From the equation (2.40)

$$T_{mp} = \phi_{,\alpha}\phi_{,\beta}T^{\alpha\beta} = \phi_{,\alpha}\phi_{,\beta}g^{\rho\beta}T^{\alpha}_{\rho}, \tag{A.6}$$

the perturbation of the above equation is shown below

$$\begin{aligned}
\delta T_{mp} &= \bar{\phi}_{,\alpha}\bar{\phi}_{,\beta}[\delta g^{\rho\beta}\bar{T}^{\alpha}_{\rho} + \bar{g}^{\rho\beta}\delta T^{\alpha}_{\rho}] = \bar{\phi}_{,0}\bar{\phi}_{,0}[\delta g^{00}\bar{T}^0_0 + \bar{g}^{00}\delta T^0_0] \\
&= \dot{\bar{\phi}}^2(2\Phi\bar{\rho}_m + \delta\rho_m) = \dot{\bar{\phi}}^2\delta\rho_m \\
&= 2\bar{X}\delta\rho_m, \tag{A.7}
\end{aligned}$$

where we neglect the terms proportional to Φ in the small scales. From the equation (2.45), the perturbation calculation for θ_1 is expressed below

$$\theta_1 = T^{\alpha\beta}\phi_{,\alpha\beta} = T^{\alpha\beta}\nabla_\alpha\partial_\beta\phi = T^{\alpha\beta}\partial_\alpha\partial_\beta\phi - T^{\alpha\beta}\Gamma^\rho_{\alpha\beta}\partial_\rho\phi,$$

$$\delta\theta_1 = \delta(T^{\alpha\beta}\partial_\alpha\partial_\beta\phi) - \delta(T^{\alpha\beta}\Gamma^\rho_{\alpha\beta}\partial_\rho\phi) = A_1 + A_2, \tag{A.8}$$

$$A_1 = \delta(T^{\alpha\beta}\partial_\alpha\partial_\beta\phi) = \partial_\alpha\partial_\beta\bar{\phi}(\delta T^{\alpha\beta}). \tag{A.9}$$

From the energy-momentum of matter

$$T^{\alpha\beta} = U^\alpha U^\beta \rho_m, \tag{A.10}$$

the calculation for perturbation of the above equation shown below

$$\begin{aligned}
\delta T^{\alpha\beta} &= U^\alpha U^\beta \delta\rho_m + 2\bar{\rho}_m U^\alpha \delta U^\beta, \\
\delta T^{00} &= U^0 U^0 \delta\rho_m + 2\bar{\rho}_m U^0 \delta U^0 = (1-\Phi)^2\delta\rho_m + 2\bar{\rho}_m(1-\Phi)(-\Phi), \\
&\approx \delta\rho_m \tag{A.11}
\end{aligned}$$

where $1 - \Phi \approx 1$ in small scales limit. From the equation (A.9), we obtain A_1 as

$$A_1 = \partial_0\partial_0\bar{\phi}\delta T^{00} \approx \ddot{\bar{\phi}}\delta\rho_m. \tag{A.12}$$

Consider A_2 from the equation (A.8)

$$A_2 = -\delta(T^{\alpha\beta}\Gamma^\rho_{\alpha\beta}\partial_\rho\phi) = -\delta(\Gamma^\rho_{\alpha\beta}g^{\sigma\beta}T^\alpha_\sigma\partial_\rho\phi)$$

$$= -(\delta\Gamma^\rho_{\alpha\beta})\bar{g}^{\sigma\beta}\bar{T}^\alpha_\sigma\partial_\rho\bar{\phi} - \bar{\Gamma}^\rho_{\alpha\beta}(\delta g^{\sigma\beta})\bar{T}^\alpha_\sigma\partial_\rho\bar{\phi} - \bar{\Gamma}^\rho_{\alpha\beta}\bar{g}^{\sigma\beta}(\delta T^\alpha_\sigma)\partial_\rho\bar{\phi}$$

$$= -(\delta\Gamma^0_{00})\bar{g}^{00}\bar{T}^0_0\partial_0\bar{\phi} - \bar{\Gamma}^0_{0\beta}\cancel{(\delta g^{0\beta})\bar{T}^0_0\partial_0\bar{\phi}} - \bar{\Gamma}^0_{\alpha\beta}\bar{g}^{\sigma\beta}(\delta T^\alpha_\sigma)\partial_0\bar{\phi}$$

$$= -\dot{\bar{\phi}}\bar{g}^{00}\bar{T}^0_0\delta\Gamma^0_{00} - \dot{\bar{\phi}}\bar{g}^{\sigma\beta}\bar{\Gamma}^0_{\alpha\beta}\delta T^\alpha_\sigma, \tag{A.13}$$

$$\delta\Gamma^\lambda_{\mu\nu} = -\bar{g}^{\lambda\beta}\delta g_{\beta\gamma}\bar{\Gamma}^\gamma_{\mu\nu} + \frac{1}{2}\bar{g}^{\lambda\alpha}(\partial_\mu\delta g_{\alpha\nu} + \partial_\nu\delta g_{\alpha\mu} - \partial_\alpha\delta g_{\mu\nu}),$$

$$\delta\Gamma^0_{00} = -\cancel{\bar{g}^{0\beta}\delta g_{\beta\gamma}\bar{\Gamma}^\gamma_{00}} + \frac{1}{2}\bar{g}^{0\alpha}(\partial_0\delta g_{\alpha0} + \partial_0\delta g_{\alpha0} - \partial_\alpha\delta g_{00}),$$

$$= \frac{1}{2}\bar{g}^{00}\partial_0\delta g_{00} = -\frac{1}{2}\partial_0(-2\Phi) = \partial_0\Phi \approx 0, \tag{A.14}$$

$$A_2 = -\dot{\bar{\phi}}\bar{g}^{\sigma\beta}\bar{\Gamma}^0_{\alpha\beta}\delta T^\alpha_\sigma = -\dot{\bar{\phi}}\bar{g}^{\sigma j}\bar{\Gamma}^0_{ij}\delta T^i_\sigma = -\dot{\bar{\phi}}\bar{g}^{kj}\bar{\Gamma}^0_{ij}\delta T^i_k \tag{A.15}$$

$$\bar{g}^{kj} = \frac{\delta^{kj}}{a^2}, \quad \bar{\Gamma}^0_{ij} = Ha^2\delta_{ij} \tag{A.16}$$

$$\delta T^\alpha_\beta = \bar{\rho}_m(\bar{U}^\alpha\delta U_\beta + \bar{U}_\beta\delta U^\alpha + \delta U^\alpha\delta U_\beta)$$

$$+ \delta\rho_m(\bar{U}^\alpha\bar{U}_\beta + \bar{U}^\alpha\delta U_\beta + \bar{U}_\beta\delta U^\alpha + \delta U^\alpha\delta U_\beta) \tag{A.17}$$

$$\delta T^i_k = \bar{\rho}_m(\cancel{\bar{U}^i\delta U_k} + \cancel{\bar{U}_k\delta U^i} + \delta U^i\delta U_k)$$

$$+ \delta\rho_m(\cancel{\bar{U}^i\bar{U}_k} + \cancel{\bar{U}^i\delta U_k} + \cancel{\bar{U}_k\delta U^i} + \delta U^i\delta U_k)$$

$$= \bar{\rho}_m\delta U^i\delta U_k + \delta\rho_m\delta U^i\delta U_k = (\bar{\rho}_m + \delta\rho_m)\delta U^i\delta U_k$$

$$= \rho_m v^i v_k \tag{A.18}$$

$$A_2 = -\dot{\bar{\phi}}\frac{\delta^{kj}}{a^2}Ha^2\delta_{ij}\rho_m v^i v_k = -\dot{\bar{\phi}}H\rho_m v^i v_k \tag{A.19}$$

Then, we obtain the perturbation for θ_1 as

$$\delta\theta_1 = \ddot{\bar{\phi}}\delta\rho_m - \dot{\bar{\phi}}H\rho_m v^i v_k. \tag{A.20}$$

The perturbation calculation for θ_2 from the equation (2.45) shown below

$$\theta_2 = \phi_{,\alpha}X_{,\beta}T^{\alpha\beta} = \phi_{,\alpha}X_{,\beta}g^{\rho\beta}T^\alpha_\rho,$$

$$\delta\theta_2 = \bar{\phi}_{,\alpha}(\delta X_{,\beta})\bar{g}^{\rho\beta}\bar{T}^\alpha_\rho + \bar{\phi}_\alpha\bar{X}_{,\beta}(\delta g^{\rho\beta})\bar{T}^\alpha_\rho + \bar{\phi}_{,\alpha}\bar{X}_{,\beta}\bar{g}^{\rho\beta}\delta T^\alpha_\rho,$$

$$= B_1 + B_2 + B_3. \tag{A.21}$$

From the kinetic energy of the scalar field $X = \frac{1}{2}g^{\lambda\sigma}\partial_\lambda\phi\partial_\sigma\phi$, thus we have

$$X_{,\beta} = -\frac{1}{2}(\partial_\beta g^{\lambda\sigma})\partial_\lambda\phi\partial_\sigma\phi - g^{\lambda\sigma}(\partial_\lambda\phi)\partial_\beta\partial_\sigma\phi, \tag{A.22}$$

$$\delta X_{,\beta} = -\frac{1}{2}(\partial_\beta\delta g^{\lambda\sigma})\partial_\lambda\bar\phi\partial_\sigma\bar\phi - \delta g^{\lambda\sigma}(\partial_\lambda\bar\phi)\partial_\beta\partial_\sigma\bar\phi. \tag{A.23}$$

Using equations (A.22) and (A.23), hence B_1, B_2 and B_3 become

$$\begin{aligned}
B_1 &= -\bar\phi_{,\alpha}\bar g^{\rho\beta}\bar T^\alpha_\rho\left[\frac{1}{2}(\partial_\beta\delta g^{\lambda\sigma})\bar\phi_{,\lambda}\bar\phi_{,\sigma} + \delta g^{\lambda\sigma}\bar\phi_{,\lambda}\bar\phi_{,\sigma\beta}\right] \\
&= -\bar\phi_{,0}\bar g^{0\beta}\bar T^0_0\left[\frac{1}{2}(\partial_\beta\delta g^{00})\bar\phi_{,0}\bar\phi_{,0} + \delta g^{00}\bar\phi_{,0}\bar\phi_{,0\beta}\right] \\
&= \dot{\bar\phi}\bar g^{0\beta}\bar\rho_m\left[\frac{1}{2}\dot{\bar\phi}^2\partial_\beta(2\Phi) + 2\Phi\dot{\bar\phi}\dot{\bar\phi}_{,\beta}\right] \\
&= -4\bar\rho_m\bar X\ddot{\bar\phi}\Phi \approx 0, \tag{A.24}
\end{aligned}$$

$$\begin{aligned}
B_2 &= -\bar\phi_{,\alpha}\bar T^\alpha_\rho\delta g^{\rho\beta}\left[\frac{1}{2}\bar\phi_{,\lambda}\bar\phi_{,\sigma}\partial_\beta\bar g^{\lambda\sigma} + \bar g^{\lambda\sigma}\bar\phi_{,\lambda}\bar\phi_{,\sigma\beta}\right] \\
&= -4\bar\rho_m\bar X\ddot{\bar\phi}\Phi \approx 0, \tag{A.25}
\end{aligned}$$

$$\begin{aligned}
B_3 &= -\bar\phi_{,\alpha}\bar g^{\rho\beta}\delta T^\alpha_\rho\left[\frac{1}{2}\bar\phi_{,\lambda}\bar\phi_{,\sigma}\partial_\beta\bar g^{\lambda\sigma} + \bar g^{\lambda\sigma}\bar\phi_{,\lambda}\bar\phi_{,\sigma\beta}\right] \\
&= 2\bar X\ddot{\bar\phi}\delta\rho_m. \tag{A.26}
\end{aligned}$$

From the equations (A.24) - (A.26), we get

$$\delta\theta_2 = 2\bar X\ddot{\bar\phi}\delta\rho_m. \tag{A.27}$$

We calculate the perturbation for θ_3 as follows

$$\theta_3 = \phi_{,\alpha}\nabla_\mu T^{\alpha\mu} = \phi_{,\alpha}g^{\alpha\nu}\nabla_\mu T^\mu_\nu,$$

$$\delta\theta_3 = \bar\phi_{,\alpha}(\delta g^{\alpha\nu})\nabla_\mu\bar T^\mu_\nu + \bar\phi_{,\alpha}\bar g^{\alpha\nu}\delta(\nabla_\mu T^\mu_\nu) = C_1 + C_2. \tag{A.28}$$

Using the definition of covariant derivative, we can write C_1 as follows

$$\begin{aligned}
C_1 &= \bar\phi_{,0}(\delta g^{00})\nabla_\mu\bar T^\mu_0 = 2\dot{\bar\phi}\Phi\left[\partial_\mu\bar T^\mu_0 + \bar\Gamma^\mu_{\mu\rho}\bar T^\rho_0 - \bar\Gamma^\rho_{\mu0}\bar T^\mu_\rho\right] \\
&= -2\dot{\bar\phi}\Phi(\dot{\bar\rho}_m + 3H\bar\rho_m) \approx 0. \tag{A.29}
\end{aligned}$$

Similarly as C_1, we can write C_2 from the equation (A.28) as follows

$$
\begin{aligned}
C_2 &= \bar{\phi}_{,\alpha} \bar{g}^{\alpha\nu} \delta [\partial_\mu T^\mu_\nu + \Gamma^\mu_{\mu\rho} T^\rho_\nu - \Gamma^\rho_{\mu\nu} T^\mu_\rho] \\
&= \bar{\phi}_{,\alpha} \bar{g}^{\alpha\nu} [\partial_\mu \delta T^\mu_\nu + \bar{\Gamma}^\mu_{\mu\rho} \delta T^\rho_\nu + \bar{T}^\rho_\nu \delta \Gamma^\mu_{\mu\rho} - \bar{\Gamma}^\rho_{\mu\nu} \delta T^\mu_\rho - \bar{T}^\mu_\rho \delta \Gamma^\rho_{\mu\nu}] \\
&= -\dot{\bar{\phi}} [\partial_\mu \delta T^\mu_0 + \bar{\Gamma}^\mu_{\mu\rho} \delta T^\rho_0 - \bar{\rho}_m \delta \Gamma^\mu_{\mu 0} - \bar{\Gamma}^\rho_{\mu 0} \delta T^\mu_\rho + \bar{\rho}_m \delta \Gamma^0_{00}].
\end{aligned}
\tag{A.30}
$$

Consider the first term in the bracket of the above equation, we have

$$
\partial_\mu \delta T^\mu_0 = \partial_0 \delta T^0_0 + \partial_i \delta T^i_0 = -\delta \dot{\rho}_m + \partial_i \delta T^i_0,
\tag{A.31}
$$

$$
T^\alpha_\beta = \rho_m U^\alpha U_\beta,
$$

$$
\delta T^\alpha_\beta = U^\alpha U_\beta \delta \rho_m + \bar{\rho}_m \delta(U^\alpha U_\beta),
$$

$$
\delta T^\alpha_0 = U^\alpha U_0 \delta \rho_m + \bar{\rho}_m \delta(U^\alpha U_0),
$$

$$
\partial_\alpha \delta T^\alpha_0 = \partial_\alpha [U^\alpha U_0 \delta \rho_m + \bar{\rho}_m \delta(U^\alpha U_0)] = \partial_\alpha [-U^\alpha \delta \rho_m + \bar{\rho}_m (U^\alpha \delta U_0 + U_0 \delta \bar{U}^\alpha)]
$$

$$
= \partial_\alpha [-U^\alpha \delta \rho_m + + \rho U_0 \delta U^\alpha]
$$

$$
= -(\partial_\alpha U^\alpha) \delta \rho_m - U^\alpha \partial_\alpha \delta \rho_m + (\partial_\alpha \bar{\rho})_m U_0 \delta U^\alpha + \bar{\rho}_m (\partial_\alpha U_0) \delta U^\alpha + \bar{\rho}_m U_0 \partial_\alpha \delta U^\alpha,
$$

$$
\partial_i \delta T^i_0 = -(\partial_i U^i) \delta \rho_m - U^i \partial_i \delta \rho_m + U_0 (\partial_i \bar{\rho}_m) \delta U^i + \bar{\rho}_m (\partial_i U_0) \delta U^i + \bar{\rho}_m U_0 \partial_i \delta U^i
$$

$$
= -(\partial_i v^i) \delta \rho_m - v^i \partial_i \delta \rho_m - \bar{\rho}_m (1 + \Phi) \partial_i v^i
$$

$$
= -(\partial_i v^i) \delta \rho_m - v^i \partial_i \delta \rho_m - \bar{\rho}_m \partial_i v^i.
\tag{A.32}
$$

From the equations (A.31) and (A.32), we obtain

$$
\partial_\mu \delta T^\mu_0 = -\delta \dot{\rho}_m - (\partial_i v^i) \delta \rho_m - v^i \partial_i \delta \rho_m - \bar{\rho}_m \partial_i v^i.
\tag{A.33}
$$

Consider the second term in the bracket of C_2, we get

$$
\begin{aligned}
\bar{\Gamma}^\mu_{\mu\rho} \delta T^\rho_0 &= \bar{\Gamma}^\mu_{\mu 0} \delta T^0_0 + \bar{\Gamma}^\mu_{\mu i} \delta T^i_0 = (\bar{\Gamma}^0_{00} + \bar{\Gamma}^i_{i0}) \delta T^0_0 + (\bar{\Gamma}^0_{0i} + \bar{\Gamma}^j_{ji}) \delta T^i_0 = \bar{\Gamma}^i_{i0} \delta T^i_0 \\
&= -3H \delta \rho_m.
\end{aligned}
\tag{A.34}
$$

Consider the third term in the bracket of C_2, we get

$$
\begin{aligned}
\delta\Gamma^{\mu}_{\mu 0} &= \cancel{\delta\Gamma^{\mu}_{\mu 0}} + \delta\Gamma^{i}_{i0} = -\bar{g}^{i\beta}\delta g_{\beta\gamma}\bar{\Gamma}^{\gamma}_{i0} + \frac{1}{2}\bar{g}^{i\alpha}(\partial_i\delta g_{\alpha 0} + \partial_0\delta g_{i\alpha} - \partial_\alpha\delta g_{io}) \\
&= -\bar{g}^{ij}\delta g_{jk}\bar{\Gamma}^{k}_{i0} + \frac{1}{2}\bar{g}^{ij}(\cancel{\partial_i\delta g_{j0}} + \partial_0\delta g_{ij} - \cancel{\partial_j\delta g_{io}}) \\
&= -\bar{g}^{ij}\delta g_{jk}\delta^{k}_{i}H + \frac{1}{2}\bar{g}^{ij}\partial_0(-2a^2\Phi\delta_{ij}) = -\bar{g}^{ij}\delta g_{ij}H - \delta_{ij}\bar{g}^{ij}\partial_0(a^2\Phi) \\
&= -3(\frac{1}{a^2})(-2a^2\Phi)H - 2a\dot{a}\Phi(3\delta_{11}\bar{g}^{11}) = 6H\Phi - 6H\Phi \\
&= 0.
\end{aligned}
\tag{A.35}
$$

Consider the fourth term in the bracket of C_2, we get

$$
\begin{aligned}
\bar{\Gamma}^{\rho}_{\mu 0}\delta T^{\mu}_{\rho} &= \cancel{\bar{0}^{\rho}_{00}\delta T^{0}_{0}} + \bar{\Gamma}^{i}_{j0}\delta T^{j}_{i} = \delta^{i}_{j}H\rho_m v^j v_i \\
&= \rho_m H v^i v_i.
\end{aligned}
\tag{A.36}
$$

The last term of C_2 equal to 0, then we obtain

$$
C_2 = \dot{\bar{\phi}}[\delta\dot{\rho}_m + (\partial_i v^i)\delta\rho_m + v^i\partial_i\delta\rho_m + \bar{\rho}_m\partial_i\delta v^i + 3H\delta\rho_m + \rho_m H v^i v_i].
\tag{A.37}
$$

From the equations (A.29) - (A.37), we obtian the perturbation for θ_3 as

$$
\delta\theta_3 = \dot{\bar{\phi}}[\delta\dot{\rho}_m + \rho_m\partial_i v^i + v^i\partial_i\delta\rho_m + 3H\delta\rho_m + \rho_m H v^i v_i].
\tag{A.38}
$$

The perturbation calculation for θ_4 shown below

$$
\begin{aligned}
\theta_4 &= \phi^{,\alpha}\nabla_\alpha T_{mp} = g^{\alpha\beta}\phi_\beta\nabla_\alpha(\phi_{,\rho}\phi_\sigma T^{\rho\sigma}), \\
\delta\theta_4 &= \bar{\phi}_{,\beta}(\delta g^{\alpha\beta})\bar{\nabla}_\alpha(\bar{\phi}_{,\rho}\bar{\phi}_{,\sigma}\bar{T}^{\rho\sigma}) + \bar{g}^{\alpha\beta}\bar{\phi}_{,\beta}\delta[\nabla_\alpha(\phi_{,\rho}\phi_{,\sigma}T^{\rho\sigma})] \\
&= D_1 + D_2.
\end{aligned}
\tag{A.39}
$$

Consider D_1 from the above equation

$$D_1 = \bar{\phi}_{,\beta}(\delta g^{\alpha\beta})\bar{g}^{\sigma\lambda}\left[\partial_\alpha(\bar{\phi}_{,\rho}\bar{\phi}_{,\sigma}\bar{T}^\rho_\lambda) - \bar{\Gamma}^\gamma_{\alpha\sigma}\bar{\phi}_{,\rho}\bar{\phi}_{,\gamma}\bar{T}^\rho_\lambda - \bar{\Gamma}^\gamma_{\alpha\lambda}\bar{\phi}_{,\rho}\bar{\phi}_{,\sigma}\bar{T}^\rho_\gamma\right]$$

$$= D_{1a} + D_{1b} + D_{1c}, \tag{A.40}$$

$$D_{1a} = \bar{\phi}_{,\beta}(\delta g^{\alpha\beta})\bar{g}^{\sigma\lambda}\partial_\alpha(\bar{\phi}_{,\rho}\bar{\phi}_{,\sigma}\bar{T}^\rho_\lambda) = \bar{\phi}_{,0}(\delta g^{00})\bar{g}^{00}\partial_0(\bar{\phi}_{,0}\bar{\phi}_{,0}\bar{T}^0_0)$$

$$= \dot{\bar{\phi}}(2\Phi)(-1)\partial_0[\dot{\bar{\phi}}^2(-\bar{\rho}_m)]$$

$$= 4\bar{X}\Phi(2\ddot{\bar{\phi}}\bar{\rho}_m + \dot{\bar{\phi}}\dot{\bar{\rho}}_m) \approx 0, \tag{A.41}$$

$$D_{1b} = -\bar{\phi}_{,\beta}\bar{\phi}_{,\rho}\bar{\phi}_{,\gamma}(\delta g^{\alpha\beta})\bar{g}^{\sigma\lambda}\bar{\Gamma}^\gamma_{\alpha\lambda}\bar{T}^\rho_\lambda = -\bar{\phi}_{,0}\bar{\phi}_{,0}\bar{\phi}_{,0}(\delta g^{00})\bar{g}^{00}\bar{\Gamma}^0_{00}\bar{T}^0_0$$

$$= 0, \tag{A.42}$$

$$D_{1c} = -\bar{\phi}_{,\beta}\bar{\phi}_{,\rho}\bar{\phi}_{,\sigma}(\delta g^{\alpha\beta})\bar{g}^{\sigma\lambda}\bar{\Gamma}^\gamma_{\alpha\lambda}\bar{T}^\rho_\gamma$$

$$= 0. \tag{A.43}$$

Then, we get

$$D_1 \approx 0. \tag{A.44}$$

The calculation for D_2 from the equation (A.39) shown below

$$D_2 = \bar{g}^{\alpha\beta}\bar{\phi}_{,\beta}\delta[\nabla_\alpha(\phi_{,\rho}\phi_{,\sigma}T^{\rho\sigma})]$$

$$= \bar{g}^{\alpha\beta}\bar{\phi}_{,\beta}[(\delta g^{\sigma\lambda})\nabla_\alpha(\bar{\phi}_{,\rho}\bar{\phi}_{,\sigma}\bar{T}^\rho_\lambda) + \bar{g}^{\sigma\lambda}\delta\{\nabla_\alpha(\phi_{,\rho}\phi_{,\sigma}T^{\rho\sigma})\}]$$

$$= D_{2a} + D_{2b}, \tag{A.45}$$

$$D_{2a} = \bar{g}^{\alpha\beta}\bar{\phi}_{,\beta}(\delta g^{\sigma\lambda})\nabla_\alpha(\bar{\phi}_{,\rho}\bar{\phi}_{,\sigma}\bar{T}^\rho_\lambda)$$

$$= 4\bar{X}\Phi(2\ddot{\bar{\phi}}\bar{\rho}_m + \dot{\bar{\phi}}\dot{\bar{\rho}}_m) \approx 0, \tag{A.46}$$

$$D_{2b} = \bar{\phi}_{,\beta}\bar{g}^{\alpha\beta}\bar{g}^{\sigma\lambda}\delta[\nabla_\alpha(\bar{\phi}_{,\rho}\bar{\phi}_{,\sigma}\bar{T}^\rho_\lambda)]$$

$$= \bar{\phi}_{,\beta}\bar{g}^{\alpha\beta}\bar{g}^{\sigma\lambda}\delta[\nabla_\alpha(\phi_{,\rho}\phi_{,\sigma}T^\rho_\lambda)]$$

$$= \bar{\phi}_{,\beta}\bar{g}^{\alpha\beta}\bar{g}^{\sigma\lambda}\delta[\partial_\alpha(\phi_{,\rho}\phi_{,\sigma}T^\rho_\lambda) - \Gamma^\gamma_{\alpha\sigma}\phi_{,\rho}\phi_{,\gamma}T^\rho_\lambda - \Gamma^\gamma_{\alpha\lambda}\phi_{,\rho}\phi_{,\sigma}T^\rho_\gamma]$$

$$= \bar{\phi}_{,\beta}\bar{g}^{\alpha\beta}\bar{g}^{\sigma\lambda}\partial_\alpha(\bar{\phi}_{,\rho}\bar{\phi}_{,\sigma}\delta T^\rho_\lambda) = \bar{\phi}_{,0}\bar{g}^{00}\bar{g}^{00}\partial_0(\bar{\phi}_{,0}\bar{\phi}_{,0a}\delta T^0_0)$$

$$= \dot{\bar{\phi}}(-1)(-1)\partial_0[\dot{\bar{\phi}}^2(-\delta\rho_m)] = -2\dot{\bar{\phi}}(\dot{\bar{\phi}}\ddot{\bar{\phi}}\delta\rho_m + \bar{X}\delta\dot{\rho}_m). \tag{A.47}$$

From the equations (A.44) - (A.47), we obtain the perturbation for θ_4 as

$$\delta\theta_4 = -2\dot{\bar{\phi}}(\dot{\bar{\phi}}\ddot{\bar{\phi}}\delta\rho_m + \bar{X}\delta\dot{\rho}_m). \tag{A.48}$$

We show the perturbation calculation for $\theta_5 T_{mp}$ below

$$\theta_5 T_{mp} = g^{\alpha\beta}\phi_{,\beta}X_{,\alpha}T_{mp} = g^{\alpha\beta}g^{\sigma\lambda}\phi_{,\beta}X_{,\alpha}\phi_{,\rho}\phi_{,\sigma}T^\rho_\lambda,$$

$$\delta(\theta_5 T_{mp}) = \bar{\phi}_{,\beta}\bar{\phi}_{,\rho}\bar{\phi}_{,\sigma}\Big[(\delta g^{\alpha\beta})\bar{g}^{\sigma\lambda}\bar{X}_{,\alpha}\bar{T}^\rho_\lambda + \bar{g}^{\alpha\beta}(\delta g^{\sigma\lambda})\bar{X}_{,\alpha}\bar{T}^\rho_\lambda + \bar{g}^{\alpha\beta}\bar{g}^{\sigma\lambda}(\delta X_{,\alpha})\bar{T}^\rho_\lambda$$

$$+ \bar{g}^{\alpha\beta}\bar{g}^{\sigma\lambda}\bar{X}_{,\alpha}\delta T^\rho_\lambda\Big]$$

$$= E_1 + E_2 + E_3 + E_4, \tag{A.49}$$

$$E_1 = \bar{\phi}_{,\beta}\bar{\phi}_{,\rho}\bar{\phi}_{,\sigma}(\delta g^{\alpha\beta})\bar{g}^{\sigma\lambda}\bar{X}_{,\alpha}\bar{T}^\rho_\lambda = \bar{\phi}_{,0}\bar{\phi}_{,0}\bar{\phi}_{,0}(\delta g^{00})\bar{g}^{00}\bar{X}_{,0}\bar{T}^0_0$$

$$= 8\bar{\rho}_m\bar{X}^2\ddot{\bar{\phi}}\Phi \approx 0, \tag{A.50}$$

$$E_2 = \bar{\phi}_{,\beta}\bar{\phi}_{,\rho}\bar{\phi}_{,\sigma}\bar{g}^{\alpha\beta}(\delta g^{\sigma\lambda})\bar{X}_{,\alpha}\bar{T}^\rho_\lambda$$

$$= 8\bar{\rho}_m\bar{X}^2\ddot{\bar{\phi}}\Phi \approx 0, \tag{A.51}$$

$$E_3 = \bar{\phi}_{,\beta}\bar{\phi}_{,\rho}\bar{\phi}_{,\sigma}\bar{g}^{\alpha\beta}\bar{g}^{\sigma\lambda}\bar{T}^\rho_\lambda\delta X_{,\alpha}$$

$$= 8\bar{\rho}_m\bar{X}^2\ddot{\phi}\Phi \approx 0,$$

$$E_4 = \bar{\phi}_{,\beta}\bar{\phi}_{,\rho}\bar{\phi}_{,\sigma}\bar{g}^{\alpha\beta}\bar{g}^{\sigma\lambda}\bar{X}_{,\alpha}\delta T^\rho_\lambda$$

$$= -4\bar{X}^2\ddot{\phi}\delta\rho_m. \tag{A.52}$$

From the equations (A.49) - (A.52), we obtain

$$\delta(\theta_5 T_{mp}) = -4\bar{X}^2\ddot{\bar{\phi}}\delta\rho_m. \tag{A.53}$$

The computation for the perturbation of $T_{mp}\Box\phi$ shown below

$$T_{mp}\Box\phi = \phi_{,\alpha}\phi_{,\beta}T^{\alpha\beta}\nabla_\rho\partial^\rho\phi = \phi_{,\alpha}\phi_{,\beta}T^{\alpha\beta}\frac{1}{\sqrt{-g}}\partial_\rho(\sqrt{g}\partial^\rho\phi)$$

$$= \phi_{,\alpha}\phi_{,\beta}T^{\alpha\beta}\frac{1}{\sqrt{-g}}\partial_\rho(\sqrt{-g}g^{\rho\sigma}\partial_\sigma\phi),$$

$$\delta(T_{mp}\Box\phi) = \delta\Big(\phi_{,\alpha}\phi_{,\beta}T^{\alpha\beta}\frac{1}{\sqrt{-g}}\Big)\partial_\rho(\sqrt{-g}\bar{g}^{\rho\sigma}\partial_\sigma\bar{\phi}) + \Big(\phi_{,\alpha}\phi_{,\beta}T^{\alpha\beta}\frac{1}{\sqrt{-g}}\Big)\delta\partial_\rho(\sqrt{-g}g^{\rho\sigma}\partial_\sigma\phi)$$

$$= (\delta A)\partial_\rho\bar{B} + \bar{A}\delta(\partial_\alpha B) = \delta Z_1 + \delta Z_2. \tag{A.54}$$

From the metric perturbation given in equation (4.5), we obtain the determinant of this metric as

$$g = \det(g_{\alpha\beta}) = -a^6(1+2\Phi)(1-2\Phi)^3,$$

$$\sqrt{-g} = a^3\sqrt{(1+2\Phi)(1-2\Phi)^3}. \tag{A.55}$$

Using the binomial series

$$(1+x)^\alpha = 1 + \alpha x + \frac{1}{2!}\alpha(\alpha-1)x^2 + ..., \tag{A.56}$$

equation (A.55) becomes

$$\sqrt{-g} = a^3[1 + \frac{1}{2}(2\Phi) + ...][1 + \frac{3}{2}(-2\Phi) + ...] \simeq a^3(1+\Phi)(1-3\Phi)$$
$$= a^3(1-2\Phi). \tag{A.57}$$

We also obtain the inverse of the above equation as follows

$$\frac{1}{\sqrt{-g}} = \frac{1}{a^3} \cdot \frac{1}{\sqrt{1+2\Phi}} \cdot \frac{1}{\sqrt{(1-2\Phi)^3}}$$
$$= \frac{1}{a^3}[1 - \frac{1}{2}(2\Phi) + ...][1 - \frac{3}{2}(2\Phi) + ...] \simeq= \frac{1}{a^3}$$
$$= \frac{1}{a^3}(1-4\Phi). \tag{A.58}$$

From the equation (A.54), we can write A, A background $(\bar{A})$, B and B background $(\bar{B})$ respectively as

$$A = \phi_{,\alpha}\phi_{,\beta}T^{\alpha\beta}\frac{1}{\sqrt{-g}} = \phi_{,\alpha}\phi_{,\beta}g^{\gamma\beta}T^\alpha_\gamma\frac{1}{a^3}(1-2\Phi), \tag{A.59}$$

$$\bar{A} = \bar{\phi}_{,\alpha}\bar{\phi}_{,\beta}\bar{g}^{\gamma\beta}\bar{T}^\alpha_\gamma\frac{1}{a^3}, \tag{A.60}$$

$$B = \sqrt{-g}g^{\rho\sigma}\partial_\sigma\phi = a^3(1-2\Phi)g^{\rho\sigma}\partial_\sigma\phi, \tag{A.61}$$

$$\bar{B} = a^3\bar{g}^{\rho\sigma}\partial_\sigma\bar{\phi}, \tag{A.62}$$

The perturbation for A is shown below

$$\delta A = \bar{\phi}_{,\alpha}\bar{\phi}_{,\beta}\delta[g^{\gamma\beta}T^\alpha_\gamma\frac{1}{a^3}(1-2\Phi)]$$

$$= \bar{\phi}_{,\alpha}\bar{\phi}_{,\beta}[(\delta g^{\gamma\beta})\bar{T}^\alpha_\gamma\frac{1}{a^3} + \bar{g}^{\gamma\beta}(\delta T^\alpha_\gamma)\frac{1}{a^3} - \bar{g}^{\gamma\beta}\bar{T}^\alpha_\gamma\frac{1}{a^3}]$$

$$= \delta A_1 + \delta A_2 + \delta A_3, \tag{A.63}$$

$$\delta A_1 = \bar{\phi}_{,\alpha}\bar{\phi}_{,\beta}(\delta g^{\gamma\beta})\bar{T}^\alpha_\gamma\frac{1}{a^3} = \bar{\phi}_{,0}\bar{\phi}_{,0}(\delta g^{00})\bar{T}^0_0\frac{1}{a^3}$$

$$= -\frac{4}{a^3}\bar{X}\bar{\rho}_m\Phi = 0, \tag{A.64}$$

$$\delta A_2 = \bar{\phi}_{,\alpha}\bar{\phi}_{,\beta}\bar{g}^{\gamma\beta}(\delta T^\alpha_\gamma)\frac{1}{a^3} = \bar{\phi}_{,0}\bar{\phi}_{,0}\bar{g}^{00}(\delta T^0_0)\frac{1}{a^3}$$

$$= \frac{2}{a^3}\bar{X}\delta\rho_m, \tag{A.65}$$

$$\delta A_3 = \bar{\phi}_{,\alpha}\bar{\phi}_{,\beta}\bar{g}^{\gamma\beta}\bar{T}^\alpha_\gamma\frac{1}{a^3} = \bar{\phi}_{,0}\bar{\phi}_{,0}\bar{g}^{00}\bar{T}^0_0\frac{1}{a^3}$$

$$= -\frac{4}{a^3}\bar{X}\bar{\rho}_m\Phi = 0. \tag{A.66}$$

From the equations (A.54), (A.62) - (A.66), We can write δZ_1 as

$$\delta Z_1 = \frac{1}{a^3}2\bar{X}\delta\rho_m\partial_\rho(a^3\bar{g}^{\rho\sigma}\partial_\sigma\bar{\phi}) = \frac{1}{a^3}2\bar{X}\delta\rho_m\partial_0(a^3\bar{g}^{00}\partial_0\bar{\phi})$$

$$= -\frac{1}{a^3}2\bar{X}\delta\rho_m\partial_0(a^3\partial_0\bar{\phi})$$

$$= -2\bar{X}\delta\rho_m(3\bar{H}\dot{\bar{\phi}} + \ddot{\bar{\phi}}). \tag{A.67}$$

We derive the perturbation for δZ_2 as

$$\partial_\rho B = \partial_\rho[a^3(1-2\Phi)g^{\rho\sigma}\partial_\sigma\phi],$$

$$\delta(\partial_\rho B) = \partial_\rho[-2a^3\Phi\bar{g}^{\rho\sigma}\partial_\sigma\bar{\phi} + a^3(\delta g^{\rho\sigma})\partial_\sigma\bar{\phi} + a^3\bar{g}^{\rho\sigma}\partial_\sigma\delta\phi],$$

$$\delta Z_2 = \bar{\phi}_{,\alpha}\bar{\phi}_{,\beta}\bar{g}^{\gamma\beta}\bar{T}^\alpha_\gamma\frac{1}{a^3}\partial_\rho\Big[a^3\{\cancel{(\delta g^{\rho\sigma})\partial_\sigma\bar{\phi}} - \cancel{2\Phi\bar{g}^{\rho\sigma}\partial_\sigma\bar{\phi}} + \bar{g}^{\rho\sigma}\partial_\sigma\delta\phi\}\Big]$$

$$= \bar{\phi}_{,0}\bar{\phi}_{,0}\bar{g}^{00}\bar{T}^0_0\frac{1}{a^3}[\partial_0\{a^3\bar{g}^{0\sigma}\partial_\sigma\delta\phi\} + \partial_i\{a^3\bar{g}^{i\sigma}\partial_\sigma\delta\phi\}]$$

$$= \frac{1}{a^3}\dot{\bar{\phi}}^2\bar{\rho}_m[\partial_0\{a^3\bar{g}^{00}\partial_0\delta\phi\} + \partial_i\{a^3\bar{g}^{ij}\partial_j\delta\phi\}]$$

$$= \frac{2}{a^3}\bar{X}\bar{\rho}_m[-\{3a^2\dot{a}\delta\dot{\phi} + a^3\delta\ddot{\phi}\} + a\partial_i\partial_i\delta\phi]$$

$$= \frac{2}{a^2}\bar{X}\bar{\rho}_m\partial_i\partial_i\delta\phi = 2\bar{X}\bar{\rho}_m\nabla^2\delta\phi. \tag{A.68}$$

From the equations (A.67) and (A.68), we obtain

$$\delta(T_{mp}\Box\phi) = -2\bar{X}\delta\rho_m(3\bar{H}\dot{\bar{\phi}} + \ddot{\bar{\phi}}) + 2\bar{X}\bar{\rho}_m\nabla^2\delta\phi. \qquad (A.69)$$

APPENDIX B TOP HAT MODEL

In this appendix, we show explicit details for the calculation of the non-linear second order evolution equation for matter density contrast. We also apply top hat model to our calculation [105]. From simple symmetric, we have

$$\partial_i \delta_m|_{\mathbf{x}=0} = v_m^i(0,t) = 0\,, \tag{B.1}$$

where $v_m^i(0,t)$ is the comoving velocity. The equation (4.76) becomes

$$\dot{\delta}_m\Big|_{\mathbf{x}=0} = -\left[(1+\delta_m)\partial_i v_m^i\right]\Big|_{\mathbf{x}=0}\,, \tag{B.2}$$

or

$$\partial_i v_m^i\Big|_{\mathbf{x}=0} = -\frac{\dot{\delta}_m}{1+\delta_m}\Big|_{\mathbf{x}=0}\,. \tag{B.3}$$

Differentiating the equation (B.2) with respect to time t, and using the equation (4.66), we obtain non-linear second order evolution equation for δ_m at $\mathbf{x} = \mathbf{0}$ as follows

$$\ddot{\delta}_m\Big|_{\mathbf{x}=0} = -\left(2H + \widetilde{Q}_0\dot{\phi}\right)\dot{\delta}_m\Big|_{\mathbf{x}=0} + \frac{4}{3}\frac{\dot{\delta}_m^2}{1+\delta_m}\Big|_{\mathbf{x}=0}$$
$$+ \frac{1+\delta_m}{a^2}(\partial_i\Phi + \widetilde{Q}_0\partial_i\delta\phi)\Big|_{\mathbf{x}=0}\,. \tag{B.4}$$

To obtained the above equation we have used the identity

$$\nabla(\mathbf{v}_m\,\nabla)\mathbf{v}_m|_{\mathbf{x}=0} = \frac{1}{3}\left(\nabla\cdot\mathbf{v}_m\right)^2\Big|_{\mathbf{x}=0} = \frac{1}{3}\frac{\dot{\delta}_m^2}{(1+\delta_m)^2}\Big|_{\mathbf{x}=0}\,. \tag{B.5}$$

We then obtain linear second order evolution equation for δ_m as follows

$$\ddot{\delta}_m = -(2H + \widetilde{Q}_0\dot{\phi})\dot{\delta}_m + \frac{1+\delta_m}{a^2}(\partial_i\Phi + \widetilde{Q}_0\partial_i\delta\phi)\,. \tag{B.6}$$

BIOGRAPHY

BIOGRAPHY

Name-Surname   Stharporn Sapa

Date of Birth   26 February 1984

Place of Birth   Bangkok, Thailand

Address   14/69, Village No. 9, Sumrongkrang Sub-district, Phrapradaeng, Samutprakarn 10130

Education Background

2007   B.Sc. (Physics), Ramkhamhaeng University, Bangkok, Thailand

2013   M.Sc. (Physics), Ramkhamhaeng University, Bangkok, Thailand